

## 16. SITE 684<sup>1</sup>

### Shipboard Scientific Party<sup>2</sup>

#### HOLE 684A

**Date occupied:** 2300 L, 20 November 1986

**Date departed:** 1545 L, 21 November 1986

**Time on hole:** 16 hr 45 min

**Position:** 8°59.49'S, 79°54.35'W

**Water depth (sea level; corrected m, echo-sounding):** 426.0

**Water depth (rig floor; corrected m, echo-sounding):** 436.5

**Bottom felt (m, drill pipe):** 437.7

**Penetration (m):** 136.1

**Number of cores:** 15

**Total length of cored section (m):** 136.1

**Total core recovered (m):** 72.5

**Core recovery (%):** 53.3

#### Oldest sediment cored

Depth (mbsf): 136.1

Nature: diatomaceous mud

Age: middle Miocene

Measured velocity (km/s): ~1.55

#### HOLE 684B

**Date occupied:** 1545 L, 21 November 1986

**Date departed:** 2030 L, 21 November 1986

**Time on hole:** 28 hr 45 min

**Position:** 8°59.49'S, 79°54.35'W

**Water depth (sea level; corrected m, echo-sounding):** 426.5

**Water depth (rig floor; corrected m, echo-sounding):** 437.0

**Bottom felt (m, drill pipe):** 438.5

**Penetration (m):** 55.0

**Number of cores:** 6

**Total length of cored section (m):** 55.0

**Total core recovered (m):** 37.17

**Core recovery (%):** 67.6

#### Oldest sediment cored

Depth (mbsf): 55.0

Nature: diatomaceous mudstone

Age: Pliocene

Measured velocity (km/s): ~1.56

#### HOLE 684C

**Date occupied:** 2030 L, 21 November 1986

**Date departed:** 0815 L, 22 November 1986

**Time on hole:** 11 hr 45 min

**Position:** 8°59.49'S, 79°54.35'W

**Water depth (sea level; corrected m, echo-sounding):** 426.5

**Water depth (rig floor; corrected m, echo-sounding):** 437

**Bottom felt (m, drill pipe):** 438.2

**Penetration (m):** 115.0

**Number of cores:** 13

**Total length of cored section (m):** 115.0

**Total core recovered (m):** 56.23

**Core recovery (%):** 48.9

#### Oldest sediment cored

Depth (mbsf): 115.0

Nature: mudstone

Age: middle Miocene

Measured velocity (km/s): ~1.56

**Principal results:** Site 684, the northern point of a transect along the Peruvian coastal upwelling regime, was located in a small sediment pond on the flank of the Trujillo Basin, in an area on the upper slope otherwise devoid of sediments. The continental shelf off north-central Peru is a broad, shallow, current-swept platform, and the sedi-

<sup>1</sup> Suess, E., von Huene, R., et al., 1988. *Proc. ODP, Init. Repts.*, 112: College Station, TX (Ocean Drilling Program).

<sup>2</sup> Erwin Suess (Co-Chief Scientist), Oregon State University, College of Oceanography, Corvallis, OR 97331; Roland von Huene (Co-Chief Scientist), U.S. Geological Survey, Branch of Pacific Marine Geology, 345 Middlefield Rd. M/S 999, Menlo Park, CA 94025; Kay-Christian Emeis (ODP Staff Scientist), Ocean Drilling Program, Texas A&M University, College Station, TX 77843; Jacques Bourgeois, Département de Géotectonique, Université Pierre et Marie Curie, 4 Place Jussieu, 75230 Paris Cedex 05, France; José del C. Cruzado Castañeda, Petroleos del Peru S. A., Paseo de la Republica 3361, San Isidro, Lima, Peru; Patrick De Wever, CNRS, Laboratoire de Stratigraphie, Université Pierre et Marie Curie, 4 Place Jussieu, 75230 Paris Cedex 05, France; Geoffrey Eglinton, University of Bristol, School of Chemistry, Cantock's Close, Bristol BS8 1TS, England; Robert Garrison, University of California, Earth Sciences, Applied Sciences Building, Santa Cruz, CA 95064; Matt Greenberg, Lamont-Doherty Geological Observatory, Columbia University, Palisades, NY 10964; Elard Herrera Paz, Petroleos del Peru, S. A., Paseo de la Republica 3361, San Isidro, Lima, Peru; Phillip Hill, Atlantic Geoscience Centre, Bedford Institute of Oceanography, Box 1006, Dartmouth, Nova Scotia B2Y 4A2, Canada; Masako Ibaraki, Geoscience Institute, Faculty of Science, Shizuoka University, Shizuoka 422, Japan; Miriam Kastner, Scripps Institution of Oceanography, SVH, A-102, La Jolla, CA 92093; Alan E. S. Kemp, Department of Oceanography, The University, Southampton SO9 5NH, England; Keith Kvenvolden, U.S. Geological Survey, Branch of Pacific Marine Geology, 345 Middlefield Rd., M/S 999, Menlo Park, CA 94025; Robert Langridge, Department of Geological Sciences, Queen's University at Kingston, Ontario K7L 3A2, Canada; Nancy Lindsley-Griffin, University of Nebraska, Department of Geology, 214 Bessey Hall, Lincoln, NE 68588-0340; Janice Marsters, Department of Oceanography, Dalhousie University, Halifax, Nova Scotia B3H 4J1, Canada; Erlend Martini, Geologisch-Paläontologisches Institut der Universität Frankfurt, Senckenberg-Anlage 32-34, D-6000, Frankfurt/Main, Federal Republic of Germany; Robert McCabe, Department of Geophysics, Texas A&M University, College Station, TX 77843; Leonidas Ocola, Laboratorio Central, Instituto Geofísico del Peru, Lima, Peru; Johanna Resig, Department of Geology and Geophysics, University of Hawaii, Honolulu, HI 96822; Agapito Wilfredo Sanchez Fernandez, Instituto Geológico Minero y Metalúrgico, Pablo Bermudez 211, Lima, Peru; Hans-Joachim Schrader, College of Oceanography, Oregon State University, Corvallis, OR 97331 (currently at Department of Geology, University of Bergen, N-5000 Bergen, Norway); Todd Thornburg, College of Oceanography, Oregon State University, Corvallis, OR 97331; Gerold Wefer, Universität Bremen, Fachbereich Geowissenschaften, Postfach 330 440, D-2800 Bremen 33, Federal Republic of Germany; Makoto Yamano, Earthquake Research Institute, University of Tokyo, Bunkyo-ku, Tokyo 113, Japan.

ment pond lies beneath the seaward trail of frequent upwelling plumes that cross this shelf. The pond is approximately 2 km wide, is of limited extent along strike, and rests on an irregular, unconformable surface that separates the Miocene strata of the Trujillo Basin from Pliocene/Quaternary sediments.

Three holes were drilled at Site 684. Hole 684A was cored to 136.1 mbsf by first using the hydraulic piston corer (APC), with >95% of the core recovered to 69.6 m, and subsequently using the extended core-barrel (XCB) corer, with poor recovery for the remainder of the hole. The change in coring tools was necessitated by frequent dolomite layers interbedded with diatomaceous silty muds. At Hole 684B, this dolomite layer caused us to end drilling at only 55.0 mbsf. Hole 684C was cored in the APC mode above a massive dolomite layer and in the XCB mode to 115.0 mbsf below this layer. Excellent correlation was established between holes based on lithostratigraphic and biostratigraphic markers.

The sediments at Site 684, compared with the previously drilled sites along the transect, record the latitudinal variability of upwelling. Three distinct time stratigraphic sections of late Quaternary, Pliocene, and Miocene age are separated by two hiatuses. The first hiatus at 13.5 mbsf divides well-laminated, olive and gray diatomaceous muds interbedded with coarse, calcareous, phosphatic and terrigenous beds (<0.9 Ma) from underlying (3.5–4 Ma) bioturbated, dark to olive gray mud with microfossil- and macrofossil-bearing units. The second hiatus at 56.2 mbsf in Hole 684A (59.5 mbsf at Hole 684C) separates these deposits from olive gray, nanofossil-bearing, diatomaceous mud with laminated and mottled beds of Miocene age (>7.8 Ma), that extend to the bottom of the holes. The six lithologic units and subunits that comprise these sections alternate between sections dominated by hemipelagic upwelling sediments and reworking (Quaternary lithologic Subunit IA, Pliocene lithologic Unit III, and Miocene lithologic Unit V) and those that show the influence of current deposition (Quaternary lithologic Subunit IB and Pliocene lithologic Units II and IV). The late Quaternary upwelling environment is characterized by well-preserved diatom and coccolith assemblages. In the current-dominated section, normally graded beds of shell debris, foraminifers, bone fragments, and glauconitic and phosphatic grains are common. The shallow-water Pliocene depositional environment was generally less influenced by coastal upwelling, as indicated by bioturbation, erosional contacts, coarse-grained beds, and rare diagnostic diatom and coccolith upwelling assemblages. The Miocene "upwelling" environment is characterized by frequent blooms of diatoms and coccoliths that show little evidence of reworking. These indicate a high nutrient supply to surface waters during brief alternating cold and warm phases.

The current-induced, shallow-water deposits of lithologic Subunit IB and lithologic Units II and IV contain abundant, dense, phosphate peloids and glauconite. We believe these phosphate-glauconite beds represent lag deposits produced by short winnowing episodes, when the diatomaceous matrix (in which grains of these authigenic phases had formed) was resuspended. Beds in lithologic Units II and IV are condensed sequences associated with major hiatuses that correlate with eustatic low sea-level stands. The diatomaceous sediments from coastal upwelling of lithologic Subunit IA and Units III and V contain authigenic carbonates and friable phosphates. Calcite and dolomite are present as disseminated crystals in unlithified muds and as fully lithified nodules and beds. Intervals with pronounced concentrations of calcite and dolomite coincide with zones of significant changes in the  $Ca^{2+}/Mg^{2+}$  ratio of hypersaline pore waters. These fluids were discovered in the subsurface of the Peru outer shelf at Sites 680 and 681 and were also present at Site 684, 200 km farther north. The areal extent of the subsurface brine over the Peru shelf is unknown. Chloride and dissolved major ion contents at the bottom of Hole 684C increased to concentrations twice those of seawater. Microbial sulfate reduction and methanogenesis, the important driving mechanisms of carbonate and organic-matter diagenesis, respond quickly to the replenishment of sulfate from an influx of brine.

The recovered section contains parts of late Quaternary, middle Pliocene, and late Miocene sediments deposited in the coastal upwelling regime alternating with periods of hemipelagic and current-dominated deposition. These sediments undergo early diagenesis, which is affected by an influx of highly saline pore fluids, which promotes the widespread formation of dolomite and calcite.

## BACKGROUND AND SCIENTIFIC OBJECTIVES

Site 684 is the northern point of a north-south transect of three sites along the upper-slope deposits of the Peruvian margin. This transect extends for almost 500 km in areas of strong coastal upwelling. It traverses three prominent centers of recurring upwelling plumes at 9°S, 11°S, and 13°S latitude in a water depth of about 400–500 m (Fig. 1). Three objectives were addressed by the drilling at Site 684 and relate to (1) latitudinal variability of upwelling parameters, (2) facies differentiation from reworking of sediments by poleward-flowing undercurrent, and (3) the impact of hypersaline pore fluids on early diagenesis in general and on dolomitization in particular.

These objectives were previously discussed in detail at Site Chapter 679, located in the center of the north-south transect, and were also the subject of drilling at Sites 686 and 687. Therefore, this introduction is intended for all these sites and will be referred to in the respective site chapters.

The north-south transect covers water depths between 416 m at 9°S (Site 684), 473 m at 11°S (Site 679), and 443 m at 13°30'S (Site 686). This interval is situated just beneath the center of today's oxygen minimum zone. During lowered sea levels in the past, this interval may have been located in the center. If this reasoning were correct, "oxygen minimum sediments" deposited throughout the age of the upper slope should have been recovered. The sediment record at Site 684 was expected to resolve, through Quaternary and perhaps late Neogene times, the latitudinal variability in faunal and floral composition of upwelling assemblages and in stable-isotope signals of calcareous plankton and benthos responding to water properties. When compared with companion sites along the transect, shifts of maximum bioproduction should become evident to outline the history of the Peruvian upwelling regime.

Two different sedimentary facies characterize the upper continental slope and outer shelf along the north-south transect. Organic-carbon-rich muds accumulate around 11°S and 13°S, where the shelf is narrow and steep. Calcareous organic-rich muds, coarser in texture and containing phosphorites and other evidence of reworking, accumulate on the much wider and shallower shelf around 9°S. This results from reworking and exporting of fine-grained constituents by the poleward-flowing undercurrent. This process controls accumulation of the more "calcareous" upwelling facies at Site 684. Drilling at this site was intended to establish the period of time over which the calcareous and residual facies have been accumulating in the northern part of the transect and, thus, how long the influence of the undercurrent has been operating here.

The shelf-slope morphology determines the upwelling facies. The difference in morphology between the northern and southern parts of the transect appears to be controlled by the different subsidence rates and histories of the forearc basins. Site 684 is situated on the landward flank of the Trujillo Basin. This basin and the northern part of the Salaverry Basin, both separated by a prominent outer shelf high, appear to have undergone less and slower subsidence than the southern part of the Salaverry Basin and the Lima Basin. The contrasting tectonic styles and the resulting difference in upwelling facies continue to be amplified during diagenesis. Kulm et al. (this volume) proposed a series of different diagenetic pathways of dolomitization of these deposits by which the characteristically "light" and "heavy" carbon-isotope signals of dolomites dredged from these two areas could be explained. Diagenetic dolomites in the Lima Basin appear to form in an environment dominated by methanogenesis and, hence, incorporate "heavy" residual carbon isotopes from dissolved bicarbonate. In contrast, dolomites of the Trujillo Basin may form under the influence of sulfate reduction and may incorporate "light" carbon isotopes. Originally, this

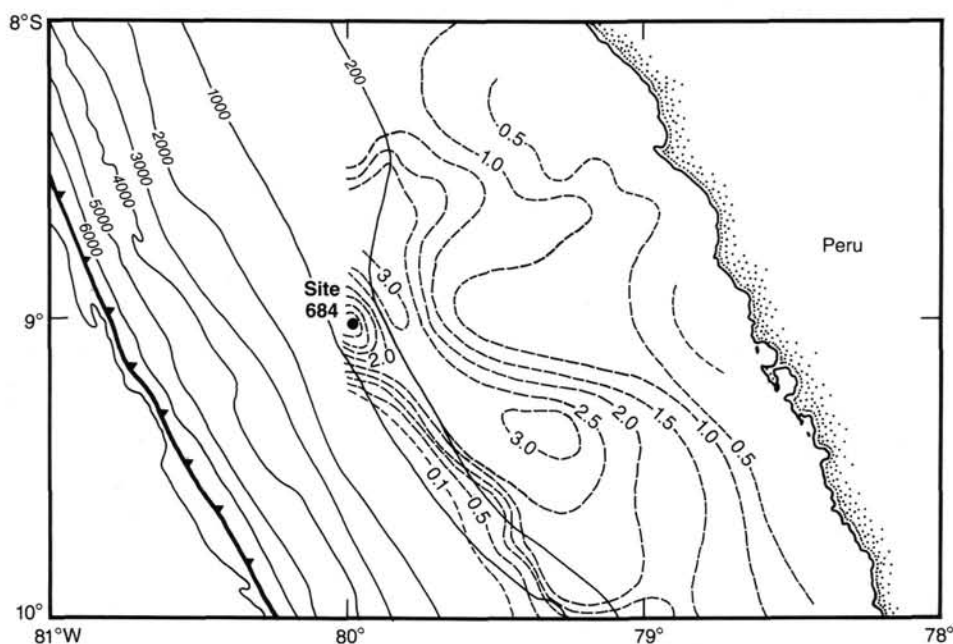


Figure 1. Bathymetry and sediment isopachs along Peru continental margin at 9°S; depths are in intervals of 1000 m, beginning at a water depth of 200 m. Sediment isopachs are in increments of 0.5 km, starting at 0.1 km thickness. For an overview of all sites, see Figure 1 in Site 679 chapter (this volume).

hypothesis was to be tested at several drill sites along the north-south transect. Because of time constraints during Leg 112, we decided to drill only at Site 684 so as not to jeopardize the remaining sites along the north-south transect.

A new objective emerged while drilling during Leg 112. This objective relates to the environment for dolomitization. Hypersaline pore fluids discovered in the subsurface at Sites 680 and 681 overprint the diagenetic reaction pathways, as envisioned for dolomitization in the forearc basins. Most likely, as ship-board interstitial-water and gas analyses suggest, sulfate is continuously being replenished from this brine and is the oxygen source used by sulfate-reducing bacteria. Consequently, the less effective microbial methanogenesis pathway is suppressed. Such a process would greatly alter the carbon-isotope signal of the metabolic carbon dioxide that is incorporated in dolomites or other authigenic carbonate minerals. Therefore, we planned to intensify sampling of interstitial water at Site 684. Special attention was given to elevated salinity, sulfate, magnesium, calcium contents, and any change in the intensity of methanogenesis.

Three holes were planned for drilling at this site to about 200 mbsf using the APC and XCB corers. This was expected to provide enough samples for our new objective as well as for high-resolution studies of the uppermost sediment sequence. The seismic data across the site show poor sediment coverage at the desired water depth of around 400 m and scattered distribution of sediment ponds between fault blocks at the western flank of the outer shelf high (Thornburg, 1985). Sediment thickness of around 160 m was confirmed from the SCS survey line YALOC 22-03-74, on which Site 684 was located.

### OPERATIONS

The ship was under way by 2300 UTC (1800 L) 20 November for the transit to Site 684. Our approach was to follow along SCS survey line YALOC 22-03-74 to locate the new site, which was situated in a small sediment pond bounded by fault blocks at the seaward flank of the outer shelf high. Our geophysical gear was not streamed out so as to maintain better maneuverability for deploying a beacon once the site had been located.

This was crucial because our global positioning system (GPS) was not available until about 0900 UTC the next day.

After intersecting YALOC line 22-03-74 at 0100 hr on 21 November, the *Resolution* set course to the new site (Fig. 2). During this run, we used 3.5-kHz shallow seismic profiling and 12-kHz precision depth recording to track our approach. At 0218 hr, within 1 nmi of the site, a SatNav position showed a northwesterly offset of 1.7 nmi. A course correction at this time would have resulted in an undesirable oblique crossing of the site. Therefore, we maintained the existing course for another 45 min until the vessel had passed the site and the target area could be approached on a reversed course. The 3.5-kHz profile confirmed that the prominent ledges and pinnacles of the target area had been passed and also indicated that the sediment patch had been missed.

On the return course, we dropped a marker buoy at 0407 hr at a water depth of 423 m; here, the 3.5-kHz profile indicated the presence of well-stratified sediments. We lowered a positioning beacon on a taut wire over the site. However, by the time the beacon was on the seafloor bottom and the vessel was operating in the dynamic positioning mode, we received two more SatNav fixes that again showed a northwesterly offset of more than 2 nmi. The 3.5-kHz shallow seismic profile confirmed that the vessel had drifted away from the sediment patch. We decided to "leap frog" the beacon toward the site and simultaneously to track the change in bottom morphology and sediment cover. This proved successful, and after we moved the ship twice in a southeasterly direction, the new site was established above a sequence of well-stratified sediments. The first APC core was drilled at 0350 L (0850 UTC).

Hole 684A was drilled to a total depth of 136.1 mbsf, using the APC to 69.6 mbsf and the XCB for the rest of the hole. Core 112-684A-4H was retrieved with a severely bent core barrel and damaged cutting shoe, both of which evidently had hit a hard layer. We found fragments of dolomite in the core catcher. However, recovery from this core and all APC cores was excellent (99%). After exceeding 50,000 lb of force to pull out Core 112-684A-8H, we switched to the XCB, and recovery decreased

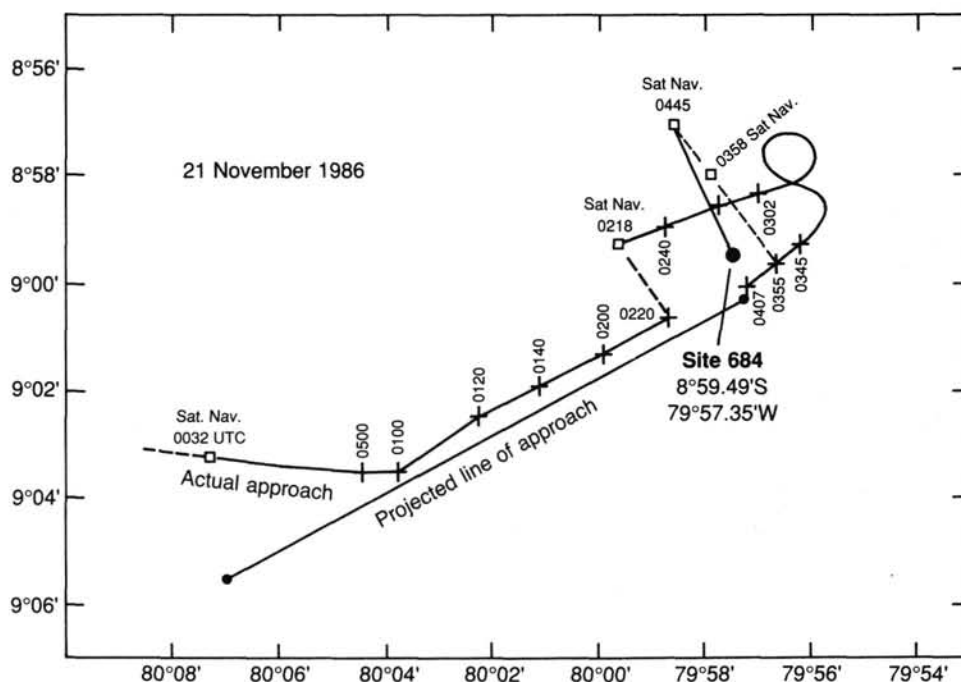


Figure 2. Track chart of approach to Site 684 locations. Time is Universal Time Coordinated.

dramatically. Invariably, we found fragments of dolomite and calcite layers mingled with soft diatomaceous mud in the core-catcher samples. We terminated the hole because of exceedingly poor recovery (<3%).

Hole 684B was started after moving 10 m south. The first four cores were cored flawlessly with the APC system and yielded high recovery rates. When drilling Core 112-684B-5H, we encountered a massive dolomite layer at the same depth as was seen in Hole 684A, but we were unable to penetrate it. A subsequent attempt using the XCB also was unsuccessful. We decided to abandon this hole at a total depth of only 55 mbsf and moved about 8 m east to achieve deeper penetration closer to the depositional center of the sediment patch. A stuck core barrel in the drill collar contributed to this decision.

Hole 684C was cored rapidly using the APC system, which again yielded maximum recovery (100%). The first five cores were frozen for shore-based organic-geochemical sampling because these intervals had been cored twice before. Excellent cross-correlation was established, based on a number of prominent marker beds (Table 1). One of markers was the massive dolomite layer at the base of Hole 684B, which we then penetrated and from which we successfully recovered sediments by means of the XCB. Subsequent coring yielded moderate recovery (average 20%) from soft diatomaceous mud and beds of phosphatic silt and sand. Dolomite and calcite layers were rare. Hole 684C was terminated at 115.0 mbsf when it became obvious that the lower part of the sediment column contained numerous hiatuses of various lengths. We considered such a discontinuous sediment record unsuitable for our stated scientific objectives.

## LITHOSTRATIGRAPHY

### Lithologic Units

The sediments recovered at Site 684 are divided into five lithologic units (Fig. 3 and Table 2) on the basis of visual core descriptions, smear-slide analysis, carbonate determinations (Fig. 4 and Table 3), and correlation with biostratigraphic data (see "Biostratigraphy" section, this chapter).

### Unit I

Cores 112-684A-1H through 112-684A-2H-6, 70 cm; depth, 0-13.5 mbsf; age, Quaternary (<0.9 Ma).

Cores 112-684B-1H through 112-684B-2H-3, 150 cm; depth, 0-12.0 mbsf; age, Quaternary (<0.9 Ma). First four cores of Hole 684C were not opened.

Lithologic Unit I is divided into two subunits (Fig. 3). Subunit IA consists of dark olive diatomaceous mud and extends from the surface to 8.7 mbsf in Hole 684A (Sample 112-684A-2H-3, 40 cm) and 7.5 m in Hole 684B (Section 112-684B-1H, CC). Subunit IB consists of two sand beds, each separated by laminated diatomaceous mud.

### Subunit IA

Subunit IA is characterized by dark olive, well-laminated diatomaceous mud and silty mud. Diatom content ranges from 15% to 40% and averages 30%. The 1-mm-thick, pale yellow laminae of nannofossil- and foraminifer-bearing diatomaceous oozes (10% foraminifers, 10% nannofossils, 65% diatoms) and of diatom-bearing nannofossil ooze (60% nannofossils, 15% diatoms) are common (Fig. 5). Gray layers are sandy foraminifer-nannofossil-diatom mud, which contained 20% foraminifers, 10% nannofossils, 25% diatoms, and 30% clay. Sandy interbeds contain foraminifers (35%), feldspar, quartz, and rock fragments (all together, 45%). Minor amounts of these terrigenous components are also dispersed throughout the diatomaceous mud. Glauconite is found in the silty and sandy interbeds, and contents of this mineral range from traces to 5%. Pyrite is common and mostly present as framboids that fill foraminifer or diatom tests. Fragments of bivalve shells are found occasionally. Near the base of the subunit, bioturbated sections and several sand layers can be found. In Hole 684B, interbeds of silty and sandy layers with normal bedding are more common than in Hole 684A. A single, 4-cm-diameter, rounded volcanic rock fragment, identified on board ship as porphyritic andesite, was present in Section 112-684B-1H-5.

Table 1. Coring summary for Site 684.

Core/ section	Date (Nov. 1986)	Time (Local)	Depth (mbsf)	Length cored (m)	Length recovered (m)	Recovery (%)
112-684A-1H	21	0453	0-5.3	5.3	5.31	100.0
2H	21	0510	5.3-14.8	9.5	9.92	104.0
3H	21	0540	14.8-24.3	9.5	9.90	104.0
4H	21	0610	24.3-33.8	9.5	9.74	102.0
5H	21	0630	33.8-43.3	9.5	9.56	100.0
6H	21	0645	43.3-52.8	9.5	8.19	86.2
7H	21	0725	52.8-62.3	9.5	9.20	96.8
8H	21	0800	62.3-69.6	7.3	7.28	99.7
9X	21	1030	69.6-79.1	9.5	2.26	23.8
10X	21	1120	79.1-88.6	9.5	0.20	2.1
11X	21	1200	88.6-98.1	9.5	0.05	0.5
12X	21	1240	98.1-107.6	9.5	0.20	2.1
13X	21	1315	107.6-117.1	9.5	0.30	3.2
14X	21	1400	117.1-126.6	9.5	0.20	2.1
15X	21	1440	126.6-136.1	9.5	0.19	2.0
112-684B-1H	21	1635	0-7.5	7.5	7.55	100.0
2H	21	1650	7.5-17.0	9.5	9.88	104.0
3H	21	1710	17.0-26.5	9.5	9.80	103.0
4H	21	1725	26.5-36.0	9.5	9.79	103.0
5H	21	1745	36.0-45.5	9.5	0.15	1.6
6X	21	1935	45.5-55.0	9.5	0.00	0.0
112-684C-1H	21	2120	0-7.8	7.8	7.87	101.0
2H	21	2145	7.8-17.3	9.5	9.88	104.0
3H	21	2210	17.3-26.8	9.5	9.77	103.0
4H	21	2235	26.8-36.3	9.5	9.78	103.0
5H	21	2305	36.3-39.0	2.7	2.70	100.0
6X	22	0030	39.0-48.5	9.5	2.02	21.2
7X	22	0110	48.5-58.0	9.5	3.64	38.3
8X	22	0205	58.0-67.5	9.5	2.73	28.7
9X	22	0300	67.5-77.0	9.5	1.12	11.8
10X	22	0400	77.0-86.5	9.5	0.60	6.3
11X	22	0500	86.5-96.0	9.5	2.31	24.3
12X	22	0550	96.0-105.5	9.5	2.15	22.6
13X	22	0630	105.5-115.0	9.5	1.66	17.5

H = hydraulic piston; X = extended-core barrel.

Carbonate content is relatively high (between 10% and 15%) in the first 4.5 m and decreases to 6% to 9% in the interval from 4.5 to 7.5 mbsf (Table 3).

#### Subunit IB

Subunit IB consists of two 1-m-thick sand beds that are separated by a laminated section of diatomaceous mud. The olive gray graded sands consist primarily of shell debris, foraminifers, and phosphorite grains, but also contain up to 30% lithogenic grains. A 2.3-m-thick layer of olive gray laminated diatomaceous mud occurs between the two sand beds. Anomalously high carbonate values of 33.4% and 59% reflect the high content of biogenic carbonate within these sand beds. Bone fragments and fish vertebrae are also present in these beds. Contacts with the underlying muds are sharp (Fig. 6). The interbedded diatomaceous mud contains numerous thin (1-cm-thick) graded beds made up of 15% foraminifers and 10% lithogenic grains. Black layers in this section are pyritic phosphatic sands that contain 35% lithogenic grains, 20% fish remains, 10% phosphatic peloids, and 20% pyritized grains (especially foraminifers), as well as glauconite and rock fragments.

#### Unit II

Cores 112-684A-2H-6, 70 cm, through 112-684A-3H-2, 150 cm; depth, 13.5-17.8 mbsf; age, late Pliocene.

Cores 112-684B-2H-4 through 112-684B-3H-1; depth, 12.0-17.0 mbsf; age, late Pliocene.

First four cores of Hole 684C were not opened.

In Hole 684A, Unit II consists of black, silty or sandy, homogeneous to mottled, bioturbated mud. Glauconite and phosphorite grains are common. Diatoms are absent or rare. Carbonate content is low and does not exceed 1% (Fig. 4 and Table 3). In Hole 684B, the black mud includes irregular layers of very

dark gray to black, medium to coarse phosphatic-glaucconitic sands. Large burrows filled with gray sand and sandy mud (Fig. 7) are conspicuous in the top 2 m of Unit II (Section 112-684B-2H-4, Fig. 7). These burrows are more than 40 cm long and 3 cm wide and possibly were produced by shrimplike *Callianassa*. Some of the burrows are filled with calcareous sandy mud, which contains 15% foraminifers, 15% terrigenous components, and 5% glauconite, as well as 10% brownish fine-grained material, possibly iron oxides or apatite(?). Burrows filled with phosphatic-glaucconitic sands can be found in the bottom part of lithologic Unit II (Section 112-684B-2H-7, Fig. 8). The middle part of Unit II is moderately bioturbated. Sandy material is present in irregular lenses, which presumably represent bioturbation structures.

#### Unit III

Cores 112-684A-3H-3 through 112-684A-5H-3; depth, 17.8-38.3 mbsf; age, Pliocene.

Cores 112-684B-3H-1 through 112-684B-4H; depth, 17.0-33.8 mbsf (base not reached); age, Pliocene.

Cores 112-684C-5H to 112-684C-6X, CC; depth, 36.3-41.0 mbsf; age, Pliocene.

(Cores 112-684C-1H through 112-684C-4H were not opened.)

Unit III is characterized by dark olive gray to black, homogeneous to mottled, bioturbated diatomaceous mud. Diatom content ranges from 5% to 40% and averages 20%. Black phosphatic-glaucconitic silts and sands are present as layers or blebs. Phosphorite and glauconite contents range from trace quantities to 65% (average 10%), with highest concentrations in the upper part of the unit. Pyrite framboids are present throughout the unit (trace to 10%), as well as foraminifers and nannofossils (trace to 30%, average 15%). These are rare in the uppermost meters of the unit and more abundant below 26 mbsf, resulting in the higher carbonate contents observed in the deeper part of the unit (Fig. 4). Large burrows, filled with olive-colored mud, are common in Hole 684A in Sections 112-684A-3H-7 to 112-684A-4H-2 and 112-684A-4H-5. In the lower part of this unit, the sediment is partly laminated. The first occurrence of an extensional fault was observed at Sample 112-684A-4H-5, 50-70 cm. Fluid-escape structures occur in Sections 112-684A-4H-2 and 112-684A-4H-4, while we observed thin mud veins in Section 112-684A-4H-6. A distinct layer containing dolomite fragments occurs in Sample 112-684A-5H-1, 100-120 cm (Fig. 9), but not in Hole 684B. The fragments have a hard center and a soft rim. Dolomitization probably took place preferentially within burrows. The cutting shoe was bent in Core 112-684B-5H, which indicates that the barrel hit a hard surface. This probably was the dolomite layer recovered in Section 112-684A-5H-1. We recovered hard fragments from Hole 684C at three zones: Samples 112-684C-5H, CC (0-8 cm), 112-684C-6X-1, 0-30 cm, and 112-684C-6X, CC (15-30 cm).

The transition between lithologic Units II to III is gradational (not present as a sharp break in lithology). Within an interval of about 7 m, the black, almost carbonate-free mud of Unit II changes to nannofossil- and foraminifer-bearing diatomaceous mud. The first common presence (about 20%) of diatoms was observed at the top of Unit III. Calcareous microfossils first become abundant several meters below this boundary.

#### Unit IV

Cores 112-684A-5H-4 to 112-684A-7H-1; depth, 38.3-54.3 mbsf; age, Pliocene.

Cores 112-684C-7X-1 to 112-684C-8X-1; depth, 41.3-59.5 mbsf; age, Pliocene.

Very dark gray or black, massive, diatom-bearing calcareous muds are characteristic of lithologic Unit IV in Hole 684A. Diatom contents range from 0% to 15% and average 5%. A shelly,



**Table 2. Lithologic Units of Site 684.**

Unit	Lithology	Core/section interval (cm)	Depth (mbsf)
I	Diatomaceous mud and sand	684A: 1H-1-2H-6, 70 684B: 1H-1-2H-3, CC 684C: first 4 cores not opened	0-13.5 0-12.0
IA	Diatomaceous mud, laminated	684A: 1H-1-2H-3, 40 684B: 1H-1-1H, CC	0-8.7 0-7.5
IB	Sand beds, interrupted by laminated diatomaceous mud	684A: 2H-3, 40-2H-6, 70 684B: 2H-1-2H-3	8.7-13.5 7.5-12.0
II	Black mud, calcareous	684A: 2H-6, 70-3H-2 684B: 2H-4-3H-1 684C: first 4 cores not opened	3.5-17.8 12.0-17.0
III	Diatomaceous mud, calcareous	684A: 3H-3-5H-3 684B: 3H-1-4H 684C: 5H-1-6X, CC	<sup>a</sup> 17.8-38.3 17.0-33.8 36.3-41.0
IV	Black mud, calcareous, phosphorite-rich, sandy	684A: 5H-4-7H-1 684C: 7X-2-8X-1	38.3-54.3 41.3-59.5
V	Diatomaceous mud, calcareous, laminated	684A: 7H-2-15X, CC 684C: 8X-1-13X, CC	54.3-136.1 59.5-115.0

<sup>a</sup> Base not reached.

150 cm, and 112-684C-7X, CC), yellow-brown mammalian bone fragments (Fig. 12) were found. Black 1-cm-thick phosphate nodules are present in Sections 112-684C-7X-1, 112-684C-7X-2, and 112-684C-8X-1.

The transition between lithologic Units III and IV is marked by a decrease in diatom content and an increase in coarse material containing high amounts of reworked phosphate nodules at Site 684C. Although Holes 684A and 684C are only about 10 m apart, lithologic Unit IV is a black sandy mud in Hole 684A, while this unit is a muddy glauconitic-phosphatic sand having a basal gravel layer in Hole 684C.

#### Unit V

Cores 112-684A-7H-2 to 112-684A-15X; depth, 54.3-136.1 mbsf; age, Miocene.

Cores 112-684C-8X-1 to 112-684C-13X; depth, 59.5-115.0 mbsf; age, Miocene.

Lithologic Unit V consists of olive gray to dark olive gray nannofossil- and/or foraminifer-bearing diatomaceous mud, locally laminated or mottled. Diatom content ranges from 5% to 50% and averages 30%. Nanofossils are common (20%) below about 61 m, whereas foraminifers are rare (3%). Carbonate contents show large differences throughout the unit, ranging from 0.25% at the top (dark olive, laminated diatomaceous mud) to 50% (thin laminae of nannofossil ooze) (Fig. 4). Lighter laminae are diatom or nannofossil oozes having up to 75% diatoms or nannofossils. Thickness of the laminae ranges from one to several millimeters. The diatomaceous ooze is typically dominated by the diatom species *Thalassiothrix longissima*, a cold water indicator. Minor lithologies are micritic calcite as infills of veins and sand-sized phosphorite grains. From Cores 112-684A-10X to 112-684A-15X in Hole 684A, core recovery was poor, and only the core-catcher samples contained sediment. Micritic limestone fragments were found in Sections 112-684A-10X, CC, 112-684A-12X, CC, and 112-684A-13X, CC. Section 112-684A-11X, CC contained one phosphate nodule, and Section 112-684A-15X, CC had one dolomite fragment. Vein structures are common in this unit. In the deeper part of Hole 684C (below Core 112-684C-11X), discontinuity surfaces, slump folds, small-scale truncations, and microfaults were observed.

The contact between lithologic Units IV and V was observed in Hole 684A. The lithology changes from black sandy mud to dark olive gray diatomaceous mud between Sections 112-684A-7H-1 and 112-684A-7H-2. Sections 112-684A-7H-2 and 112-684A-7H-3 contain large burrows filled with black phosphorite and glauconite sands (Fig. 10). The strongly bioturbated top

section of lithologic Unit V supports the suspected biostratigraphic hiatus between Units IV and V, where middle Miocene to early Pliocene strata are missing. Thus, the top of Unit V may be a hardground.

#### Diagenesis

The five lithologic units present at Site 684 alternate between those dominated by hemipelagic upwelling sediments (Subunit IA and Units III and V) and those that show the influence of current deposition (Subunit IB and Units II and IV). As discussed next in detail, we observed indications that authigenic carbonates and F-phosphates at Site 684 occur mainly in the hemipelagic upwelling units, while D-phosphates and glauconite are most abundant in the current-deposited, shallower water units.

#### Phosphate and Glauconite

*F-phosphates* (friable phosphates; see "Lithostratigraphy" section of the Site 680 chapter [this volume] for definitions) are comparatively rare at Site 684. They occur as small (1-3 cm), light-colored, friable nodules only in the diatom-rich, upwelling sediments of Subunit IA (Sample 112-684B-1H-4, 35 cm), Unit III (Sample 112-684A-4H-4, 137 cm), and Unit V (Sections 112-684A-7H-3, 112-684A-7H-4, and 112-684A-7H-5; see Fig. 11). F-phosphate nodules typically consist of 80% to 85% finely crystalline apatite and include small amounts of diatoms, foraminifers, and siliciclastic grains; they appear to record *in-situ* phosphatization of organic-rich muds (Burnett, 1977).

*D-phosphates* (dense phosphates) are much more abundant at Site 684 and occur as dark, hard, irregularly shaped nodules (Fig. 13), as well as sand-sized peloids and coated grains in gravels, sands, silts and, more rarely, also in muds. Commonly co-occurring grains in the gravels and sands are glauconite, foraminifers, and (in some beds) fragments of bone and bivalve shells. D-phosphates are present in all five lithologic units but are most abundant in Subunit IB and Units II and IV.

Most D-phosphate grains have dark, shiny exterior surfaces and some of the larger nodules have prominent cavities (Fig. 13) that result from boring organisms or dissolution or both processes. As seen in Figure 13, D-phosphate nodules are compound bodies formed by successive generations of apatite cementation; individual nodules thus record repeated episodes of phosphatization; the details warrant further study. We speculate that, as at Site 680, D-phosphate nodules evolved from F-nodules through repeated cycles of apatite precipitation, exhumation, reburial, and renewed apatite precipitation. However, we did not observe direct evidence for this cycle at Site 684.

For the most part, D-phosphate nodules and peloids occur in relatively well-sorted beds of silt, sand, or gravel that range from about 1 cm to more than 2 m thick. The thicker and coarser beds typically are graded (with D-nodules most abundant in the coarse basal part) and have scoured basal contacts above diatomaceous muds. In some instances, phosphatic and other granular material is piped down into the underlying muds along burrows (Figs. 8 and 10).

The phenomena noted above can be seen particularly well at the levels of the two major hiatuses at Site 684 (Fig. 14). The combination of textures and structures indicates (1) imposition of high-energy conditions and coarse-grained sedimentation on a low-energy environment where fine-grained muds accumulated and (2) increases in oxygenation at the seafloor that allowed colonization by large burrowing organisms.

In Figure 14, column C, note that below the contact between Units IV and V (which marks the major hiatus at this site), large burrows filled with phosphatic sand extend into the underlying diatomaceous mud. What is not shown in Figure 14 is that such burrows appear more than 2 m below the base of the phosphatic

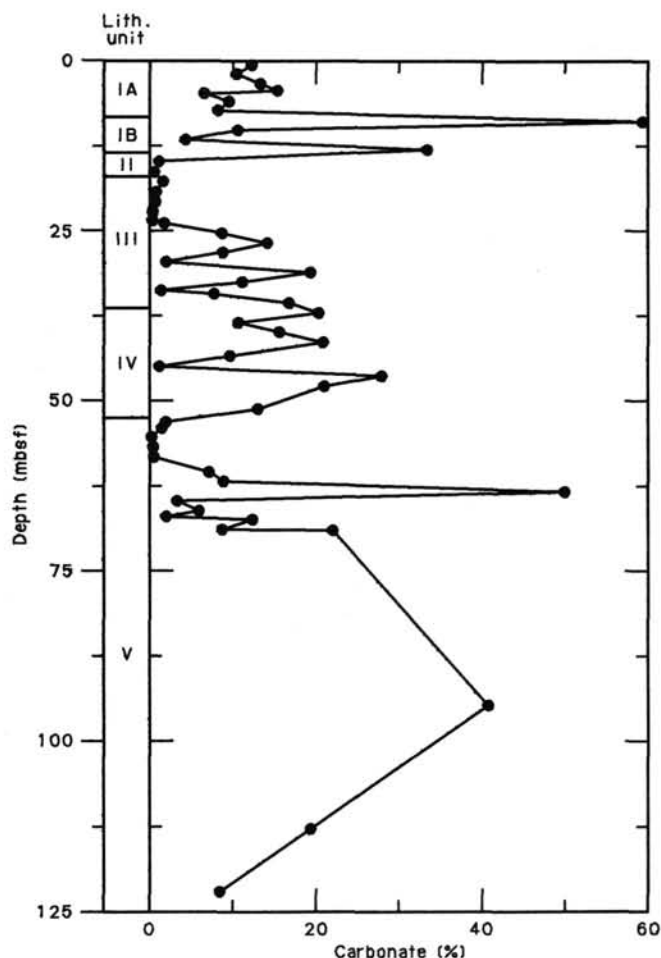


Figure 4. Carbonate contents at Hole 684A. Note extreme low values in lithologic Unit II (black mud), top sections of Unit III (Pliocene diatomaceous mud), and Unit V (Miocene diatomaceous mud). Also see Table 3 for downhole data.

sand layer, which itself is more than 2 m thick. Thus, if the burrowing had occurred *after* the deposition of this sand bed, the burrowing animals would have had to penetrate through more than 4 m of sediment. This appears unlikely, and we must conclude that the large burrow system in the top of lithologic Unit V formed during the long hiatus *before* deposition of the phosphatic sand. The size and extent of the burrow system suggests it can be assigned to the ichnogenus *Thalassinoides*. *Thalassinoides* is commonly associated in the Upper Cretaceous chalks of western Europe with hiatuses that are marked by omission surfaces, firmgrounds, or carbonate hardgrounds (Ekdale et al., 1984).

Burrowing within the thicker phosphatic beds apparently disrupted and destroyed all primary structures except size grading. Therefore, we were unable to determine what mechanism or mechanisms were responsible for their deposition, although we surmised that such deposition occurred under high-energy conditions at comparatively shallow depths. Possible mechanisms for emplacement of thick phosphate beds, such as those illustrated in Figure 14, include wind- or tide-forced currents, storm-generated turbidity currents, or intruding ocean currents (Walker, 1984).

#### Phosphatic-Glauconitic Sands and Silts

Phosphatic-glauconitic or glauconitic sand and silt layers, generally a few centimeters or less in thickness and containing abundant reworked foraminifer tests, occur in all five lithologic

Table 3. Summary of carbonate contents at Site 684.

Core/section interval (cm)	Depth (mbsf)	CaCO <sub>3</sub> (%)
112-684A-1H-1, 40-42	0.40	12.18
1H-2, 40-42	1.90	10.51
1H-3, 40-41	3.40	13.34
1H-3, 135-136	4.35	15.26
1H-4, 40-42	4.90	6.59
2H-1, 66-67	5.96	9.59
2H-2, 66-67	7.46	8.26
2H-3, 66-67	8.96	59.05
2H-4, 66-67	10.46	10.59
2H-5, 66-67	11.96	4.34
2H-6, 66-67	13.46	33.36
3H-1, 66-67	15.46	1.08
3H-2, 66-67	16.96	0.58
3H-3, 66-67	18.46	1.58
3H-4, 66-67	19.96	0.75
3H-5, 66-67	21.46	0.58
3H-6, 66-67	22.96	0.33
3H-7, 66-67	24.46	0.33
4H-1, 50-51	24.80	1.75
4H-2, 50-51	26.30	8.76
4H-3, 50-51	27.80	14.09
4H-4, 50-51	29.30	8.84
4H-5, 50-51	30.80	2.00
4H-6, 50-51	32.30	19.27
4H-7, 50-51	33.80	11.18
5H-1, 120-121	35.00	1.33
5H-2, 20-21	35.50	7.84
5H-3, 20-21	37.00	16.68
5H-4, 20-21	38.50	20.27
5H-5, 20-21	40.00	10.68
5H-6, 20-21	41.50	15.51
5H-7, 20-21	43.00	20.77
6H-2, 28-29	45.08	9.76
6H-3, 28-29	46.58	1.17
6H-4, 28-29	48.08	27.86
6H-5, 28-29	49.58	20.93
7H-1, 30-31	53.10	13.01
7H-2, 90-91	55.20	1.92
7H-3, 30-31	56.10	1.42
7H-4, 30-31	57.60	0.25
7H-5, 30-31	59.10	0.50
7H-6, 30-31	60.60	0.50
8H-1, 41-42	62.71	7.17
8H-2, 41-42	64.21	8.92
8H-3, 41-42	65.71	49.96
8H-4, 41-42	67.21	3.34
8H-5, 41-42	68.71	6.00
8H,CC, 15-16	69.63	2.00
9X-1, 40-41	70.00	12.34
9X-2, 40-41	71.50	8.76
9X,CC, 10-11	71.74	22.02
12X,CC, 17-18	98.27	40.87
14X,CC, 4-5	117.14	19.35
15X,CC, 7-8	126.67	8.42

units; they are particularly common in lithologic Unit II, where some layers have up to 60% glauconite peloids (e.g., Sample 112-684A-3H-2, 51 cm). These layers are commonly interlayered with diatomaceous muds that contain dispersed glauconite and/or phosphate peloids. In Unit II some of these muds have 15% to 40% of dispersed, very small apatite crystals, suggesting *in-situ* precipitation (e.g., Sample 112-684B-2H-5, 31 cm). Examination of concentrations of glauconite peloids from Sections 112-684A-2H, CC, 112-684A-684-7H, CC, and 112-684C-7X, CC showed that most peloids are the internal casts of foraminifer shells (in some instances, glauconite has also replaced the shell wall). Thus, foraminifer chambers appear to be favored sites for the formation of glauconite.

We interpreted these types of thin sandy and silty beds as products of moderate, short-lived winnowing of diatomaceous muds in which peloids of glauconite and phosphate had formed, commonly within the reduced or slightly reduced microenvironments provided by foraminifer tests.

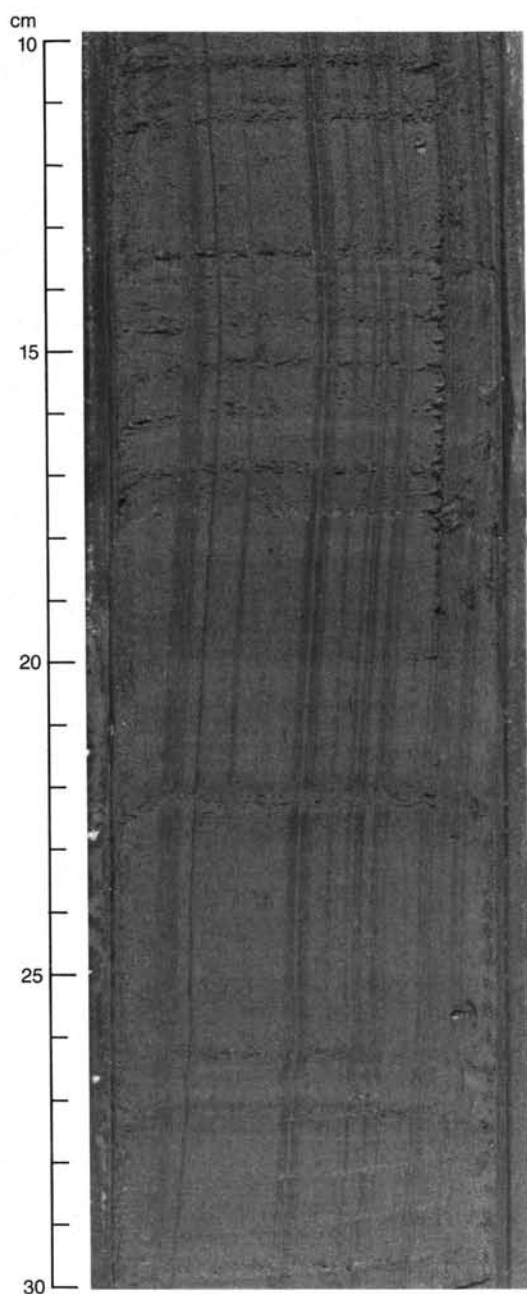


Figure 5. Example of well-laminated diatomaceous mud of lithologic Unit I. Gray layers are enriched in clay, and light olive green layers are diatomaceous oozes (112-684A-1H-2, 10–30 cm).

The phosphatic-glaucinitic beds of lithologic Unit II and the basal part of lithologic Unit IV are condensed sequences associated with major hiatuses (Fig. 14). In simplified form, we suggest that several principal stages in the genesis of these sequences occur, following the general scheme first outlined by Baturin (1971). These are (1) formation of phosphate and/or glauconite peloids or nodules (F-phosphate nodules) in suboxic to anoxic pore waters of diatomaceous muds, perhaps during periods of upwelling, high fertility, and high stands of sea level; and (2) winnowing of fines as a consequence of high-energy events or a series of such events (e.g., large storms), probably during intervals of low sea-level stands. The actual course of events was undoubtedly much more complex; large D-phosphate nodules, for example, must have experienced repeated cycles of this kind, so that thick

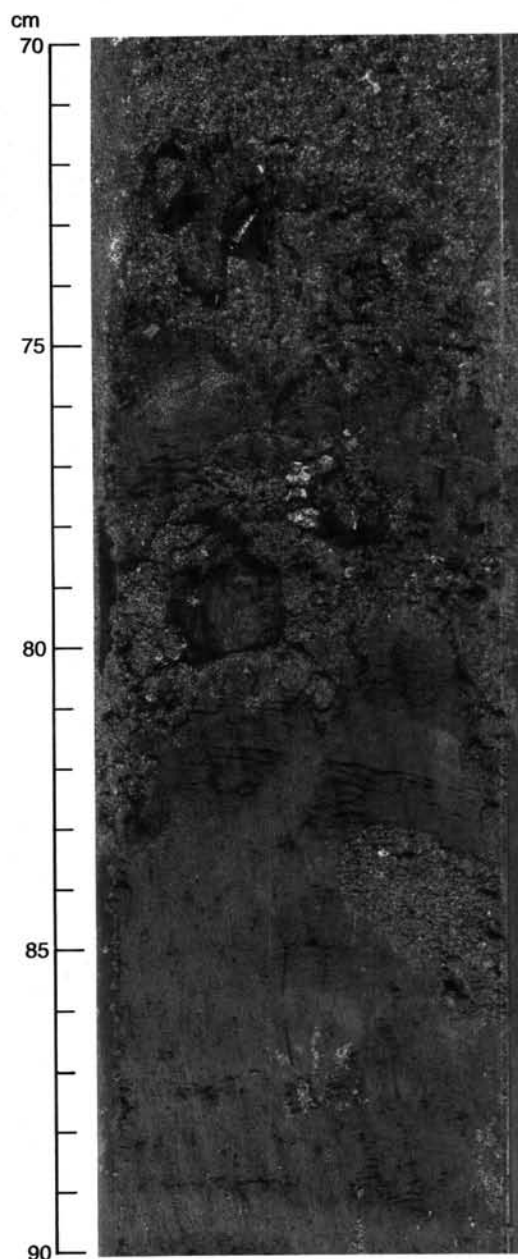


Figure 6. Contact between Subunit IB and Unit 2 (Sample 112-684A-2H-6, 70–90 cm). The bottom part of Subunit IB is the coarse basal portion of a thick graded bed containing D-phosphate nodules and peloids, glauconite, fragments of bones, and bivalve shells. A sharp, erosional contact separates this bed from underlying burrowed muds of Unit II. See Figure 14 for other views of this contact.

beds containing such nodules (Fig. 14) may represent the winnowing and erosion of tens of meters of organic-rich mud (which may in turn be redeposited in secondary upwelling lenses downslope). In this regard, we find it significant that the two major hiatuses marked by condensed phosphatic sequences at Site 684 (Fig. 14) appear to correlate with eustatic low stands of sea level.

#### *Authigenic Carbonates*

Both authigenic calcite and dolomite are present in the sediments at Site 684 as disseminated crystals in unlithified muds and as fully lithified nodules and beds. These sediments are most abundant in Subunit IA and Units III and V, which are

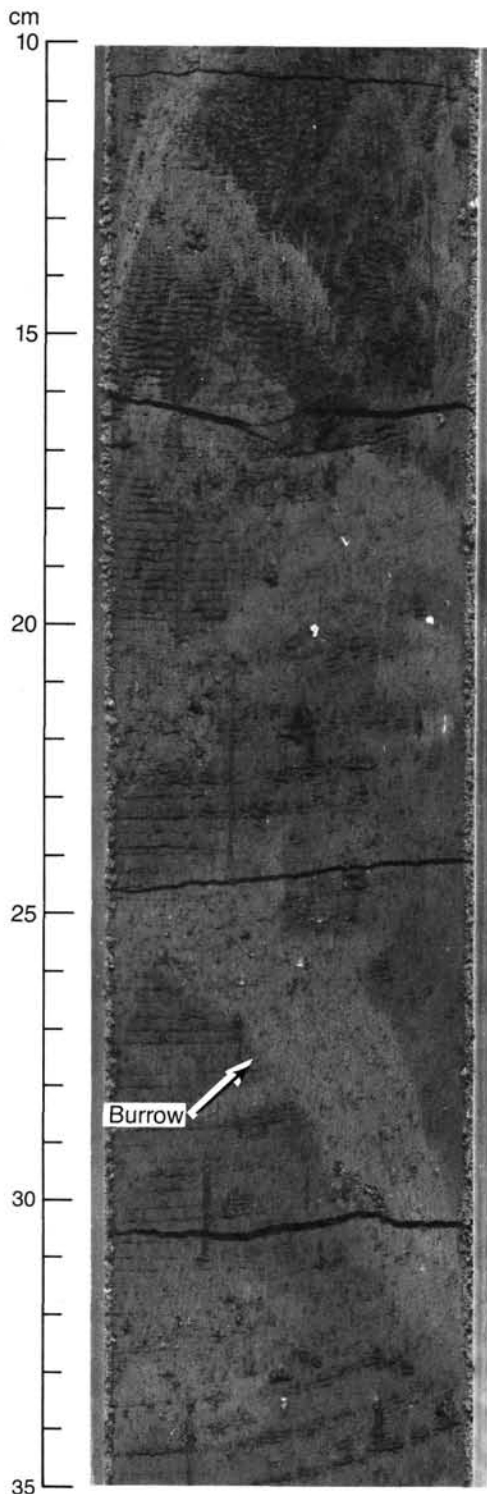


Figure 7. Top section of Unit II in Hole 684B (Sample 112-684B-2H-4, 10–35 cm). Large burrows filled with gray calcareous sandy mud.

mainly diatomaceous muds. Lithologic Unit I and the upper part of lithologic Unit II contain a few unlithified layers with 5% to 85% of authigenic calcite; this interval coincides with a zone in which the calcium content of pore waters decreases and the  $Mg^{2+}/Ca^{2+}$  ratio increases (see “Inorganic Geochemistry” section, this chapter).

Lithologic Unit III contains both dolomite and authigenic calcite. The first lithified carbonate encountered at Site 684 is a

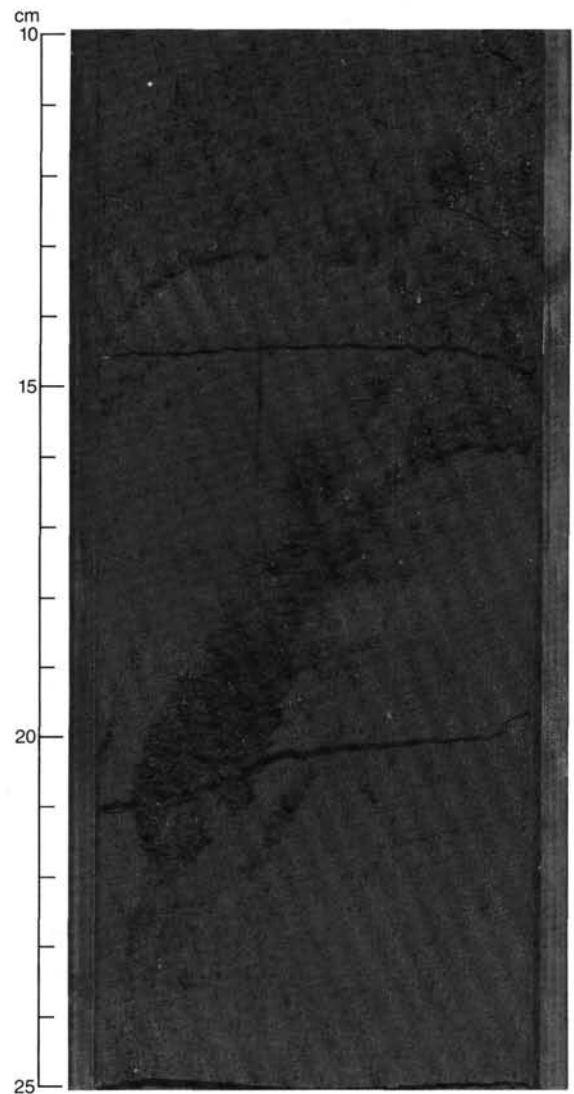


Figure 8. Large burrows filled with black sand (bottom part of Unit II) (Sample 112-684B-2H-7, 10–25 cm).

small calcite nodule in diatomaceous mud at a depth of about 31 mbsf (Sample 112-684C-4H-4, 32 cm). The first lithified dolomite is a 24-cm-thick bed that occurs in diatomaceous mud at a depth of approximately 35 mbsf (Sample 112-684A-5H-1, 98–122 cm). Nearby, unlithified beds in the same core contain 10% to 20% anhedral authigenic calcite crystals (along with 10% to 20% foraminifers and nannofossils), demonstrating a close spatial juxtaposition of the two authigenic carbonate phases. However, these phases may have formed at distinctly different times. Near the base of lithologic Unit III, Core 112-684C-6X contains two calcite-cemented sandstone beds (Figs. 15 and 16). Hole 684B was terminated by a bent core barrel, which was probably caused by a lithified carbonate bed at the base of Unit III.

Lithologic Unit IV yielded a single small piece of brown dolomite. It is significant that this dolomite occurs in a sandy phosphatic-glaucanitic bed just above the hiatus separating Units IV and V (Fig. 14), and thus it is almost certainly reworked.

The most abundant lithified carbonates at Site 684 were encountered in lithologic Unit V, where roughly equal amounts of limestone and dolomite were recovered in Holes 684A and 684C. Small pieces of micritic limestone or calcite-cemented siltstone were recovered in Cores 112-684A-7H, 112-684A-8H, 112-684A-

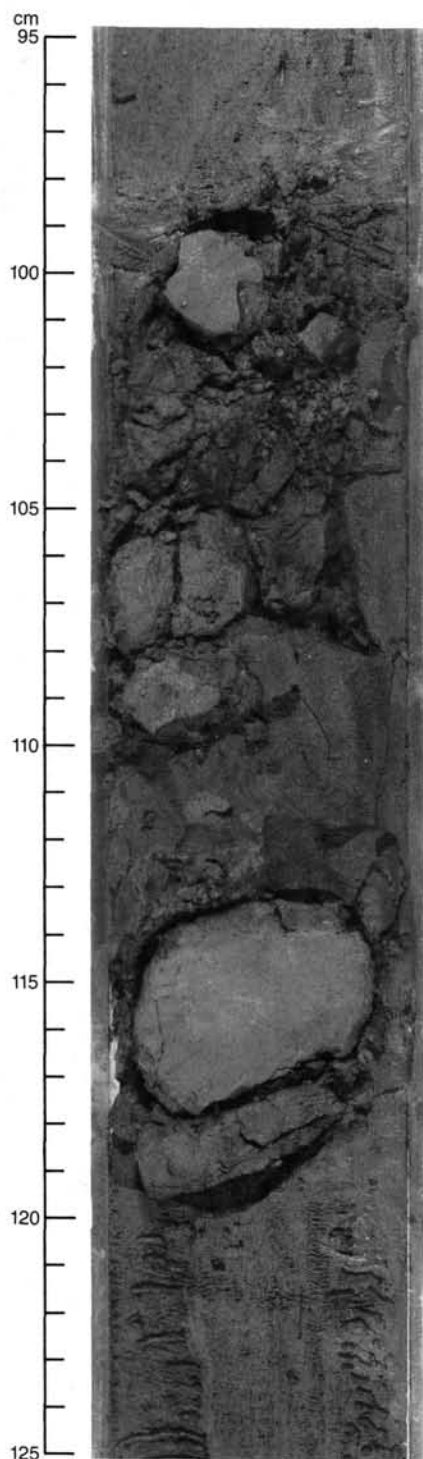


Figure 9. Dolomite layers near the base of lithologic Unit II (Sample 112-684A-5H-1, 95-125 cm). Along with other distinct breaks in lithology, these layers were used to correlate between Holes 684A and 684B.

10X, and 112-684A-12X. Fine-grained dolomite fragments were recovered in Cores 112-684A-13X, 112-684A-15X, 112-684C-9X, and 112-684C-10X. Dolomites in the latter two cores have small fractures filled with white calcite veins. Section 112-684A-13X, CC contains a particularly interesting and complexly fractured dolomite (Fig. 17). Most of this rock consists of a hard, dolomitized foraminifer mud in which dolomitized foraminifer shells

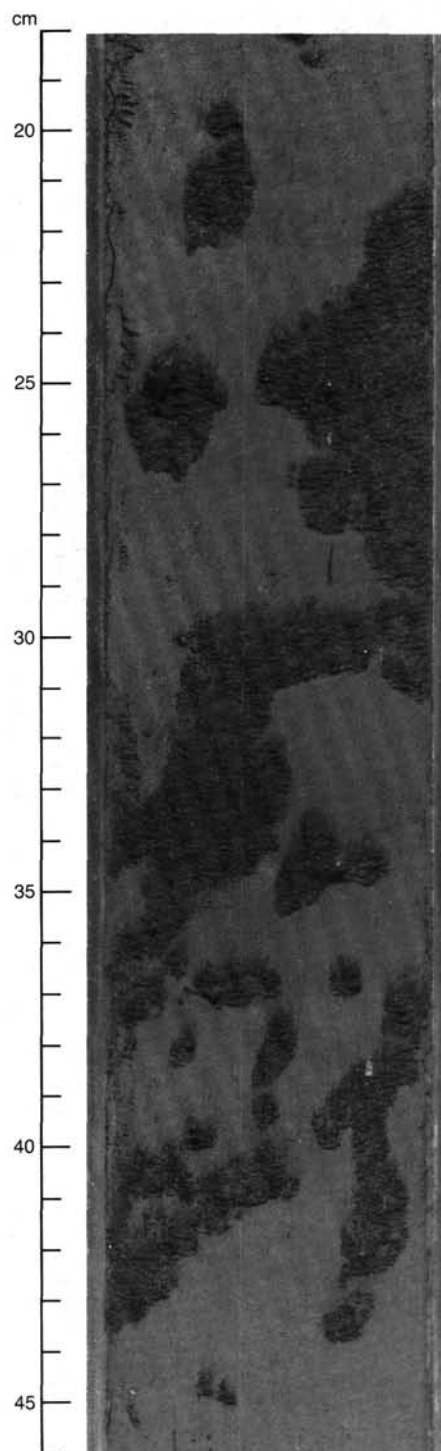


Figure 10. Near the contact between lithologic Units IV and V, burrows filled with black phosphorite sand of Unit IV extend to 2 m below top of Unit V (Sample 112-684A-7H-2, 18-46 cm).

are prominent. This dolomite is traversed by numerous fractures, most of which are parallel or subparallel to bedding. A variety of internally deposited or injected sediments and precipitated cements, including the prominent sparry dolomite visible in Figure 17, fills these fractures. Several generations of cement can be discerned, and some of these cements are in turn fractured and recemented by later generations of carbonates. This

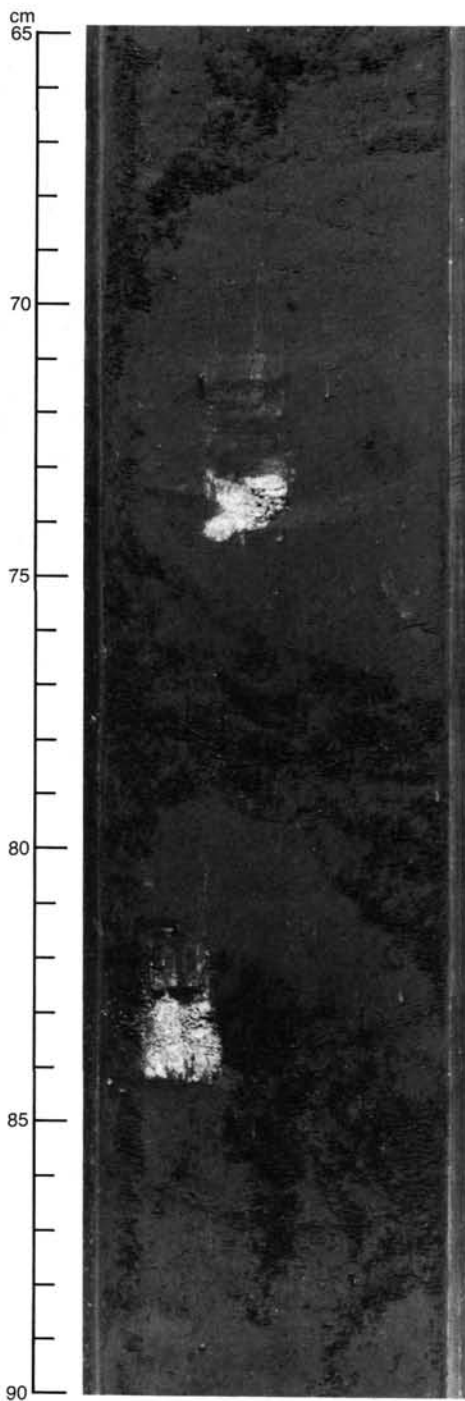


Figure 11. The two light-colored patches are F-phosphate nodules in diatomaceous mud of lithologic Unit V (Sample 112-684A-7H-3, 65–90 cm). Dark granular material is phosphatic-glaucanitic sand in thin layers and burrows.

single specimen thus contains evidence for repeated episodes of fracturing and cementation, which perhaps are a consequence of persistent tectonism at Site 684 since the late Miocene.

The authigenic carbonates in lithologic Units III and V occur within a zone of increasing calcium and magnesium and decreasing  $Mg^{2+}/Ca^{2+}$  ratios in pore waters that contain essentially no sulfate (see “Inorganic Geochemistry” section, this chapter). Dolomite should be the stable phase under these circumstances, and the co-occurrence of dolomite and calcite may

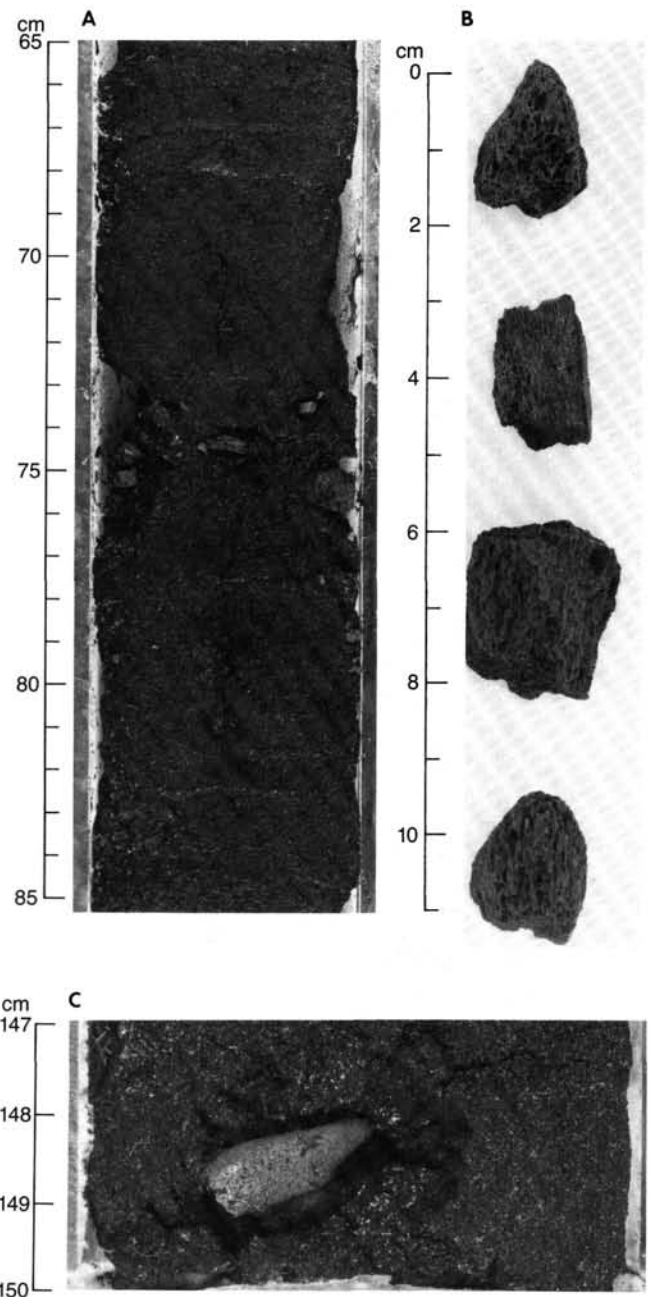


Figure 12. A) Black, phosphoritic-glaucanitic muddy sand of lithologic Unit IV (Sample 112-684C-7X-1, 65–85 cm) with mammalian bone fragments. B) Close-up of bones from Sample 112-684C-7X-1, 73–76 cm. C) Phosphoritic-glaucanitic muddy sand with bone fragment (Sample 112-684C-7X-1, 147–150 cm).

indicate that authigenic calcite formed first but was not fully replaced by later dolomitization. This hypothesis is supported by the trends of calcium and magnesium abundances with depth, which suggest that dolomite forms at Site 684 by precipitation rather than by replacement of preexisting calcite (see “Inorganic Geochemistry” section, this chapter).

#### **Barite**

Authigenic barite was observed at two places in the sediment column at Site 684. The shallowest occurrence is a small, discontinuous vein filled by finely crystalline barite in lithologic Unit III at a depth of about 31 mbsf (Sample 112-684B-4H-6,



Figure 13. Phosphate nodule with holes of boring organisms (bivalves?) (Sample 112-684A-11X, CC [0-4 cm]).

35-41 cm; see Fig. 18). The other occurrence was observed at about 49 mbsf in Unit IV. Here, a phosphatic-glaucanitic mud and sandy silt contains 10% to 35% of coarse barite crystals, some of which form rosettes (Sample 112-684A-6H-4, 81-82 cm; see Fig. 19 for an X-ray diffractogram of this sample).

### Environments of Deposition

Lithologic Subunit IA represents Quaternary coastal upwelling sediments similar to the "calcareous mud facies" described by Kulm et al. (1984). Laminated diatomaceous mud sections probably were deposited during high sea-level stands (interglacial). We assume that the coarse beds of Subunit IB represent periods of stronger current flow and that they were deposited during low sea-level stands (glacial). We remain uncertain whether the coarsely graded beds represent single high-energy events or whether they are steadily deposited during the periods of increasing water depth of deglaciation.

Lithologic Unit II is believed to have been deposited at relatively shallow water depths outside the coastal upwelling plume. The diatoms that indicate upwelling are absent. Current activity is indicated by the 1-cm-thick sandy layers that are common in the middle part of the unit. The hiatus between Units II and I, indicated from the biostratigraphic data (see "Biostratigraphy" section, this chapter) is also marked by a lithological break in the form of an erosional contact between Unit II and the overlying sand bed of Subunit IB (Fig. 6 and Fig. 20). Deep burrows in the black muds of Unit II just below the contact are filled with sandy, shelly material derived from Subunit IB. Furthermore, wood and bone fragments and fish remains found in the 20-cm-thick transition zone between Lithologic Units II and I (Sample 112-684A-2H-6, 70-90 cm, Fig. 6) indicate erosion after deposition of Unit II.

Lithologic Unit III contains sediments similar to those of Unit I, although diatom content might be slightly lower. Glaucanites and phosphorites are more common in Unit III than in Unit I, and the sediment is more bioturbated. Laminated sections occur only in the lower part of Unit III. We suggest that Unit III also represents upwelling sediments of the "calcareous mud facies," but that the sedimentation rate may have been lower during the Pliocene, as compared to the Quaternary Unit

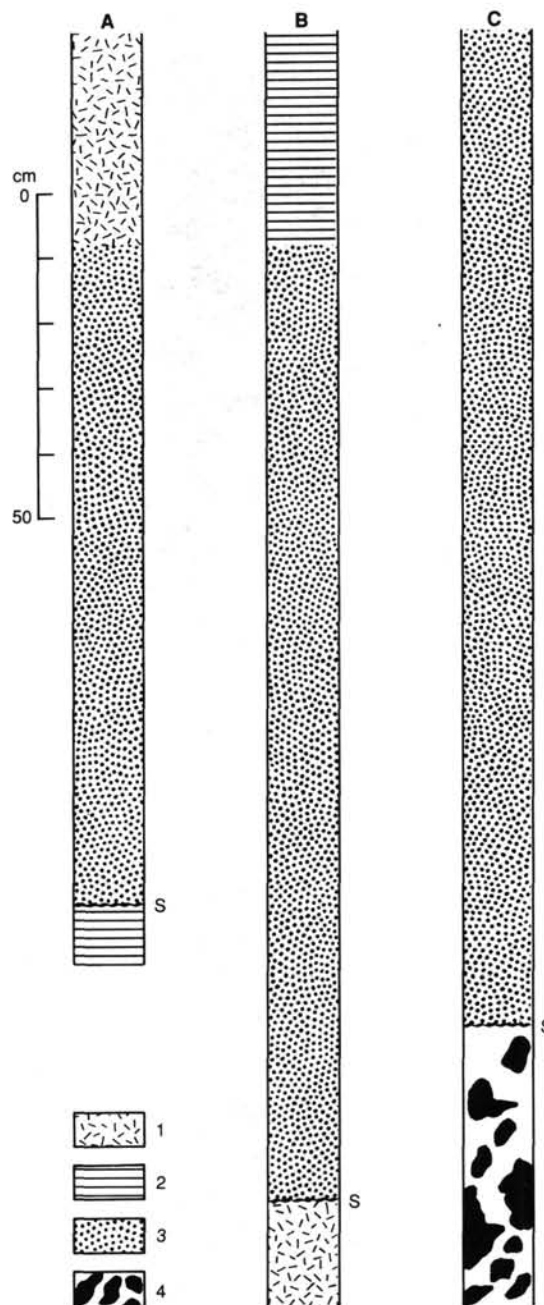


Figure 14. Selected examples of graded phosphatic beds traced from core photographs. Symbols are 1 = burrowed diatomaceous mud, 2 = laminated diatomaceous mud, 3 = phosphatic silty sand, 4 = large burrows filled with phosphatic sand, and S = scoured erosional surface. A) Section 112-648A-2H-3, the graded bed contains abundant shell debris, foraminifer tests, and phosphatic grains; Subunit IB. B) Sections 112-684A-2H-5 and 112-684A-2H-6; a single, thick graded bed that contains shell debris, foraminifer tests, and peloids and nodules of D-phosphates, along with scattered bone fragments. The scoured basal contact of this bed separates Subunit IB from Unit II (see also Fig. 6) and marks the unconformable surface between Pliocene and upper Quaternary sediments. C) Sections 112-684A-7H-1 and 112-684A-7H-2; the scoured basal contact of the thick phosphatic-glaucanitic bed marks an unconformity that separates coarse Pliocene sediments of Unit IV from the underlying Miocene diatomaceous muds of Unit V. The unconformity is marked by a network of large burrows that are filled with Pliocene phosphatic sandy silt to a depth of more than 2 m below the contact.

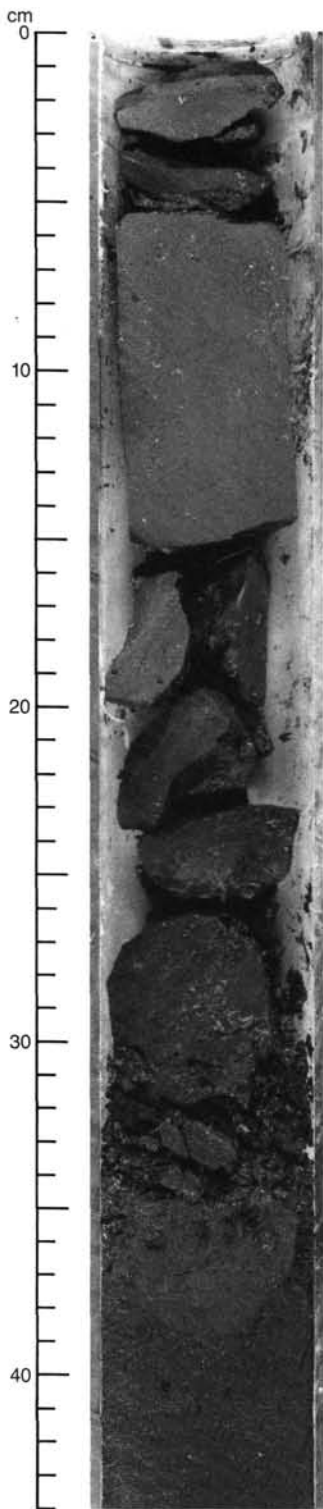


Figure 15. Bed of calcite-cemented glauconitic silty sand, Unit III (Sample 112-684C-6X-1, 0-44 cm).

I, owing to winnowing by bottom currents. This is suggested from the common presence of phosphorites (indication of reworking) and from the more bioturbated (more oxygenated bottom water) sediments.

We suggest that lithologic Unit IV was deposited in relatively shallow water in a nonupwelling area similar to the depositional environment of Unit II. Diatoms are more common in Unit IV

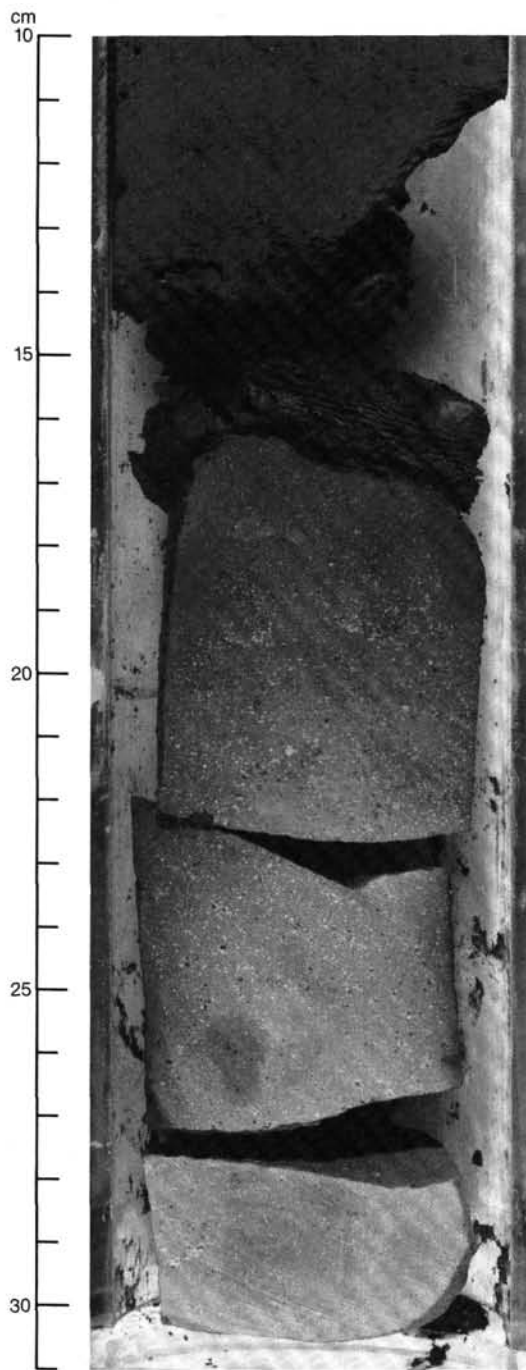


Figure 16. Bed of calcite-cemented sandstone, Unit III (Sample 112-684C-6X, CC [10-31 cm]).

than in Unit II, but the content is much lower than in the diatomaceous muds of Units I, III, and V. One indication of shallow water depths is the presence of coarse, black phosphorite sands, especially in Hole 684C. Although the holes were only meters apart, sediments in Hole 684C were generally much coarser. Instead of the muds, muddy silts, and sandy muds in Hole 684A, the sediments are muddy sands, sands, or gravels in Hole 684C, which possibly represent a filled channel. Seismic records (see "Geophysics" section, this chapter) show that Site 684 is located within a small basinlike structure. It is possible that the main seismic reflector is the eroded top of the Miocene (Unit V) and that the Pliocene and Quaternary sediments at Site 684 rep-

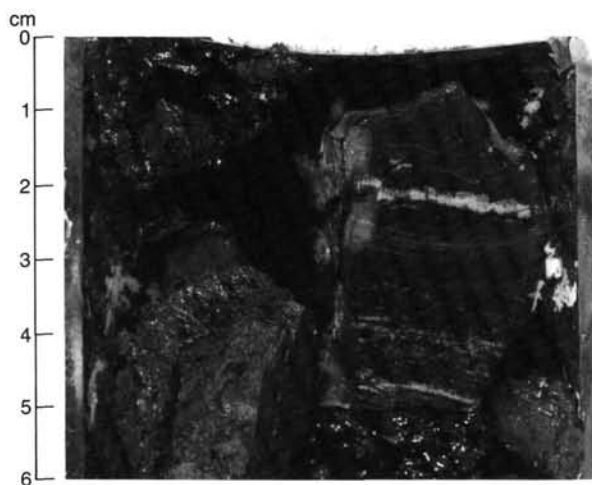


Figure 17. Dolomite fragment having numerous bedding-parallel fractures that are partly filled by coarse white dolomite. Some of this void-filling dolomite has itself been fractured (lower part of the rock). See text for discussion (Sample 112-684A-13X, CC [0-6 cm]).

resent infilling of the structural depression. Further indication of transportation of sediments is the presence of numerous bone fragments found in these sands.

The recovered Pliocene sections (Units II, III, and IV) represent possibly one cycle of a change in sea level from shallower water (Unit IV) to deeper water (deposition of diatomaceous mud, Unit III) then again to shallower water during deposition of sediments of Unit II. The boundaries with the overlying Quaternary sand beds and diatomaceous muds and with the underlying Miocene diatomaceous mud are marked by hiatuses. These hiatuses may represent low sea-level stands during the late Miocene and the late Pliocene, respectively (Hsü et al., 1977; Haq et al., 1987).

Like Units I and III, Unit V is a typical upwelling sediment of the "calcareous mud facies." Diatom and nannofossil contents are higher than in Unit III. This may indicate differences in productivity or preservation, e.g., shift of the upwelling cell or winnowing by bottom currents.

### BIOSTRATIGRAPHY

Diatoms and radiolarians were rare to abundant in all three holes drilled at Site 684. Their preservation was generally excellent, except in those intervals that were characterized by organic-rich pyritic muds.

Calcareous nannoplankton and foraminifers occurred sporadically, even though frequent thin layers of calcareous nannoplankton blooms occurred in the dominant diatomaceous muds of Miocene age.

Two major hiatuses were revealed by diatom, silicoflagellate, calcareous nannoplankton, and radiolarian biostratigraphy (H-1 and H-2 in Figs. 20 and 21). Based on diatom and calcareous nannoplankton stratigraphy, hiatus H-1 occurred between Cores 112-684C-1H and 112-684C-2H, whereas based on radiolarian stratigraphy, this hiatus is placed between Cores 112-684C-2H and 112-684C-3H.

Sedimentation rates for the Quaternary are about 20 m/m.y.; for the Pliocene, around 30 m/m.y.; and for the late Miocene, around 50 m/m.y. The oldest sediments at 136.1 mbsf are of late Miocene to latest middle Miocene age. These sedimentation rates are minimum values as only one zone was found for each of the three intervals.

Warm-water floras (diatoms) and faunas (planktonic foraminifers) were found in the *Thalassionema nitzschioides* bloom

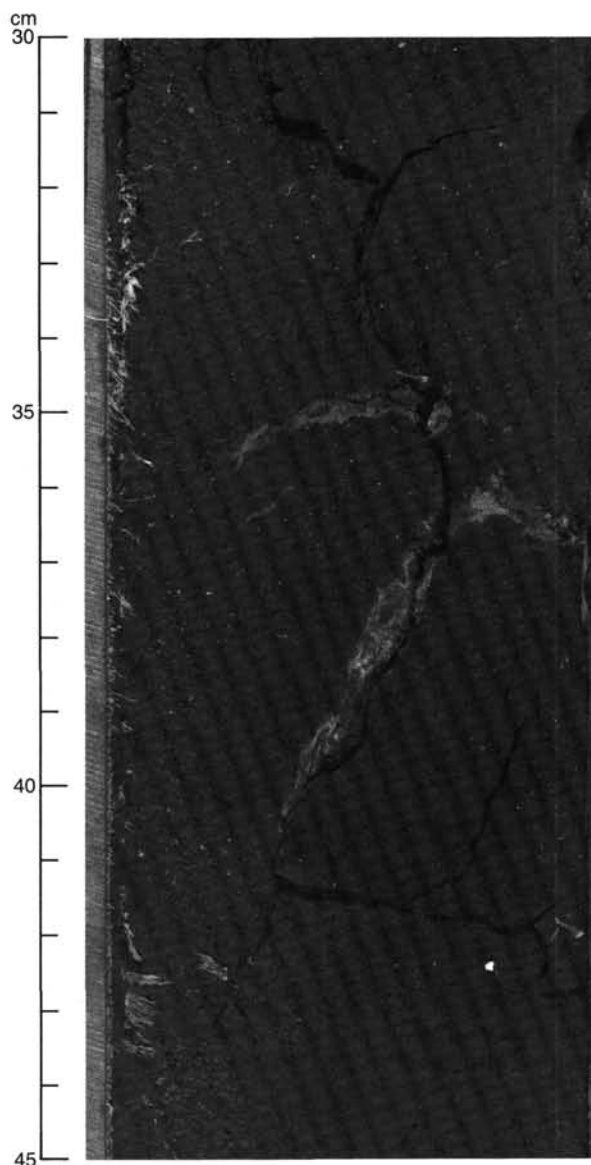


Figure 18. Irregular vein of finely crystalline barite (Sample 112-684B-4H-6, 30-45 cm).

zones. These blooms seem to be a Pacific-wide phenomenon during the late Miocene. Intercalated in these blooms are those of the cold-water *Thalassiothrix longissima*, indicating highly fluctuating surface-water temperatures. The presence of calcareous nannoplankton indicates sedimentation in a "nearshore" and "shallow-water" environment in the Miocene.

Benthic foraminifers are characteristic of upper bathyal or upper middle bathyal water depth and low-oxygen, bottom-water conditions during the Quaternary and late Miocene at Site 684.

### Diatoms

Diatoms were abundant and well preserved in most core-catcher samples studied from the three holes drilled; preservation was moderate to poor in the intervals with pyrite-rich organic muds. In these intervals, large, heavy diatom frustules are enriched, and floral composition is oceanic with a temperate to warm character. This phenomenon might be caused by selective winnowing of the normally light and delicate "upwelling" diatom frustules. The poor to moderate preservation of siliceous shells indicates prolonged exposure to corrosive bottom waters;

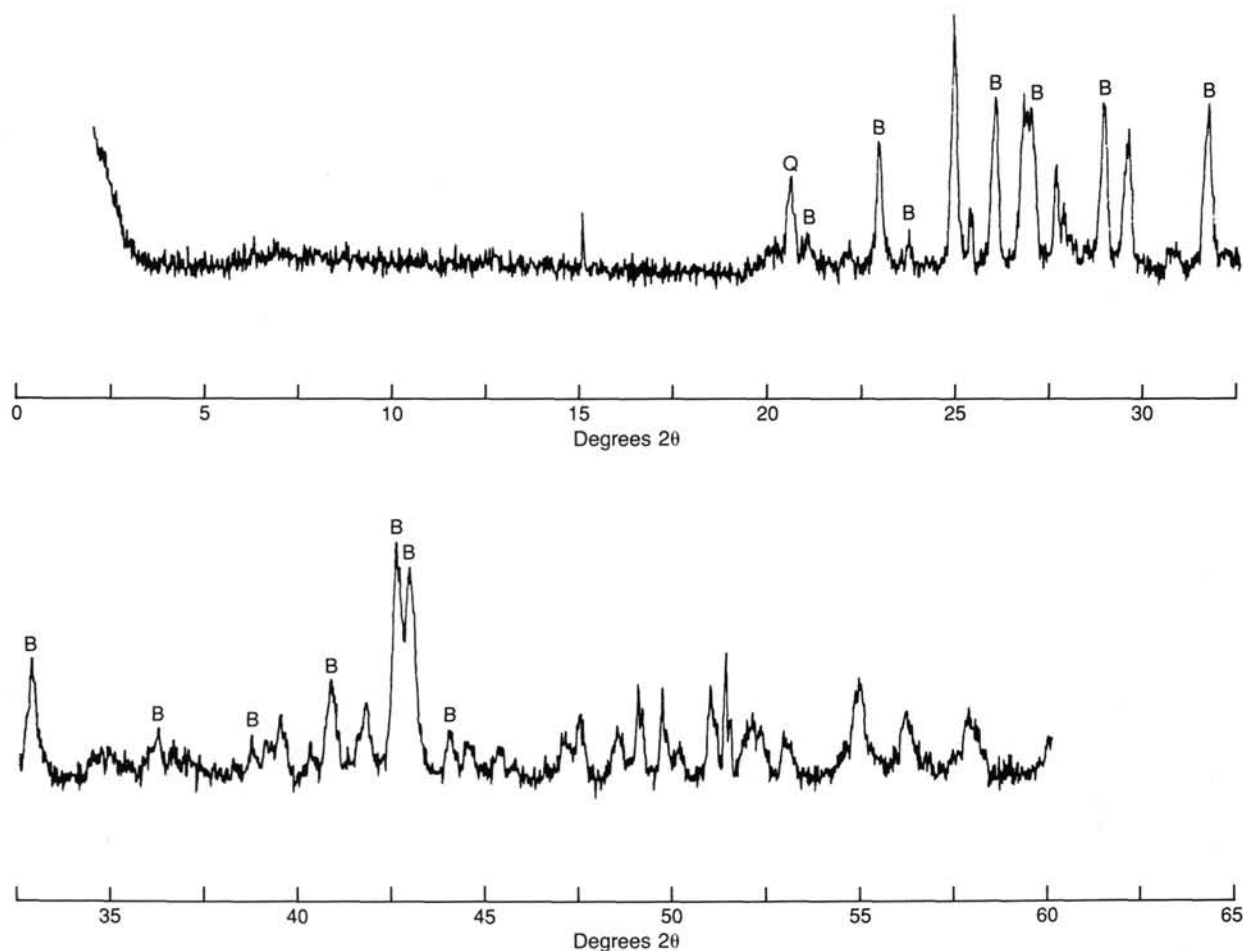


Figure 19. X-ray diffractogram of barite (Sample 112-684A-6H-4, 80 cm). Peaks marked are B = barite and Q = quartz.

the organic matter occurs in larger amorphous clumps and may well withstand winnowing. The high organic-carbon contents of these muds may not be the result of increased bioproduction, but rather winnowing of bottom currents in a coastal upwelling system having low-oxygen bottom waters. The water depth at Site 684 is just below today's poleward-flowing undercurrent (low-accumulation vs. the high-accumulation model of organic-matter-rich deposits).

Two hiatuses, H-1 and H-2, were found at Site 684 (Fig. 21). H-1 occurs at 15 mbsf in Hole 684A and at 17 mbsf in Hole 684B. In Hole 684C, it occurs at 17.5 mbsf in Core 112-684C-2H (note that only core-catcher samples were studied). This hiatus separates the Quaternary from the Pliocene and produces a gap in sedimentation of around 2 m.y. Sediments younger than the *Rhizosolenia matuyama* range (as defined at Site 683) occur at this site.

H-2 occurs at 51.0 mbsf in Section 112-684A-6H, CC and at 51.8 mbsf in Section 112-684C-7X, CC, and separates the Pliocene from the Miocene. This hiatus represents a gap in time of more than 2.4 m.y. All of the lower Pliocene and some of the upper Miocene deposits are missing.

Floods of *Thalassionema nitzschioides*, interlayered with floods of *Thalassiothrix longissima*, were observed in Sections 112-684A-9C, CC (71.6 mbsf) through 112-684A-14X, CC, the deepest sample available. The same assemblage association occurred at Hole 684C in Sections 112-684C-8X, CC through 112-684C-12X, CC (60.4–97.9 mbsf). Pacific-wide floods of *Thalassionema nitzschioides* were reported by several authors. Barron (1985) dated

this event in the equatorial Pacific (DSDP Leg 85, Sites 574 and 572) to occur at the *Coscinodiscus yabei* and *Actinocyclus moronensis* Zones. Maximum abundances were observed in the equatorial Pacific between 11.2 to 11.0 Ma (after adjusting to the time scale used on ODP Leg 112, 8.8 to 8.7 Ma). Because these floods at Site 684 occur stratigraphically within the same time interval, namely the *Coscinodiscus yabei* Zone, implications are that a Pacific-wide circulation must have existed that permitted migration of large populations across biogeographic belts. This is not possible today because of the strong isolation of the belts by the Equatorial Pacific Current system. *Thalassionema nitzschioides* is a cosmopolitan species that is well adapted to large temperature and salinity variations. In the "needle" zone, about 20% of the total diatom population consists of *Thalassionema nitzschioides* var. *parva*, which is a warm-water indicator. Today, this species preferentially thrives in the equatorial belts of the world oceans. Since the diatom population at Site 684 consisted of a large proportion of this species, warm surface-water conditions must have prevailed during deposition of this zone (60.4–97.9 mbsf). *Thalassiothrix longissima* is a true cold-water indicator and occurs in similarly high abundances in today's North Pacific. This species was found in several zones interlayered with the *T. nitzschioides* Zone and was most abundant in Section 112-684A-11X, CC (88.6 mbsf). The surface-water nutrient supply must have been high during both cold and warm phases to accumulate these deposits.

The co-occurrence of *Thalassionema convexa* var. *convexa* with *Nitzschia jousea* in Sections 112-684A-2H, CC through

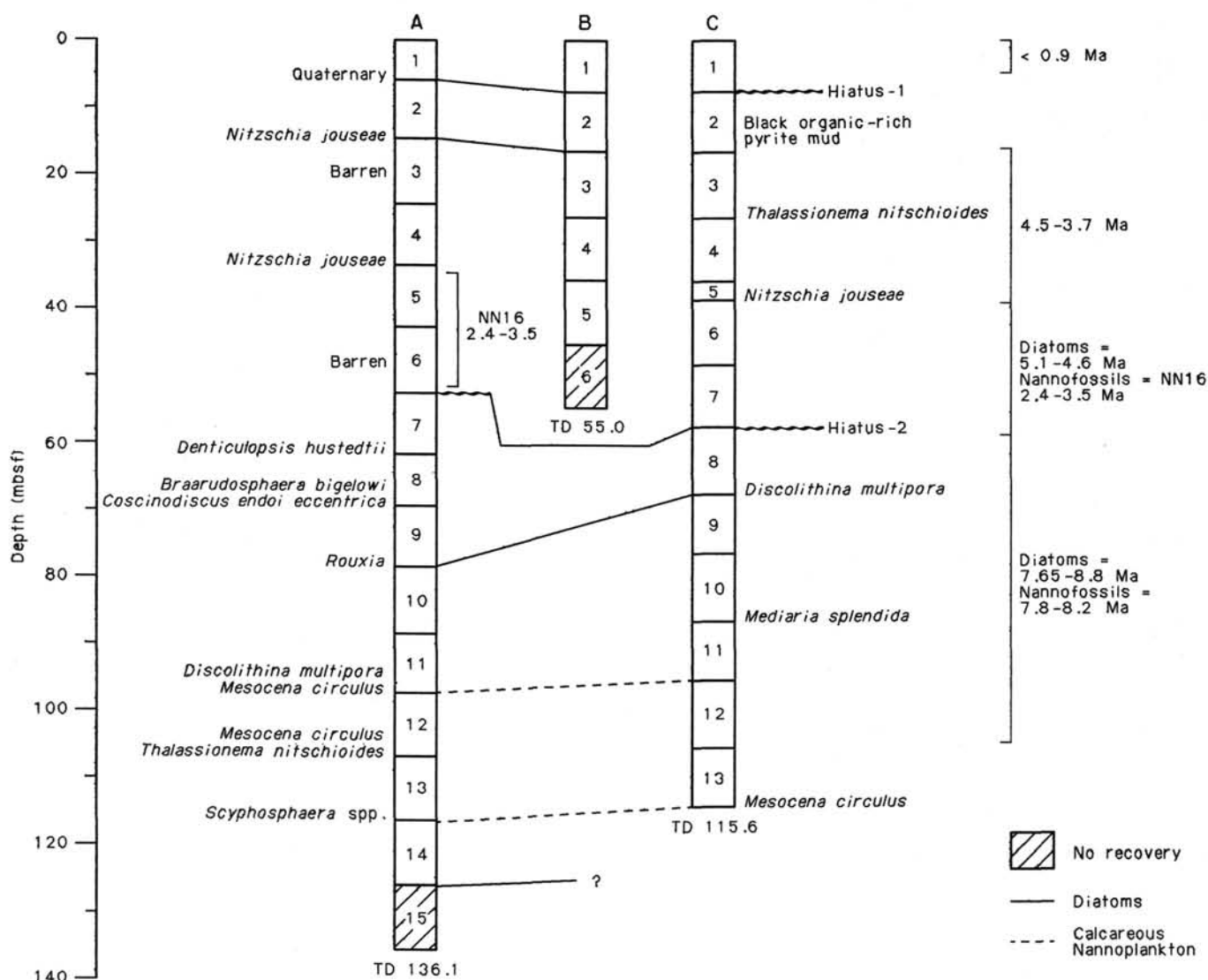


Figure 20. Biostratigraphic and lithostratigraphic correlation of the three holes cored at Site 684, based on diatom and calcareous-nannofossil events. Note diatom data are solely based on core-catcher samples, whereas calcareous nannofossil data are based on samples taken from within cores.

112-684A-4H, CC (15.0–33.6 mbsf), 112-684B-2H, CC to 112-684B-5H, CC (17.2–36.0 mbsf), and 112-684C-2H, CC to 112-684C-5H, CC (17.5–38.8 mbsf) and the absence of *Rhizosolenia praebergonii* places these intervals in the *Nitzschia jouseae* Zone (Barron, 1985; early Pliocene to early late Pliocene, 4.5 to 3.0 Ma). The remaining cores above H-2 can be placed in the upper *Thalassiosira convexa* Zone of Barron (1985), Subzone C, 5.1 to 4.6 Ma. This latter assignment is not well constrained owing to the scarcity of *Nitzschia jouseae* throughout the Pliocene section of all three holes. However, calcareous nannoplankton indicate Zone NN16 (2.4 to 3.5 Ma) for the interval of Cores 112-684-5 through 112-684-6. As true *Thalassiosira oestrupii* specimens were found in Holes 684A, 684B, and 684C right above H-2, the Miocene/Pliocene boundary was not crossed (boundary at 5.1 Ma).

The floral association in the lower sections of Hole 684A (below Core 112-684A-6X) and at Hole 684C (below Core 112-684C-7X) includes the following important stratigraphic species: *Denticulopsis hustedtii*, *Rossiella praepaleacea*, *Thalassiosira yabei*, *Rouxia* aff. *peragalli* in several new species, *Nitzschia heteropolica*/*Nitzschia pliocena*, *Thalassiosira* aff. *eccentrica*,

and a few *Actinocyclus ellipticus* forma *lanceolata* (first appearance datum [FAD] slightly predates the base of the *Thalassiosira yabei* Zone). This section was placed in the *Coscinodiscus yabei* Zone (Barron, 1985) and is of late Miocene age, 8.8 to 7.65 Ma. *Nitzschia cylindrica* and *Thalassiosira burckliana* were not found. A few isolated occurrences of forms that resemble *Nitzschia porteri* were noted. These new forms differ in shape and apical structures.

### Silicoflagellates

All core-catcher and some additional samples were studied for silicoflagellates in Hole 684A. None were investigated from Holes 684B and 684C. Preliminary data show three intervals with different silicoflagellate assemblages.

Core 112-684A-1H and most of Core 112-684A-2H contain a meager Quaternary assemblage that includes *Distephanus bioctonarius bioctonarius*, which has its lowest occurrence at this hole in Sample 112-684A-2H-4, 27–28 cm (10.7 mbsf).

In Cores 112-684A-3H to 112-684A-6H, the most common silicoflagellates belong to *Dictyocha messanensis stapedia* and related forms with a vertical apical bar and *Distephanus specu-*

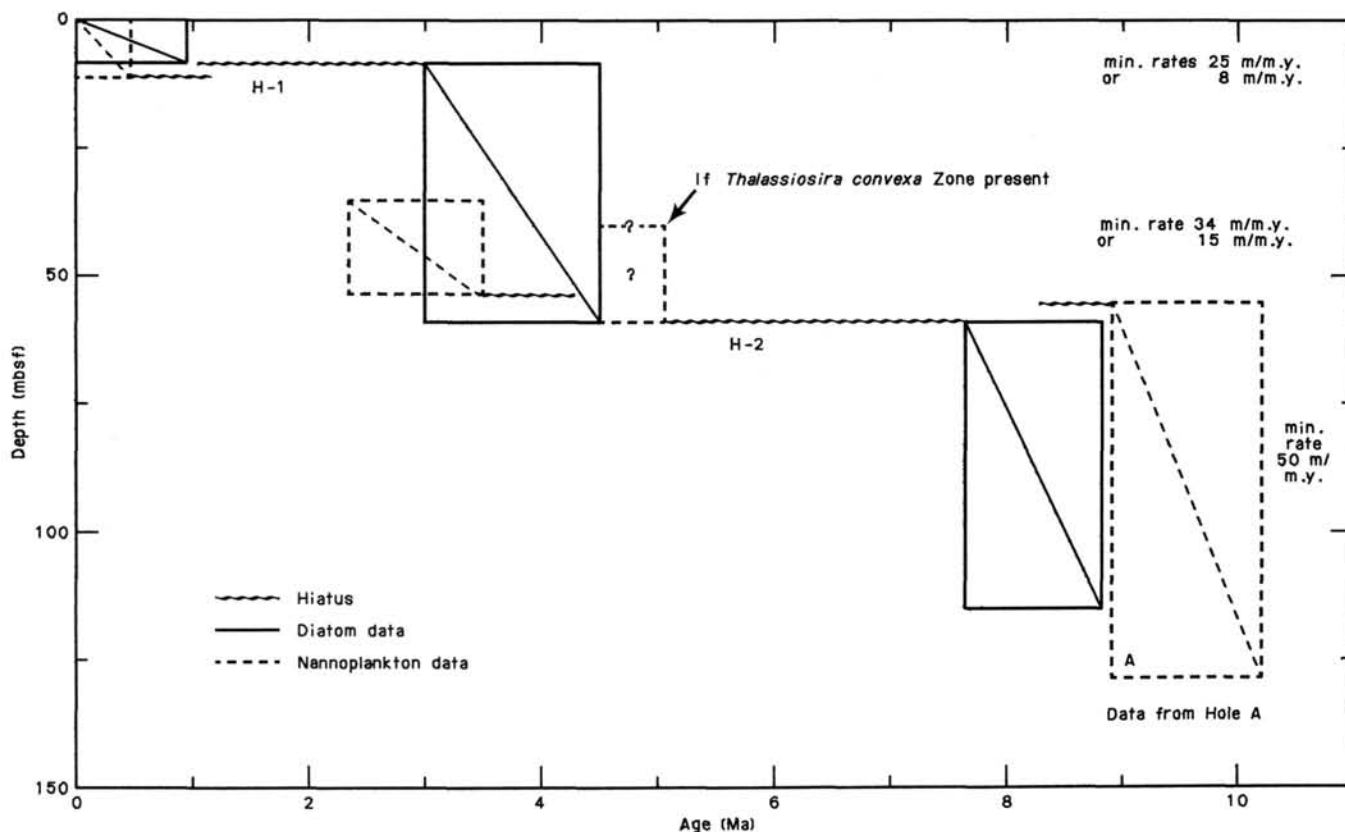


Figure 21. Conservative age vs. depth plot based on diatom and calcareous-nannofossil zonal assignments. Note position of hiatuses H-1 and H-2. Note diatom data are solely based on core-catcher samples, whereas calcareous-nannofossil data are based on samples taken from within cores.

*lum speculum* f. *speculum*. We found *Paramesocena circulus* in Sample 112-684A-3H-4, 109–110 cm (20.4 mbsf). This species, together with calcareous nannoplankton data for this part of the sequence, indicates a late Pliocene age for this interval.

Samples from Cores 112-684A-7H through 112-684A-14X are dominated by *Distephanus crux crux* and *Dictyochoa varia*. In Sample 112-684A-7H, CC (61.8 mbsf) we observed frequent *Mesocena didodon*, which ranges throughout the middle and late Miocene into the earliest Pliocene (calcareous nannoplankton Zones NN5 to NN13). We noted rare *Paramesocena circulus* in Samples 112-684A-8H-1, 9–10 cm (62.4 mbsf) and 112-684A-12X, CC (98.1 mbsf). The assemblage of this interval can be placed in the late middle to early late Miocene *Dictyochoa varia* Zone (Locker and Martini, 1986).

Two hiatuses are postulated, based on the silicoflagellate assemblages and their age assignment. The first was recognized in the lowest part of Core 112-684A-2H at approximately 15 mbsf with the lower Pleistocene and part of the upper Pliocene missing, and the second between Cores 112-684A-6H and 112-684A-7H at approximately 51 mbsf. Here, the lower Pliocene and most of the upper Miocene are missing.

Actiniscidians and ebridians were found scattered throughout the sequence and include *Actiniscus pentasterias*, *A. ? elongatus*, and *Parathranium clathratum*.

#### Calcareous Nannoplankton

Calcareous nannoplankton in distinct assemblages were found in three different intervals of Hole 684A. Core 112-684A-1H and part of Core 112-684A-2H contain a monotonous nannoplankton assemblage of the late Quaternary. *Gephyrocapsa oceanica* and *Gephyrocapsa aperta* are always present and are accompanied by rare to few *Helicosphaera carteri*. Some reworked

specimens from the Neogene were observed in Sample 112-684A-1H-2, 84–86 cm (2.3 mbsf).

The lowest part of Cores 112-684A-2H, and 112-684A-3H and the upper part of Core 112-684A-4H are barren of calcareous nannoplankton.

We noted rare *Discoaster surculus* in Sections 112-684A-4H, CC (33.6 mbsf) and 112-684A-5H, CC. *Discoaster brouweri* was found in several samples from Cores 112-684A-5H and 112-684A-6H, together with *Discoaster tamalis* in Sample 112-684A-6H-3, 98 cm (47.3 mbsf). As *Reticulofenestra pseudoumbilica* is absent in all samples, this interval was placed in the late Pliocene nannoplankton Zone NN16 (*Discoaster surculus* Zone). The interval between Section 112-684A-6H, CC and Sample 112-684A-7H-5, 57–58 cm (51–59.4 mbsf) also was barren.

From Sample 112-684A-7H-6, 80–81 cm, down to Core 112-684A-14X (61.1–117.3 mbsf), an assemblage dominated by *Reticulofenestra pseudoumbilica* and related species was observed. Rare *Discoaster hamatus* in Samples 112-684A-7H-6, 80–81 cm, and 684A-8H-1, 9–10 cm (61.1 and 62.4 mbsf, respectively) down to Section 112-684A-13X, CC allows us to place this assemblage in nannoplankton Zone NN9 (*Discoaster hamatus* Zone). Section 112-684A-14X, CC probably also belongs in Zone NN9 because *Catinaster coalitus*, a species indicative of the next lower Zone NN8, was not found even though it was found at Site 683. *Braarudosphaera bigelowi* was observed frequently in Sections 112-684A-8H-2 and 112-684A-8H-3, as well as in Section 112-684C-8X, CC (60.4 mbsf). Together with *Discolithina* species in Cores 112-684A-11X to 112-684A-14X, *Braarudosphaera bigelowi* indicates “nearshore” and “shallow-water” conditions for the area during deposition of this late middle Miocene sequence. Blooms of *Reticulofenestra* species were noted at several levels. Preliminary study of selected light-coloured thin layers in equiv-

alent strata of Hole 684C indicate the presence of many *Reticulofenestra* blooms. Complete spheres resulting from blooms are common in these layers, which indicates rapid accumulation and undisturbed settlement. *Scyphosphaera* species occur frequently in Cores 112-684A-13X and 112-684C-13X at the same level near the bottom of the drilled sequence (at approximately 107 mbsf in both cases). A nearly identical assemblage was observed in the slightly younger sequence (nannoplankton Zone NN10, *Discoaster calcaris* Zone) in Gabun, on the west coast of Africa (Martini, 1969), but it is associated there with *Coccolithus pelagicus*, which commonly indicates cold-water influences. This species is missing in the assemblage of late middle Miocene age at Site 684.

According to these nannoplankton data, two hiatuses divide the assemblages. One hiatus is present in the lowest part of Core 112-684A-2H at approximately 15 mbsf, with the lower part of the Quaternary and the uppermost Pliocene (<2.0 Ma) missing. The other is between Cores 112-684A-6H and 112-684A-7H at approximately 52 mbsf, where the lower Pliocene and most of the upper Miocene (5.4 Ma) are missing.

We did not investigate samples from Hole 684B and from the upper part of Hole 684C because of meager nannoplankton assemblages encountered in Hole 684A at these levels.

### Radiolarians

Two hiatuses are documented by radiolarians (mainly from data of Hole 684A), one between the Quaternary and the lower Pliocene (between Section 112-684A-2H, CC at 15 mbsf and Section 112-684A-3H, CC at 24.5 mbsf) and the other between a Pliocene level near the upper-middle Miocene boundary. The latter is characterized by the presence of abundant glauconite, but it is not well constrained because of the absence of radiolarians in Section 112-684A-6X, CC.

#### Hole 684A

All core-catcher samples from this hole were studied for signs of radiolarians. The species are well preserved in all samples and are generally rare to few (diluted by diatoms), except in Section 112-684A-5H, CC (43.1 mbsf), where they are common.

*Lamprocyrtis nigrinae*, *Pterocorys zancleus*, and *Stichocorys* cf. *peregrina* were found in Section 112-684A-1H, CC. This assemblage indicates a Quaternary age.

*Lamprocyrtis nigrinae* (abundant) and *Dictyophimus hirundo* were found in Section 112-684A-2H, CC. These species indicate a Quaternary age.

*Didymocyrtis tetrathalamus*, *Lamprocyrtis heteroporos*, *Phormostichoartus doliolum*, *Pterocanium praetextum*, and *Theocorythium vetulum* were found in Section 112-684A-3H, CC (24.4 mbsf). This assemblage indicates the middle part of the *Spongaster pentas* Zone, which represents the upper part of the lower Pliocene.

*Didymocyrtis tetrathalamus*, *Theocorythium trachelium*, *Stichocorys peregrina*, and *Dictyoprora amphora* were found in Section 112-684A-4H, CC (33.6 mbsf). These species indicate a mixture from different stratigraphic levels. *D. amphora* indicates a reworking of an Eocene fauna, *D. tetrathalamus* and *Th. trachelium* are from the Quaternary, and *S. peregrina* is from early to middle Pliocene. According to the age of Section 112-684A-3H, CC, the Quaternary species could represent down-hole contamination, while the Eocene species could represent reworking.

*D. tetrathalamus*, *L. nigrinae*, and *L. heteroporos* were found in Section 112-684A-5H, CC (43.1 mbsf). As for the previous sample, we have no further evidence of reworking, but we suspect contamination. Section 112-684A-6H, CC (51.0 mbsf) was barren.

*Didymocyrtis laticonus*, *D. huguesi*, *D. pettersoni*, and *D. antepenultimus* were found in Sections 112-684A-7H, CC to

112-684A-10X, CC (61.8–79.1 mbsf). This assemblage indicates the lower part of the *Didymocyrtis antepenultimus* Zone, which represents the lowermost upper Miocene or the uppermost part of the middle Miocene. Section 112-684A-11X, CC (88.6 mbsf) was barren.

*Didymocyrtis laticonus* was found in Section 112-684A-12X, CC (98.1 mbsf). It ranges from the base of the *D. antepenultimus* Zone to the top of the *Dorcadospyris alata* Zone, which represents the lowermost upper Miocene to the uppermost middle Miocene.

*D. pettersoni* and *Stichocorys wolffii* were found in Sections 112-684A-13X, CC to 112-684A-14X, CC (107.6–117.1 mbsf). This assemblage indicates the *D. pettersoni* Zone, which represents the uppermost middle Miocene.

#### Hole 684C

All core-catcher samples from this hole were studied for radiolarians. These are well preserved in all samples and are generally rare to few (diluted by diatoms).

An assemblage with *Lamprocyrtis nigrinae* was found in Sections 112-684C-1H, CC and 112-684C-2H, CC (0.0–17.5 mbsf). It indicates a Quaternary age. No collospherid species were encountered.

*Lamprocyrtis neoheteroporos* and *Didymocyrtis tetrathalamus* were found in Sections 112-684C-3H, CC and 112-684C-5H, CC (26.8–38.8 mbsf). This assemblage indicates the upper lower Pliocene to the Quaternary. Nevertheless, the absence of *L. nigrinae*, common in previous samples, suggests that it is older than the Quaternary.

*Theocorythium vetulum*, *Lamprocyrtis heteroporos*, *L. neoheteroporos*, and *Didymocyrtis tetrathalamus* were found in Section 112-684C-6X, CC (40.7 mbsf). This assemblage indicates an early Pliocene to late late Pliocene age. Section 112-684C-7X, CC (51.8 mbsf) was barren.

*Didymocyrtis laticonus*, *D. huguesi*, and *D. pettersoni* were found in Sections 112-684C-8X, CC to 112-684C-11X, CC (60.4–88.5 mbsf). This assemblage indicates the lower *D. antepenultimus* Zone, which represents the earliest part of the early Miocene. Section 112-684C-12X, CC (97.9 mbsf) was barren.

### Planktonic Foraminifers

All core-catcher samples were examined for planktonic foraminifers. These were barren in the following sequences: Cores 112-684A-2H through 112-684A-8X, 112-684B-3H through 112-684B-6X, and 112-684C-2H through 112-684C-7X. The first cores of each hole and Section 112-684B-2H, CC did contain foraminifers. Planktonic foraminifers are small when first encountered downhole in Sections 112-684A-9X, CC, (71.6 mbsf) and 112-684C-8X, CC, (60.4 mbsf). The genus *Globigerinoides* was common in this lower zone (Cores 112-684A-9X to 112-684A-13X). The habitat of this genus is warm surface water. Middle to late Miocene species were found in the samples from Sections 112-684A-9X, CC through 112-684A-13X, CC and 112-684C-9X, CC through 112-684C-13X, CC.

#### Hole 684A

Few planktonic foraminifers occurred in Section 112-684A-1H, CC and below Section 112-684A-7H, CC; these were well preserved. *Globigerinoides obliquus* occurred to Section 112-684A-9X, CC (71.6 mbsf); its last occurrence is at 1.8 Ma (Berggren et al., 1983). *Beella praedigitata* was found in Section 112-684A-9X, CC and in 112-684A-10X, CC (71.6 and 79.1 mbsf). The range of this species is from the *Globorotalia crassaformis* Zone to the *Globorotalia tosaensis* Zone of Kennett (1973); both zones are of Pliocene age. *Globoquadrina dehiscens dehiscens* was encountered in Sections 112-684A-11X, CC through 112-684A-13X, CC; its reported last occurrence is at 5.3 Ma (Berggren et al., 1983). *Globigerina decoraperta* was also found

in Section 112-684A-11X, CC. The range of this species is from Zone N9 to N21, middle Miocene to Pliocene. We placed this sample in N9 to N18, middle Miocene to late Miocene.

*Globorotalia challengerii* was found in Sections 112-684A-12X, CC (98.1 mbsf) and 112-684A-13X, CC (107.6 mbsf). These samples can be placed in the interval from the *Orbulina suturalis* Zone to the *Globorotalia mayeri* Zone of Srinivasan and Kennett (1981). Both samples are of middle Miocene age, based on the presence of *Globorotalia challengerii*.

#### Hole 684B

Planktonic foraminifers occurred in Sections 112-684B-1H, CC and 112-684B-2H, CC. All species are of Holocene age.

#### Hole 684C

Planktonic foraminifers occurred in Section 112-684C-1H, CC and in Sections 112-684C-9X, CC through 112-684C-13X, CC to total depth in Section 112-684C-13, CC at 115.0 mbsf. *Globigerinoides obliquus obliquus* occurred in Section 112-684C-9X, CC (71.6 mbsf); its last occurrence is at 1.8 Ma (Berggren et al., 1983). *Globoquadrina dehiscens dehiscens* occurred to Section 112-684C-11X, CC (88.6 mbsf); it occurs last at 5.3 Ma (Berggren et al., 1983). *Globigerinoides ruber* also was recognized in Section 112-684C-11X, CC. The first appearance of *Globigerinoides ruber* is in Zone N16 (Blow, 1969). Based on planktonic foraminifers, the sample was placed in Zones N16 to N18, late Miocene.

### Benthic Foraminifers

#### Hole 684A

Benthic foraminifers in this hole are present in three assemblages in which specimens are common to abundant and well preserved. Between these assemblages, the core-catcher samples are barren of foraminifers. Proceeding downhole, these assemblages are as follows:

*Bolivina seminuda humilis* Assemblage. This assemblage, which was described previously at Sites 680 and 681, occurred in Section 112-684A-1H, CC (5.1 mbsf). In contrast to previous sites, *Buliminella elegantissima* is represented by relatively few specimens at this site, and *Epistominella subperuviana* is abundant. This assemblage indicates an upper-bathyal, oxygen-minimum environment.

*Uvigerina peregrina* Assemblage. This assemblage occurs in Samples 112-684A-4H, CC (33.6 mbsf) and 112-684A-5H, CC (43.1 mbsf). In addition to the nominate species, *Uvigerina peregrina dirupta*, *Bolivina spissa*, *Cassidulina cushmani*, *Epistominella smithi*, and *E. subperuviana* are common to abundant, whereas *Plectofrondicularia californica* are few but conspicuous by their large size. This assemblage is indicative of an upper-middle bathyal environment.

*Valvulinera cf. depressa* Assemblage. This assemblage occurs in Sections 112-684A-8H, CC (69.4 mbsf) through 112-684A-14X, CC (117.1 mbsf). The nominate species is accompanied by abundant *Buliminella subfusiformis* and common *Bolivina pacifica* and *B. cf. vauhani*, which may have been transported from the shelf. These possibly transported tests are especially conspicuous in Section 112-684A-13X, CC (107.6 mbsf). A few *Bulimina cf. uvigerinaformis* and *Baggina cf. robusta* occur. The species content is similar, but not identical, to that found in Section 112-682A-19X, CC (171.9 mbsf) and is characteristic of middle-to-upper bathyal environments. Downhole displacement of specimens from the two stratigraphically higher assemblages was noted in Sections 112-684A-11X, CC and 112-684A-12X, CC (88.6 and 98.1 mbsf).

## ORGANIC GEOCHEMISTRY

At Site 684, upper-slope sediments of the Peruvian continental margin were cored at a water depth of 426 m. These sediments provided us an opportunity to examine the organic geochemistry of reworked upwelling facies seaward of the Yaquina and Trujillo basins. Sediment samples to 127 mbsf were studied to determine hydrocarbon gases, organic carbon, geochemical properties, and biogeochemical stratigraphy. Methods, procedures, and instruments used are described in "Explanatory Notes" (this volume).

### Hydrocarbon Gases

The primary record of hydrocarbon gases at this site came from our examination of the gases extracted from sediments by means of the headspace and can procedures (see "Organic Geochemistry" section, Site 679 chapter) because no gas pockets formed in the recovered cores. Thus, vacutainer samples could not be obtained. The results are compiled in Table 4. Because gases were measured in samples from three holes, we can compare with depth the sampling intervals that overlapped. Figure 22 shows this comparison for  $C_1$  concentrations. Reasonable agreement occurs in  $C_1$  concentrations (determined by the headspace procedure) among cores from the sediment surface to about 50 mbsf. The  $C_1$  concentrations increase from about 100 to 1,000  $\mu\text{L/L}$  of wet sediment over the first 36 m and then rapidly increase to about 90,000  $\mu\text{L/L}$  at 60 mbsf. Below 60 mbsf, the amount of  $C_1$  appears to decrease slightly.

$C_2$  and  $C_3$  are also present but in much lower amounts than  $C_1$  (Table 4).  $C_2$  contents range from about 4 to 57  $\mu\text{L/L}$  and  $C_3$  from about 3 to 23  $\mu\text{L/L}$ . Generally, the lowest amounts of these compounds were found toward the tops of the holes and possibly are derived from microbial sources. The concentrations of  $C_2$  below about 20 mbsf and of  $C_3$  below about 50 mbsf most likely result from microbial and early thermal diagenesis (Claypool and Kvenvolden, 1983). The ratios of  $C_1/C_2$  (Table 4) are low, less than 100 in the uppermost 36 m of all holes, increasing rapidly to about 2800 at 68 mbsf. Below this depth, this value decreases to an average of about 800. Figure 23 compares these ratios with depth for the three holes.

Both the extracted  $C_1$  concentrations and the  $C_1/C_2$  ratios show a marked increase at 36 mbsf (Figs. 22 and 23). This is the depth where sulfate concentrations decrease to 0% (see "Inorganic Geochemistry" section, this chapter). Thus, below 36 mbsf, sulfate reducers are no longer in competition with the methanogens for substrates, and  $C_1$  is produced in abundance. In the region of sulfate reduction above 36 mbsf, the low  $C_1$  concentrations are determined by a balance between  $C_1$  production, which is inhibited in the presence of sulfate ions;  $C_1$  consumption by anaerobic oxidation, which is still a debated process; and  $C_1$  diffusion from the methane-generating zone below 36 mbsf to the seafloor (Claypool and Kvenvolden, 1983).

The origin of  $C_2$  and  $C_3$  in the near-surface anaerobic sediments is not known, but these compounds are believed to come from microbial sources (reviewed by Claypool and Kvenvolden, 1983). Our data suggest that methanogenesis and "ethanogenesis" are independent processes, with  $C_2$  increasing significantly in concentration at about 22 mbsf and  $C_3$  increasing at about 49 mbsf, compared with the  $C_1$  increase at 36 mbsf. We conclude that microbial  $C_2$  and  $C_3$  production is not as inhibited by sulfate ions as  $C_1$  generation. Above 22 and 49 mbsf, respectively,  $C_2$  and  $C_3$  probably are subjected to some of the same processes that limit  $C_1$ , that is, anaerobic oxidation and diffusion. These processes lead to the very low concentrations of  $C_2$  and  $C_3$  near the sediment-water interface.

Table 4. Extracted gases at Site 684.

Core/section interval (cm)	Depth (mbsf)	C <sub>1</sub> (μL/L)	C <sub>2</sub> (μL/L)	C <sub>3</sub> (μL/L)	C <sub>1</sub> /C <sub>2</sub>
<i>Headspace gases, Hole 684A</i>					
112-684A-1H-2, 149-150	3.0	160	4.4		35
2H-5, 149-150	12.8	180	6.1		29
3H-5, 149-150	22.3	730	21		34
4H-5, 149-150	31.8	1,000	27	4.1	37
5H-5, 149-150	41.3	7,300	38		190
6H-4, 149-150	49.3	21,000	43	16	470
7H-5, 149-150	60.3	92,000	46	19	2000
8H-5, 0-1	68.3	15,000	24	14	630
9X-1, 149-150	71.1	29,000	32	12	900
<i>Headspace gases, Hole 684B</i>					
112-684B-1H-4, 0-1	4.5	120			
2H-6, 0-1	15.0	380	17		23
3H-4, 0-1	21.5	560	16		35
4H-6, 0-1	34.0	640	17		38
<i>Headspace gases, Hole 684C</i>					
112-684C-1H-4, 0-1	4.5	100			
2H-4, 0-1	12.3	120	3.9		32
3H-4, 0-1	21.8	480	15	3.1	31
4H-7, 0-1	35.8	2,000	34		59
5H-2, 0-1	37.8	1,000	16		64
6X-2, 0-1	40.5	7,300	29		250
7X-2, 149-150	51.5	70,000	48	11	1500
8X-2, 91-92	60.4	89,000	49	23	1800
9X-1, 79-80	68.3	80,000	29	11	2800
10X-1, 34-35	77.4	16,000	21	12	760
11X-2, 0-1	88.0	15,000	24	17	620
12X-2, 0-1	97.5	37,000	32	21	1200
13X-1, 139-140	106.9	41,000	57	5.4	720
<i>Canned gases, Hole 684B</i>					
112-684B-1H-3, 140-145	4.5	120	1.5		84
3H-3, 140-145	21.5	410	8.8		46
<i>Canned gases, Hole 684C</i>					
112-684C-6X-1, 140-145	40.5	18,000	36	4.3	490
9X-1, 80-85	68.4	71,000	50	17	1400

Units are in microliters (μL) of gas component per liter (L) of wet sediment. All measurements were performed on the Hach-Carle Gas Chromatograph.

### Carbon

Carbon contents in sediments from Site 684 were surveyed using 11 samples recovered in Hole 684C from the "squeeze-cakes" used from studies of pore-water chemistry. The percentages of total carbon, carbonate carbon, and organic carbon are listed in Table 5. The total organic carbon (TOC) from Rock-Eval pyrolysis also is given. In general, the organic carbon (OC) at this site is high, ranging from 1.4% to 8.7%; TOC ranges from 1.2% to 10.6%. Profiles of OC and TOC with depth are shown in Figure 24. The two shallowest samples at this site (4.5 and 12.3 mbsf) have the least organic carbon (less than 3%). The remainder of the samples contain more than 5% OC, except a sample from 57.5 mbsf that contains either 2.5 or 3.9%, depending on which result is accepted. The two minimum OC values at 12.3 and 57.5 mbsf correspond to two well-defined hiatuses at about 15 and 55 mbsf (see "Biostratigraphy" section, this chapter). The values for OC and TOC do not correlate as well at this site as they did at previous sites. Reanalyzing OC using samples that show the greatest difference did not produce significantly different results. We believe that the lack of agreement in the data may be the result of a faulty calibration of the Rock-Eval instrument. A standard run after obtaining these data demonstrated the need for recalibration, which was done in prep-

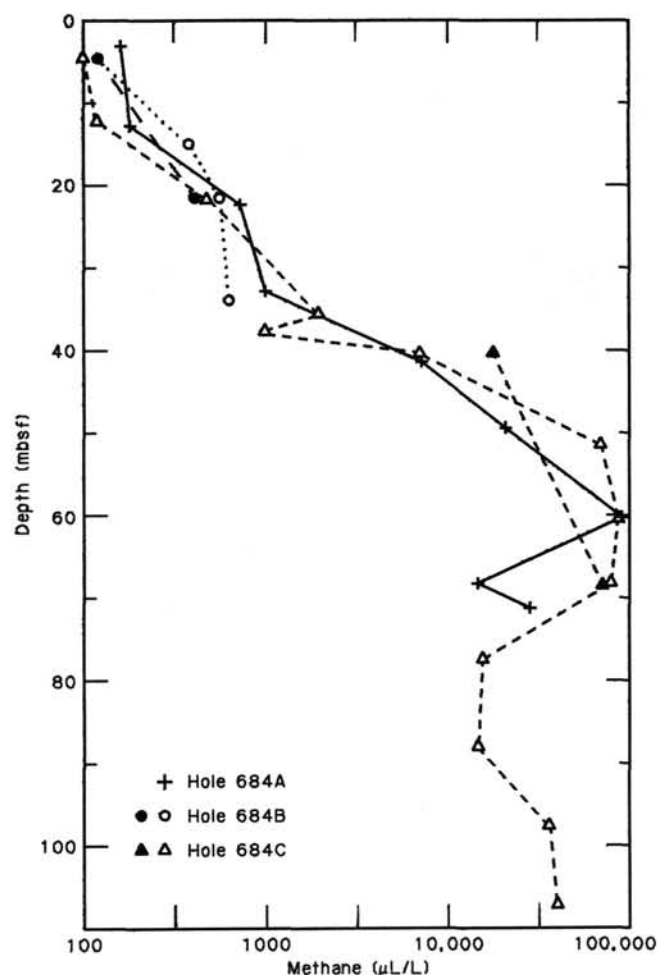


Figure 22. Comparison of extracted methane concentrations (μL/L of wet sediment) with depth as obtained from the headspace and can procedures at three holes from Site 684. Open symbols indicate results from headspace procedure; filled symbols indicate results from can procedure.

aration for samples from the next site. Time did not allow us to reanalyze all the samples for TOC.

Rock-Eval pyrolysis data are summarized in Table 6 and presented in Figure 25. The trends with depth for S<sub>1</sub>, S<sub>2</sub>, S<sub>3</sub>, TOC, and the hydrogen index (HI) are similar. In addition, the trends of T<sub>max</sub> and the oxygen index (OI) are similar but inverse to the other parameters. The lowermost sample is exceptional in that its Rock-Eval parameters do not follow the generalizations just stated. This sample (at 106.9 mbsf) contains more OC (8.7% or 10.6%) than any other sample at Site 684, but the HI value is low (290 mg/g TOC). All samples have T<sub>max</sub> values of less than 415°C, which suggests that the organic matter is immature with regard to its petroleum potential. The HI and OI values (Fig. 26) range from 200 to 462 and 29 to 89, respectively. Samples having HI values of less than 300 are believed to have a significant component of terrigenous organic material or marine organic matter that has undergone mild oxidation. The organic matter in the other samples is believed to be mainly of marine origin.

### Biogeochemical Stratigraphy

The work reported here constitutes a pilot program where organic geochemistry is linked with established stratigraphic tech-

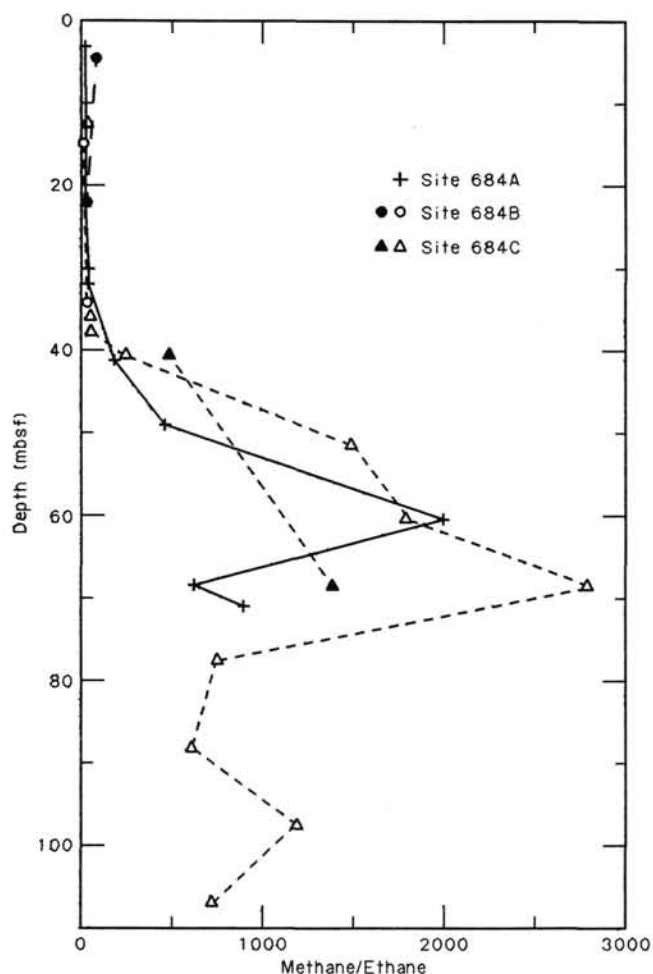


Figure 23. Methane/ethane ratios for extracted gases from three holes at Site 684. Open symbols indicate results from the headspace procedure; filled symbols indicate results from the can procedure.

Table 5. Profiles of organic carbon and carbonate carbon for Hole 684C.

Core/section interval (cm)	Depth (mbsf)	Total carbon (%)	Inorganic carbon (%)	Organic carbon (%)	TOC (%)
112-684C-1H-3, 145-150	4.5	3.62	0.83	2.79	2.85
2H-3, 145-150	12.3	1.78	0.37	1.41	1.16
3H-3, 145-150	21.8	7.09	0.15	6.94	7.65
4H-6, 145-150	35.8	10.03	1.78	8.25	7.86
5H-1, 145-150	37.8	9.47	1.52	7.95	8.99
6X-1, 145-150	40.5	9.40	1.91	7.49	8.67
7X-2, 145-150	57.5	4.07	0.19	3.88	2.51
8X-2, 92-97	60.4	8.98	1.58	7.40	8.25
10X-1, 35-40	77.4	5.91	0.80	5.11	4.99
11X-1, 145-150	88.0	6.62	1.05	5.57	5.60
13X-1, 140-150	106.9	11.25	2.51	8.74	10.57

TOC = total organic carbon from Rock-Eval pyrolysis.

niques. This study employed some of the techniques of molecular organic geochemistry that could be used on board the *Resolution*, coupled with the rapid characterization of organic matter made possible by the Rock-Eval instrument, and was linked to the routine sedimentological-micropaleontological approach.

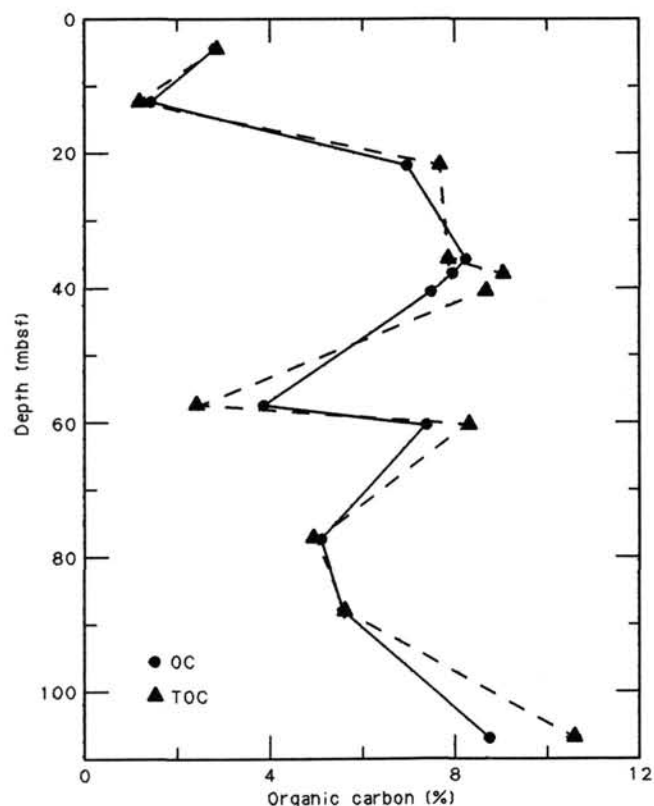


Figure 24. Comparison of organic carbon (OC) and total organic carbon (TOC) with depth in sediments from Hole 684C.

Hole 684A gave us an opportunity to examine the sediments deposited during Neogene time under upwelling conditions over some 127 m of core. The choice of this hole was dictated partly by the availability of an operational gas chromatograph having adequate resolution for the compounds of interest and by the availability of a stratigraphically suitable sequence of sediments.

We studied two classes of compounds: long-chain alkenones and pigments. To determine alkenones, Hole 684A sediments were extracted with organic solvent, the extracts derivatized with silylating reagent, and then analyzed by gas chromatography. The resulting gas chromatograms were compared with those obtained by similar procedures applied to other marine sediments and some of the peaks assigned on the basis of retention time behavior. In particular, co-injection was used to establish the identity of peaks owing to the  $C_{37}$  to  $C_{39}$  alkenones, for which a coccolithophorid origin was assumed (Brassell et al., 1986a, 1986b). The distribution patterns of these alkenones have been shown to vary with water temperature and, hence, reflect climatic signals. The analytical procedure used is described in "Explanatory Notes" (this volume). Pigment analyses were performed using the method for analysis of seawater described by Parsons et al. (1984). The procedures used also are described in "Explanatory Notes" (this volume).

#### Organic-Matter Pyrolysis and Total Organic Carbon

The data obtained with the automated Rock-Eval instrument are shown in Table 7 and Figures 27 and 28. The most useful parameters are TOC, HI, OI, and to a lesser extent,  $S_2/S_3$  and  $T_{max}$  (the temperature of maximum release of pyrolysate).

Table 6. Summary of Rock-Eval pyrolysis for Hole 684C.

Core/section interval (cm)	Depth (mbsf)	Quantity (mg)	T <sub>max</sub>	S <sub>1</sub>	S <sub>2</sub>	S <sub>3</sub>	PI	S <sub>2</sub> /S <sub>3</sub>	PC	TOC (%)	HI	OI
112-684C-1-3, 145-150	4.45	101.1	402	1.53	8.22	1.78	0.16	4.61	0.81	2.85	288	62
2-3, 145-150	12.25	101.2	406	0.29	2.35	1.04	0.11	2.25	0.22	1.16	202	89
3-3, 145-150	21.75	97.5	391	4.19	35.48	2.28	0.10	15.56	3.30	7.65	463	29
4-6, 145-150	35.75	102.0	392	4.63	35.15	3.44	0.12	10.21	3.31	7.86	447	43
5-1, 145-150	37.75	97.7	390	5.52	35.80	3.45	0.13	10.37	3.44	8.99	398	38
5-1, 145-150	40.45	100.0	395	4.69	33.70	3.61	0.12	9.33	3.19	8.67	388	41
7-2, 145-150	51.45	100.6	415	0.47	6.72	1.97	0.07	3.41	0.59	2.51	267	78
8-2, 92-97	60.42	94.7	392	4.27	36.87	3.50	0.10	10.53	3.42	8.25	446	42
10-1, 35-40	77.35	89.6	395	3.03	22.39	3.15	0.12	7.10	2.11	4.99	448	63
11-1, 145-150	87.95	93.6	395	4.77	25.92	3.52	0.16	7.36	2.55	5.60	462	62
13-1, 140-145	106.90	93.2	406	2.85	30.66	5.12	0.09	5.98	2.79	10.57	290	48

Rock-Eval parameters are defined in "Organic Geochemistry" section, Site 679 chapter.

TOC values vary from near 0% to 10%, indicated as follows:

Lithologic Units	TOC (%)	HI	OI
IA	2.4	300	100
IB	2.6	320	100
II	7.5	380	35
III	8.0	400	60
IV	8.0	450	70
V	5.0	450	60

The lithologic units are defined in the "Lithostratigraphy" section (this chapter). The unit boundaries are often sharply delineated by the Rock-Eval data, which show considerable variations in samples close to and within the boundaries. The different parameters not only show changes at the boundaries between the units, but also consistent levels within the individual units (Fig. 27). The biogeochemical boundary observed at 50 mbsf is in close, but not complete, agreement with the designated lithologic boundary between Units IV and V at 54.3 mbsf.

#### Lipid Analysis by Gas Chromatography: C<sub>37</sub> Alkenones in Hole 684A

The C<sub>37</sub> alkenones (37:2 and 37:3), when estimated by gas chromatography using n-C<sub>36</sub> as a standard, were found in the Peru margin sediments in amounts varying between 0 and 40 µg/g of sediment. This range is of the same order as that observed in Mediterranean Quaternary sapropels. The quantities observed roughly parallel the TOC values, as would be expected if there were no preferential removal of these compounds from a more or less constant influx.

The unsaturation ratio, U<sub>37</sub><sup>k</sup>, depends on the resolution of the two C<sub>37</sub> alkenone peaks (37:2 and 37:3; Fig. 29). For our survey, precise measurement was difficult because of overlapping of other peaks. Therefore, the values are not highly accurate and will be revised when gas chromatography and mass spectrometry techniques (identifying and quantifying co-elution problems) are applied. The data obtained show U<sub>37</sub><sup>k</sup> ranging from 0.7 to 0.95 but typically falling close to 0.8. A few major shifts occur, often at the boundaries between units, such as that between lithologic Units IV and V (Fig. 30). No obvious correlation can be found between the observed values and glacial and interglacial intervals, although improved data should give clearer results.

#### Pigment Analysis

Modification of the literature technique for estimating gross phaeophytin and carotenoid contents of seawater gave a useful record (Fig. 31) of both groups of pigments at Hole 684A down to 125 mbsf, which corresponds to Miocene age. More detailed analyses of the pigments will be conducted using shore-based high-precision liquid chromatography (HPLC) techniques (Ri-

dout et al., 1986). Both groups of pigments occur at nearly all intervals, with the values generally paralleling each other down-hole. The carotenoid signal displays a trend toward lower concentrations over the Pliocene, lithologic Units II and III, which may be a diagenetic effect. The concentrations decrease to very low values at or near the unit boundaries (Subunits IA and IB, Subunit IB and Unit II, and Units IV and V). Additional low and fluctuating values can be seen at other zones, notably at 50 m in Unit IV and 67 m in Unit V.

We emphasize that the data illustrated in Figure 31 provide only a qualitative estimate of the relative abundances of two generalized groups of biologically produced pigments and their degradation products. The estimation technique is based on absorbance measurements conducted at only four wavelengths. These light absorptions are the summation of the various absorptions of a considerable number of individual components. For example, the term "phaeophytin" is used here as a convenient description for a variety of chlorin-type pigments, such as phaeophorbides, phaeophytins, and so forth. Thin-layer chromatography (TLC) of sediment extracts (acetone) over silica, using 10% propan-2-ol in *n*-hexane as eluant, revealed a complex pattern of yellow, orange, pink, and pale green-brown spots, some of which fluoresced crimson under ultraviolet light, which indicates the presence of a variety of carotenoid and chlorin-related pigments. All of the sediment extracts examined gave related patterns, including the deepest (127 mbsf) at Hole 684A.

#### Microscopical Analysis

To relate the organic geochemical results to other stratigraphic methods at Hole 684A, we applied the smear-slide technique using small portions of the dry sediment remaining after extraction with methylene chloride and estimated the distribution of particles (Fig. 32).

On the average, diatoms are the most abundant fossil, with only infrequent complete absences, notably at the boundaries between Subunits IA and IB, Subunit IB and Unit II, and Units IV and V. In addition, abundances decrease to zero at the 50- and 76-m levels.

Nannofossils occur only intermittently, peaking at about 10% of the specimens counted.

Organic particles are recognized as amorphous irregular clumps that are generally quite abundant throughout the hole. These decrease to occasional low levels but are never entirely absent. These particles are usually found in some abundance at the unit boundaries.

We looked for both dinoflagellate cysts and higher plant debris, but found none. Pyrite particles were normally present in low abundances (about 5%) and occasionally peaked to 60%.

The sand/silt-sized fraction constituted zero to a few percent downhole, except for a few zones; for example, the hiatus between lithologic Units II and III.

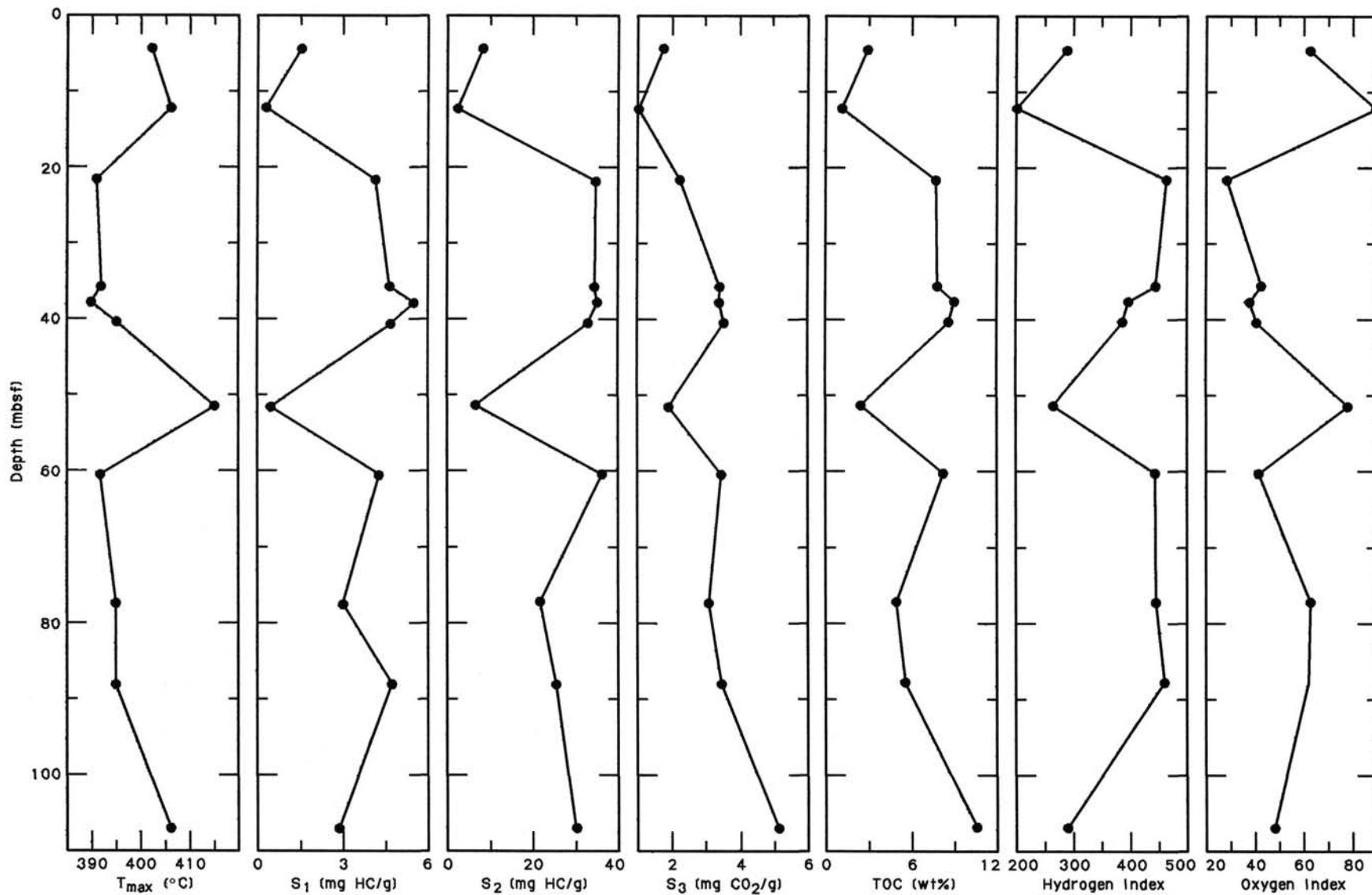


Figure 25. Comparison of Rock-Eval parameters  $T_{max}$ ,  $S_1$ ,  $S_2$ ,  $S_3$ , TOC, hydrogen and oxygen indices (HI and OI) with depth at Hole 684C.

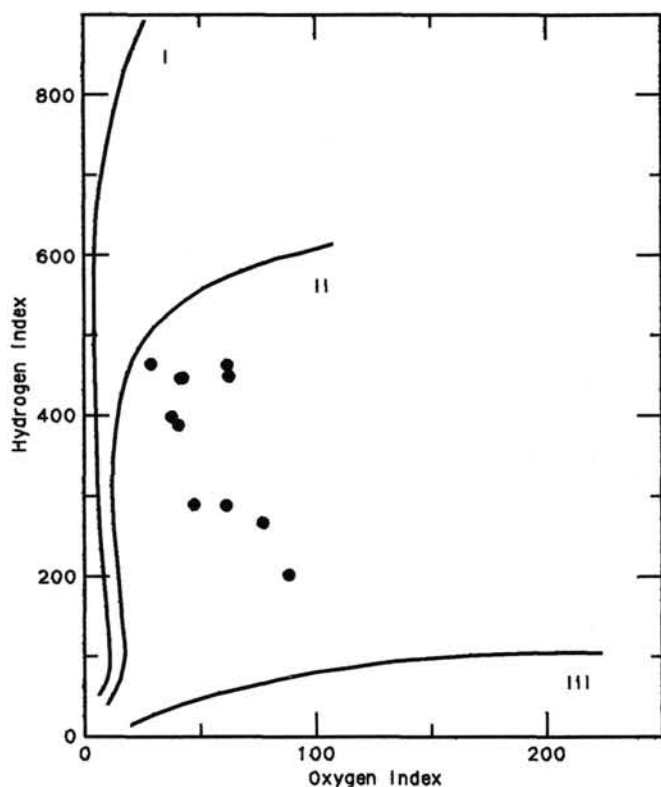


Figure 26. Hydrogen and oxygen indices (HI and OI) obtained from Rock-Eval pyrolysis of sediments from Hole 684C and plotted on a van Krevelen-type diagram (Tissot and Welte, 1984).

As with some of the other Peru margin holes, Hole 684A exhibited numerous zones where the usual distribution of particles could be described as winnowed. "Winnowed" zones are defined on the basis that the normal distribution size for hemipelagic sediments is not present. Such zones are of particular interest in terms of the "weathering," oxidation, and sorting that the organic matter might undergo. The winnowed zones occur at about 14, 18.46 to 21.46, 24.8 to 40.0, 45.08 to 51.08, and 54.6 mbsf.

### Discussion

Leg 112 sites provided a good record of the past high productivity of organic matter along the Peru margin. Where sampled, this record extends back to the Miocene, as attested by the high organic-carbon contents, typically 2% to 10%. The lipid extracts display a remarkably persistent pattern of lipids typical of a phytoplankton origin, which can be discerned even when markedly attenuated in turbiditic intervals deposited during low sea-level stands.

Of particular interest regarding phytoplankton influx (diatoms) is the survival of organic pigments of the phaeophytin-type, which we presume were derived from chlorophyll, and of the carotenoid-type. These pigments are present in Quaternary sediments at most of the sites. In a detailed study conducted downhole at Site 684A, the pigment abundances vary with depth from the Quaternary to Miocene and correlate positively with smear-slide data for diatom and nannoplankton contents (Fig. 33).

The lipid extracts were also assessed using the gas chromatograph. A detailed study involving approximately one sample per section (about 1.5 m) was performed for the first 75 m of Hole 684A. Aliquots of the same samples were examined by means of smear slides, visible absorption, and pyrolysis (Rock-Eval) tech-

niques. This work revealed significant relationships between the organic content measured by these techniques and the visual description of the samples. Not only do the pigments (e.g., the "phaeophytins") and the diatom contents run parallel (Fig. 33), but a similar relationship between the abundance of  $C_{37}$  alkenones and the TOC contents and other pyrolysis-derived parameters also occurs (Fig. 34). These relationships indicate a general constancy in the type of organic matter being deposited at this site.

The distribution patterns and amounts of lipids revealed by gas chromatography (with marked exceptions within and in the proximity of hiatuses and in the turbiditic and low-stand sections) are remarkably consistent. This observation suggests that upwelling at Site 684 was largely continuous over the recorded intervals of the Neogene. Detailed shore-based laboratory studies employing gas-chromatographic-mass-spectrometric (GC-MS) techniques should complete and validate this conclusion. These lipid distributions are typical of marine phytoplankton and show no indication of significant higher-plant input.

The correlation between diatom abundance (established microscopically) and the pigment content (determined through extraction and visible spectrometry) is consistent with the lipid input by diatoms of the upwelling system having determined the bulk of the lipid signal. Certainly, diatoms do dominate the biomass of modern upwelling systems. However, we observed a second phenomenon that was unexpected and particularly interesting. This was the marked abundance (about  $30 \mu\text{g/g}$  dry sediment) of the  $C_{37}$  alkadienone, accompanied by the usual suite of  $C_{37}$  to  $C_{39}$  alkenones, in almost all sediment samples we examined. These long-chain alkenones have been detected only in living members of the Prymnesiophyceae and in sediments. Hence, in the organic geochemical literature, specimens commonly are assigned to a coccolithophorid source. However, coccoliths were not abundant in these sediments. Possible inferences include that either the calcareous coccolithophorid nannoplankton record in the Peru sediments is grossly under represented as a result of dissolution or the alkenones have a source other than coccolithophorids.

The alkenone unsaturation index ( $U_{37}^K$ ) displays several major shifts downhole, which probably signifies fluctuations in sea-surface temperatures (Brassell et al., 1986a, 1986b). Other organic geochemical parameters (most notably the Rock-Eval pyrolysis data) display a "three-step" trend with depth (e.g., Fig. 27), with distinct hiatuses separating each step. These hiatuses, which show winnowed particle distributions, are characterized by distinctive peaks in the OI profile (Fig. 27), possibly the result of some degree of organic-matter reworking in more oxygenated conditions. Indeed, these particular levels are distinctive with respect to most of the organic geochemical parameters used here.

This preliminary study illustrates the value of a combined approach, that is, linking organic geochemical techniques with sedimentological and micropaleontological descriptions. Such an approach offers an opportunity to address cyclicity (including glacial/interglacial fluctuations), biological assemblages in the upwelling record, sediment transport and reworking, and diagenesis.

## INORGANIC GEOCHEMISTRY

### Introduction and Operation

Samples for interstitial-water analyses were obtained from two (Holes 684B and 684C) of the three holes cored at this site; all were squeezed from whole-round samples. At Hole 684B, we analyzed samples from Cores 112-684B-1H and 112-684B-3H; at Hole 684C, whole-round, 5-cm samples were taken from every core between Cores 112-684C-1H and 112-684C-8X and,

Table 7. Rock-Eval pyrolysis data for Hole 684A.

Core/section interval (cm)	Depth (mbsf)	Weight (mg)	T <sub>max</sub>	S <sub>1</sub>	S <sub>2</sub>	S <sub>3</sub>	PI	S <sub>2</sub> /S <sub>3</sub>	PC	TOC (%)	HI	OI
112-684A-1H-1, 40-42	0.40	99.4	402	2.07	9.60	2.99	0.18	3.21	0.97	3.06	313	97
1H-2, 40-42	1.90	70.1	404	2.11	10.32	2.92	0.17	3.53	1.03	3.11	331	93
1H-3, 40-42	3.40	60.9	403	1.75	8.35	2.67	0.17	3.12	0.84	2.77	301	96
1H-4, 40-42	4.90	62.3	401	1.86	8.17	2.92	0.19	2.79	0.83	2.94	277	99
2H-1, 66-67	5.96	59.4	405	1.63	7.17	2.44	0.19	2.93	0.73	2.45	292	99
2H-2, 66-67	7.46	60.0	404	1.21	6.41	1.95	0.16	3.28	0.63	2.42	264	80
2H-3, 66-67	8.96	85.9	411	0.23	1.93	1.51	0.11	1.27	0.18	1.15	167	131
2H-4, 66-67	10.46	60.5	400	1.88	9.30	2.34	0.17	3.97	0.93	2.98	312	78
2H-5, 66-67	11.96	60.2	403	1.66	9.80	2.07	0.14	4.73	0.95	3.06	320	67
2H-6, 66-67	13.46	60.2	418	0.09	0.94	1.17	0.09	0.80	0.08	0.55	170	212
2H-6, 83-84	13.63	73.0	408	0.12	1.02	2.53	0.11	0.40	0.09	0.66	154	383
2H-6, 109-110	13.89	92.3	399	3.10	28.67	4.55	0.10	6.3	2.64	7.01	408	64
2H-6, 140-141	14.20	98.6	401	2.32	24.5	4.13	0.09	5.93	2.23	6.23	393	66
3H-1, 66-67	15.46	62.3	397	2.34	28.78	2.93	0.08	9.82	2.59	8.52	337	34
3H-2, 66-67	16.96	61.9	401	2.14	24.26	2.77	0.08	8.75	2.20	7.51	323	36
3H-3, 66-67	18.46	62.5	394	3.28	27.85	2.57	0.11	10.83	2.59	7.32	380	35
3H-4, 66-67	19.96	60.3	395	3.34	29.75	2.91	0.10	10.22	2.75	7.18	414	40
3H-5, 66-67	21.46	63.5	397	2.77	33.73	3.96	0.08	8.51	3.04	8.91	378	44
3H-6, 66-67	22.96	60.4	383	4.61	29.63	3.89	0.13	7.61	2.85	7.66	386	50
3H-7, 54-55	24.34	59.4	394	2.91	30.67	4.30	0.09	7.13	2.79	7.74	396	55
4H-1, 50-51	24.80	70.8	407	1.11	17.27	3.81	0.06	4.53	1.53	5.95	290	64
4H-2, 50-51	26.30	100.1	399	2.60	20.24	3.01	0.11	6.72	1.90	5.43	372	55
4H-3, 50-51	27.80	100.2	398	3.16	23.22	3.45	0.12	6.73	2.19	4.82	481	71
4H-4, 50-51	29.30	99.2	403	2.96	30.84	3.86	0.09	7.98	2.81	7.99	385	48
4H-5, 50-51	30.80	62.7	385	5.94	40.33	4.22	0.13	9.55	3.85	9.77	412	43
4H-6, 50-51	32.30	82.3	386	5.06	31.90	4.59	0.14	6.94	3.08	8.37	381	54
4H-7, 29-30	33.59	91.0	386	5.00	33.53	4.61	0.13	7.27	3.21	8.79	381	52
5H-1, 120-121	35.00	97.4	393	5.31	39.13	4.06	0.12	9.63	3.70	8.74	447	46
5H-2, 20-21	35.50	96.9	396	5.07	34.42	4.80	0.13	7.17	3.29	9.56	360	50
5H-3, 20-21	37.00	67.7	398	4.12	29.09	4.84	0.12	6.01	2.76	7.77	374	62
5H-4, 20-21	38.50	87.3	391	5.15	32.30	4.71	0.14	6.85	3.12	8.57	376	54
5H-5, 20-21	40.00	73.9	392	4.93	35.38	4.92	0.12	7.19	3.35	8.61	410	57
5H-6, 20-21	41.50	93.5	395	4.28	31.51	4.74	0.12	6.64	2.98	7.72	408	61
5H-7, 20-21	43.00	86.4	397	5.23	31.11	4.88	0.14	6.37	3.02	8.53	364	57
6H-2, 28-29	45.08	85.5	392	4.64	32.70	5.02	0.12	6.51	3.11	7.16	456	70
6H-3, 28-29	46.58	104.7	398	5.10	40.32	6.11	0.11	6.59	3.78	8.75	460	69
6H-4, 28-29	48.08	100.9	386	7.14	45.11	5.35	0.14	8.43	4.35	9.34	482	57
6H-4, 59-60	48.39	92.5	398	5.35	47.87	7.95	0.10	6.02	4.43	6.79	705	117
6H-4, 90-91	48.80	95.8	400	1.43	21.46	5.34	0.06	4.01	1.90	2.87	747	186
6H-4, 120-121	49.20	108.8	399	3.16	35.34	5.86	0.08	6.03	3.20	7.98	442	73
6H-4, 149-150	49.50	97.8	406	1.11	16.43	4.21	0.06	3.90	1.46	5.54	296	75
6H-5, 28-29	49.58	107.1	402	1.40	23.69	3.17	0.06	7.47	2.09	4.14	572	76
6H-6, 28-29	51.08	98.1	411	1.02	12.44	2.42	0.08	5.14	1.12	4.23	294	57
7H-1, 30-31	53.10	72.9	393	4.17	26.17	3.70	0.14	7.07	2.52	5.40	484	68
7H-2, 30-31	54.60	102.1	402	1.23	18.43	2.58	0.06	7.14	1.63	4.53	406	56
7H-3, 30-31	56.10	93.1	395	2.33	22.91	2.72	0.09	8.42	2.10	5.05	453	53
7H-4, 30-31	57.60	73.5	380	6.59	32.39	2.28	0.17	14.20	3.24	6.22	520	36
7H-5, 30-31	59.10	106.8	385	4.93	30.97	2.34	0.14	13.23	2.99	6.10	507	38
7H-6, 30-31	60.60	67.8	394	3.68	28.02	3.71	0.12	7.55	2.64	6.00	467	61
8H-1, 41-42	62.71	70.5	395	4.05	30.07	3.74	0.12	8.04	2.84	5.87	512	63
8H-2, 41-42	64.21	70.2	402	3.61	27.42	4.07	0.12	6.73	2.58	5.58	491	72
8H-3, 41-42	65.71	98.3	419	0.43	5.25	1.27	0.08	4.13	0.47	2.90	181	43
8H-4, 41-42	67.21	101.2	407	0.42	3.15	1.50	0.12	2.10	0.29	2.86	110	52
8H-5, 41-42	68.71	59.7	406	3.36	26.06	1.27	0.11	20.51	2.45	5.39	483	23
8H,CC, 9-10	69.57	97.4	427	0.39	4.56	0.35	0.08	13.02	0.41	1.85	246	18
9X-1, 40-41	70.00	57.8	399	4.10	25.46	2.92	0.14	8.71	2.46	5.29	481	55
9X-2, 40-41	71.50	59.8	402	3.04	18.77	1.93	0.14	9.72	1.81	3.91	480	49
9X,CC, 10-11	71.74	46.3	403	2.13	16.00	2.35	0.12	6.80	1.51	3.37	474	69
12X,CC, 17-18	98.27	69.9	414	2.04	20.95	3.31	0.09	6.32	1.91	4.87	430	67
13X,CC, 20-21	107.80	112.3	417	0.43	6.74	1.10	0.06	6.12	0.59	1.69	398	65
14X,CC, 4-5	117.14	90.0	413	2.83	29.95	4.00	0.09	7.48	2.73	6.42	466	62
15X,CC, 7-8	126.67	68.6	402	3.93	27.04	3.04	0.13	8.89	2.58	5.49	492	55

Note: Rock-Eval parameters are defined in "Organic Geochemistry" section, Site 679 chapter.

subsequently, from Cores 112-684C-10X, 112-684C-11X, and 112-684C-13X (Table 8). No *in-situ* water samples were obtained at this site.

As at Sites 680 and 681 at the 11°S transect, large systematic downhole increases in salinity, chloride, calcium, and magnesium were observed at this site, which is located at a greater water depth (426 m) (Table 8, Figs. 35 through 42) than Sites 680 and 681. However, sulfate concentrations do not increase with depth at Site 684; the deepest sample analyzed at 107 m was still

within the sulfate-depleted (0 mmol/L) and methane-production zones.

The profiles for chloride concentration and salinity, which here are controlled by Cl<sup>-</sup> (and alkalis) concentrations, are diffusion profiles between a brine solution at greater depth and seawater. We assumed that the same brine was responsible for the increases in salinity, chloride, Mg<sup>2+</sup>, and some of the Ca<sup>2+</sup> at all three sites. For a discussion of origin of this brine, see "Inorganic Geochemistry" section of the Site 680 chapter.

Table 7 (continued).

	Microscopic parameters (%)				U <sub>37</sub> <sup>k</sup>	C <sub>37</sub>	Pheo.	Carot.	Pig. Total	Carbonate
	Diatoms	Nannofossils	C <sub>Org</sub>	Pyrite						
75	0	15	5	5	0.75	4	33	50	60	12.18
70	2	20	5	2	0.69	8	24	48	67	10.51
0	0	0	0	0			22	49	69	13.34
70	0	15	5	10	0.77	5	25	52	71	15.26
78	2	15	5	0	0.77	5	25	48	65	6.59
40	0	40	5	5	0.74	1	24	44	66	9.59
50	0	40	3	7	0.87	2	16	22	58	8.26
0	0	80	10	10	0.80	3	6	4	40	59.05
70	10	18	2	0	0.80	12	26	51	66	10.59
80	0	10	2	0	0.83	10	19	46	71	4.34
0	0	70	20	10	0.78	2	4	4	50	33.36
0	0	5	5	90	0.82	2	3	0	0	
0	0	80	10	10	0.81	31	24	50	68	
0	0	75	10	15	0.83	3	20	42	68	
10	0	40	48	2	0.80	30	19	35	65	1.08
35	0	60	5	0	0.81	23	18	32	64	0.58
45	0	50	5	0	0.77	13	24	25	51	1.58
40	0	50	5	0	0.81	24	15	19	56	0.75
20	0	70	10	0	0.83	23	15	11	58	0.58
40	0	45	10	5	0.77	21	21	26	55	0.33
60	0	35	5	0	0.77	36	17	17	50	0.33
10	0	40	50	0	0.83	15	9	9	50	1.75
43	0	50	5	2	0.82	18	15	15	50	8.76
30	0	60	10	0	0.81	22	16	18	53	14.09
20	0	60	20	0	0.83	23	18	17	49	8.84
50	0	40	10	0	0.80	20	36	34	51	2.0
60	0	30	10	0	0.74	23	23	26	53	19.27
45	5	40	10	0	0.74	22	18	14	44	11.18
10	0	70	20	0	0.74	20	21	18	46	1.33
10	0	80	10	0	0.71	25	23	26	53	7.84
70	1	28	1	0	0.83	18	26	20	57	16.68
66	2	30	2	0	0.83	23	23	19	45	20.27
45	0	45	10	0	0.87	26	21	22	51	10.68
60	5	25	10	0	0.76	25	23	24	51	15.51
43	10	40	5	2	0.72	29	26	25	51	20.77
30	1	50	10	10	0.83	30	27	24	47	9.76
19	1	60	10	10	0.72	17	23	20	53	1.17
20	0	70	10	0	0.75	26	23	20	47	27.86
10	0	80	5	5	0.71	37	25	37	60	
10	2	80	5	3	0.70	24	15	18	55	
5	0	75	20	0	0.70	30	16	19	54	
0	0	50	50	0			11	9	45	
2	0	58	30	10	0.95	8	13	13	50	20.93
0	0	50	50	0	0.95	7	9	8	53	
90	2	5	2	0	0.88	19	22	22	50	13.01
0	0	50	40	10	0.74	26	13	7	65	
60	0	40	5	0	0.72	17	16	14	53	1.42
70	0	25	5	0	0.81	33	22	17	44	0.25
55	0	40	5	0	0.81	36	22	22	50	0.50
60	0	35	5	0	0.72	28	22	18	45	0.50
90	1	5	5	0	0.75	23	25	20	56	7.17
70	0	25	5	0	0.79	32	18	15	45	8.92
80	0	10	10	0	0.85	12	5	3	63	49.96
0	0	10	60	30	0.91	10	3	2	60	3.34
72	10	10	2	0	0.93	8	17	17	50	6.00
85	5	5	5	0	0.85	33	21	23	52	12.34
0	0	0	0	0			15	17	53	8.76
85	5	5	5	0	0.79	24	15	10	40	22.02
65	10	15	10	0	0.85	19	17	10	40	
5	0	5	5	85	0.96	20	6	4	40	
80	10	3	3	0	0.87	41	17	9	35	
90	5	2	2	0	0.88	30	18	18	50	

Because of similarities, the interstitial-water data obtained at Site 684 are compared in the following paragraphs with those obtained in the two shallower sites of the 11°S transect.

#### Chloride and Salinity

Chloride concentration increases from 557 mmol/L at 4.5 mbsf to 1029 mmol/L at 107 mbsf. The diffusion gradient is considerably steeper than at previous sites: 46 mmol/L Cl<sup>-</sup>/10 m, relative to 38 and 23 mmol/L Cl<sup>-</sup>/10 m at Sites 681 and 680, respectively (Fig. 36). At 107 mbsf, the concentration of Cl<sup>-</sup> is

already 184% of the Cl<sup>-</sup> in seawater. Similarly, the salinity gradient, shown in Figure 35, is significantly steeper (Table 9). We assumed that the brine must be at a shallower depth in the vicinity of this site.

#### Alkalinity and Sulfate

Sulfate reduction proceeds rapidly; at the shallow subsurface depth of 36 m, all sulfate is reduced and methane production increases considerably. At Site 681, complete sulfate reduction occurs at a slightly shallower depth, i.e., at a depth of 28 m. Sulfate reduction was not driven to completion at Site 680 (Fig. 38).

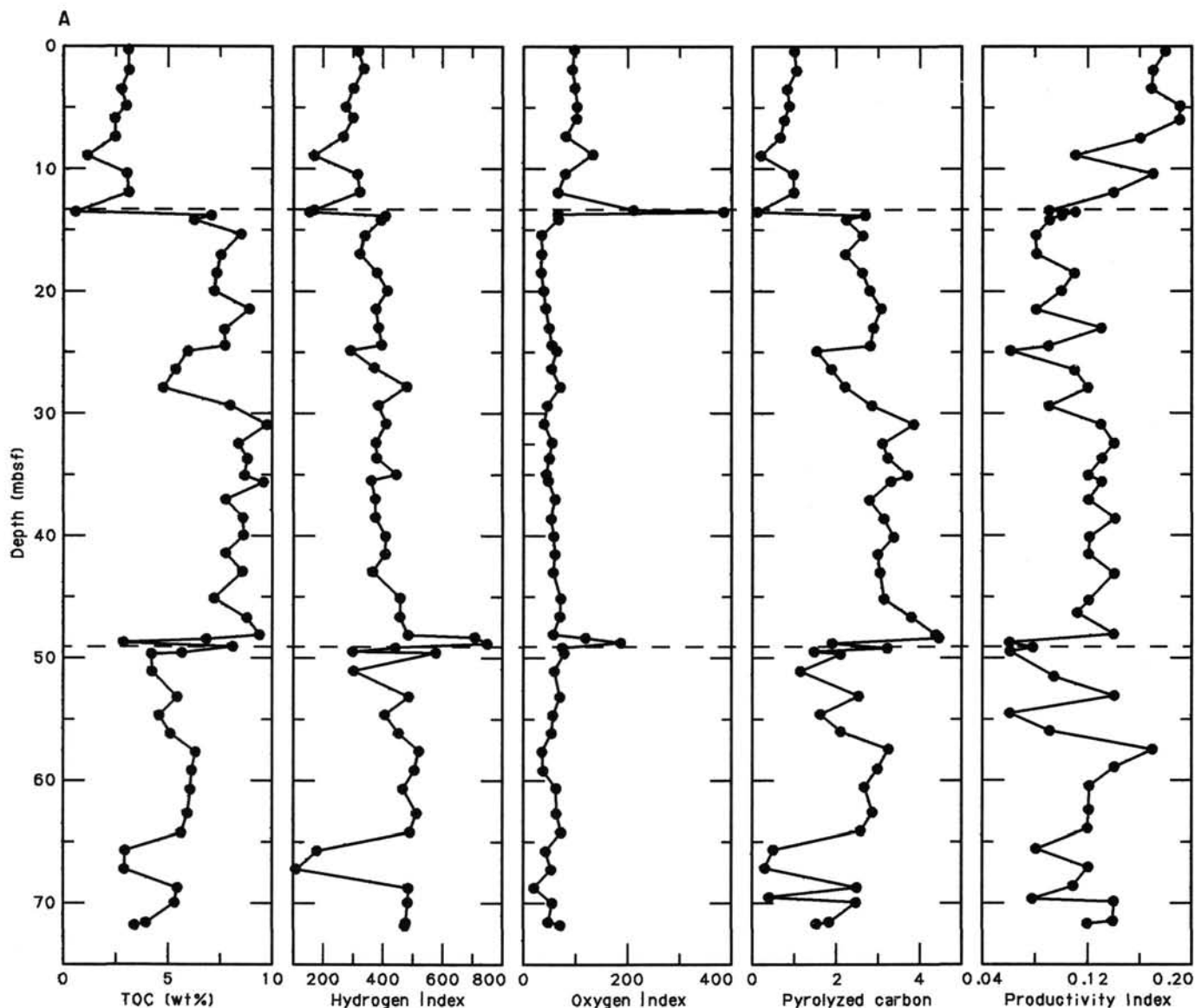


Figure 27. Rock-Eval data for Hole 684A samples plotted vs. sub-bottom depth from 0 to 75 mbsf.

Unlike Sites 680 and 681 in which sulfate concentrations increase again at greater depths, the zone of  $\text{SO}_4^{2-}$  depletion at Site 684 is thicker and extends to the bottom of the hole. However, sulfate concentrations should increase with depth at this site as well, as suggested by the decreased methane toward the bottom of the hole (see "Organic Geochemistry" section, this chapter).

Alkalinity reaches its maximum value of  $\sim 24$  mmol/L at  $\sim 36$  mbsf and decreases slowly with depth to  $\sim 13$  mmol/L at 107 mbsf. The alkalinity maxima at Sites 681 and 680 are lower (19.5 and 19.7 mmol/L, respectively; Fig. 37). The intense, diagenetic carbonate mineral formation that we observed between  $\sim 38$  and  $\sim 50$  mbsf may be at least partially responsible for the observed decrease in alkalinity with depth. Hence, the alkalinity profiles shown in Figure 37 represent only minimum values of microbially produced alkalinity from organic-matter remineralization.

### Ammonia

Ammonia concentrations increase systematically from 2.0 mmol/L at 4.5 mbsf to 14.2 mmol/L at 107 mbsf. Still higher values should occur at greater depths. The steady increase in

$\text{NH}_4^+$  in Figure 39 indicates that the maximum ammonia value has not been reached at the bottom of this hole.

As yet we are not sure why the  $\text{NH}_4^+$  concentrations at this site are so distinctly higher than those at Sites 680 and 681, where values range between 1 and 5 mmol/L. Differences in the TOC values do not explain the observed discrepancy between the  $\text{NH}_4^+$  concentrations at Site 684 vs. those at Sites 680 and 681 (for detailed gas and TOC concentrations, see "Organic Geochemistry" section, this chapter):

	Site 684	Site 681	Site 680
TOC (%)	1.4–8.7	0.6–4.4	2.9–10.0

Differences in the nature of the organic matter in the deeper water at Site 684 (438 m) compared with the shallow water at Sites 681 and 680 (161 and 272 m, respectively) could be responsible for this observation, although normally the shallow environments contain the most metabolizable organic nitrogen. Another explanation might be found in the history of the brine; i.e., addition of  $\text{NH}_4^+$  to the brine during passage through organic carbon-rich sediments. Such an effect could also account for the observed lack of sulfate at the higher salinities.

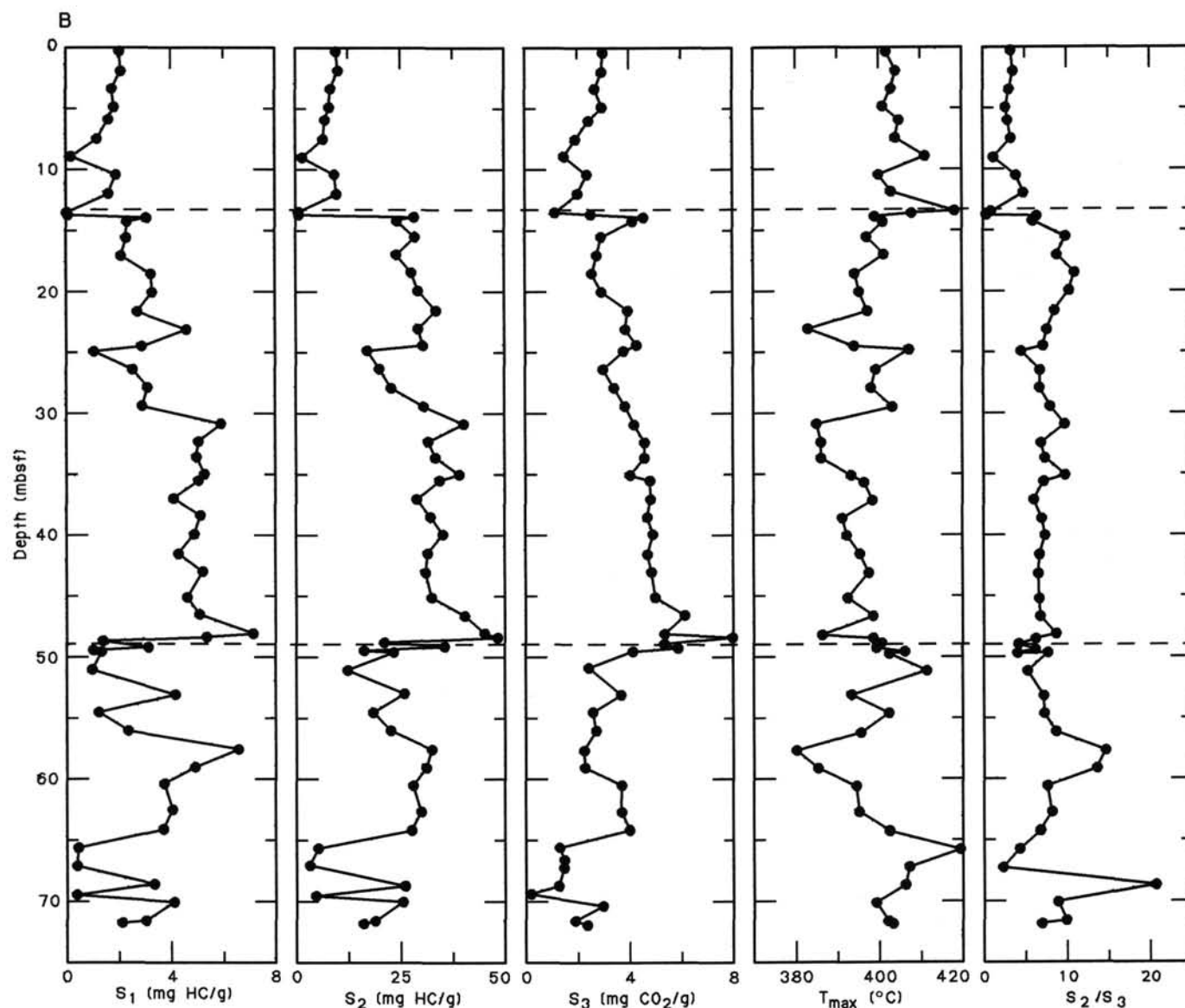


Figure 27 (continued).

### Phosphate and Silica

The same analytical problems with phosphate that were encountered at Sites 680 and 681 were also encountered here (see Site 680 chapter). Therefore, only a few results are reported in Table 9.

In the highly diatomaceous sediments and high-salinity geochemical environment at Site 684, silica concentrations reach opal-A saturation at 4.5 mbsf. Silica concentrations remain almost constant with depth; silica values are controlled by diatom dissolution in the diatomaceous Subunit IA and Unit III (described in "Lithostratigraphy" section, this chapter). The sediments of Subunit IB and Unit II, the phosphatic and glauconitic terrigenous muds and sands sandwiched between the diatomaceous units, are not recognizable in the silica concentration profiles. This may be due to diffusion of dissolved silica, which would level out concentration gradients throughout the column.

### Calcium and Magnesium

As at Sites 680 and 681, almost immediately below the sediment/water interface,  $\text{Ca}^{2+}$  and  $\text{Mg}^{2+}$  concentrations are lower than seawater concentrations.  $\text{Ca}^{2+}$  concentrations decrease to

6.58 mmol/L at 12.3 mbsf (Sample 112-684A-2H-3, 145–150 cm), and  $\text{Mg}^{2+}$  concentrations decrease to 48.2 mmol/L. Below this depth,  $\text{Mg}^{2+}$  and some of the  $\text{Ca}^{2+}$  concentrations increase by diffusive transport from the subsurface brine. As with the salinity and chloride profiles, the  $\text{Ca}^{2+}$  and  $\text{Mg}^{2+}$  gradients are steeper at Site 684 relative to those observed at Sites 680 and 681 (Figs. 40 and 41). However, the  $\text{Ca}^{2+}$  and  $\text{Mg}^{2+}$  profiles are not simple diffusion profiles but diffusion-reaction profiles. Authigenic calcite precipitation is responsible for the  $\text{Ca}^{2+}$  minimum at 12.3 mbsf, and the  $\text{Mg}^{2+} \rightleftharpoons 2\text{NH}_4^+$  ion exchange reaction may cause the small corresponding  $\text{Mg}^{2+}$  maximum. A maximum  $\text{Mg}^{2+}/\text{Ca}^{2+}$  ratio of 7.32 (molar) develops and influences the depth of onset and the rate of dolomite formation in underlying sediments. The  $\text{Mg}^{2+}/\text{Ca}^{2+}$  maximum is higher at this site than at Sites 680 and 681 (6.42 and 6.11, respectively; Fig. 42).

At Site 684, a profound lithified zone of dolomite was encountered in all three holes at the bottom of lithostratigraphic Subunit III, between ~38 and 50 mbsf. We terminated coring at Hole 684B because of this dolomite zone. The zone coincides with the subsurface depth where sulfate concentration reaches zero, alkalinity is at its maximum value, and the  $\text{Mg}^{2+}/\text{Ca}^{2+}$  ratio is that of seawater. All parameters indicate active dolomitiza-

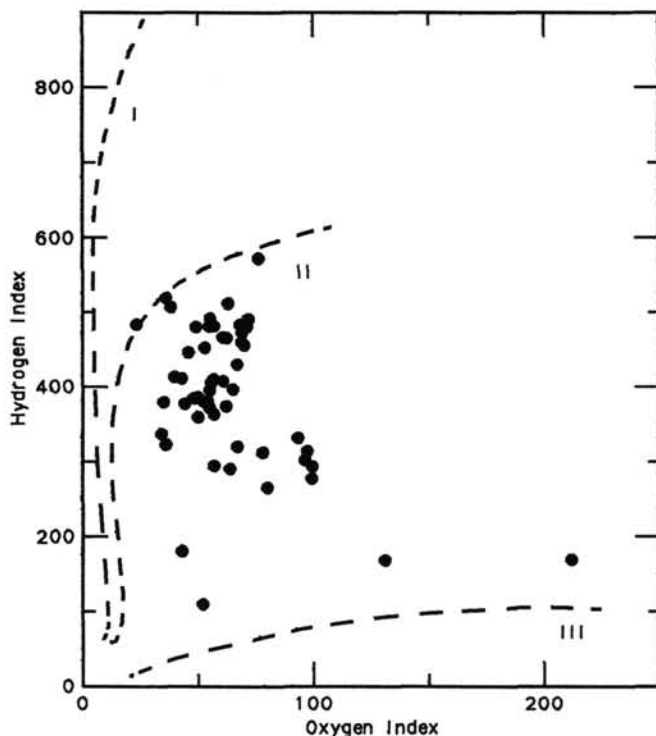


Figure 28. A van Krevelen-type diagram plotting the hydrogen and oxygen indices of Hole 684A samples.

tion. Below the dolomite zone, where the  $Mg^{2+}/Ca^{2+}$  ratios are  $<3$ , the rate of dolomite formation should decrease and, eventually, authigenic calcite could form again in the lower sections of Site 684.

$Ca^{2+}$  and  $Mg^{2+}$  concentrations increase with depth by approximately 25 mmol/L per 100 m ( $Ca^{2+}$  from ~6 to ~30 mmol/L;  $Mg^{2+}$  from ~50 to ~75 mmol/L).

## PALEOMAGNETICS

### Introduction

Shipboard paleomagnetic studies at Site 684 yielded results consistent with those obtained at earlier sites during Leg 112. Magnetic intensity decreased with depth to a level at which it could not be measured with the Molspin spinner magnetometer ( $<0.05$  mA/m). We obtained results at this site to a depth of 30 m in Holes 684A and 684B; cores covering this depth range from Hole 684C were not split and, consequently, not sampled. Later shore-based studies will involve the use of a cryogenic magnetometer. We hope that during these studies we will be able to measure successfully the weak remanent magnetization of deeper sections.

### Results

The declination, inclination, and intensity of magnetization are plotted vs. depth in Figures 43 and 44 for samples measured from Holes 684A and 684B, respectively. Cores were not oriented, and as a result the declination values have no absolute significance. The other two graphs, those of inclination and intensity of magnetization, are significant, and the correlation between the two holes is extremely good. The slight offset required to match the two sets of data is exactly that required to match up the lithologies at this level.

### Inclination

The graphs of inclination vs. depth for Holes 684A and 684B show two reversals: (1) from normal to reversed occurring (a) between Sample 112-684A-2H-5, 135 cm, and Sample 112-684A-2H-6, 135 cm (12.65–14.15 mbsf) and (b) Sample 112-684B-2H-2, 115 cm, and Sample 112-684B-2H-4, 115 cm (10.15–13.15 mbsf), and (2) from reversed to normal occurring in (a) Sample 112-684A-3H-3, 103 cm, and Sample 112-684A-3H-4, 103 cm (18.8–20.30 mbsf) and (b) Sample 112-684B-3H-3, 33 cm, and Sample 112-684B-3H-5, 33 cm (20.33–23.33 mbsf).

Interpreting either reversal requires consideration of the major lithological and paleontological boundary that coincides with the first reversal, which is the base of lithologic Unit I. Paleontologically, this boundary coincides with a hiatus representing a gap of roughly 2 m.y. Silicoflagellate and calcareous-nannoplankton studies (see "Biostratigraphy" section, this chapter) indicate that the lowest Pleistocene to uppermost Pliocene (approximately 0.4–2.4 Ma) sequence is missing.

The presence of this hiatus does not allow a clear interpretation of the younger of the two reversals. Possible interpretations include the following:

1. If the hiatus coincides with the base of lithologic Unit I, then this reversal is simply the juxtaposition of normally magnetized sediment from the Brunhes Chron with reversely magnetized material from the Gauss Chron or possibly the Matuyama Chron.
2. If the hiatus is higher in the section, then this reversal represents a later event within the Matuyama Chron or possibly the Gauss Chron.
3. However, if this hiatus is lower in the section, then this reversal most likely represents the Brunhes/Matuyama boundary.

Silicoflagellate and calcareous-nannoplankton studies do indicate that the hiatus continued until 0.4 Ma, still well within the Brunhes Chron. Therefore, we suggest that the first interpretation is correct.

The second reversal represents a later event within the Matuyama Chron or possibly the Gauss Chron. In addition, this reversal could possibly represent the Matuyama/Gauss boundary. However, the intensity values for samples from this depth range are at the limit to which the Molspin can measure. More detailed paleomagnetic and paleontological studies may help determine which interpretation is more reasonable for this reversal as well as the younger one.

### Intensity

In Holes 684A and 684B, as in the other Leg 112 holes, the intensity of magnetization of the samples decreased with increasing depth. Some variation in this general pattern can be seen (Figs. 43 and 44), as has been the case in previous holes. More detailed studies of these variations will be undertaken during post-cruise work with the hope of correlating between sites and possibly correlating these variations in intensity of magnetization with climatic variations and rates of deposition.

## PHYSICAL PROPERTIES

Physical-properties measurements at Site 684 were performed on split cores, generally at an interval of one every two sections (3 m) in good quality APC cores. XCB cores were not of sufficient quality for samples. In Holes 684A and 684B, good recovery in the APC cores allowed high sampling density. The first four cores of Hole 684C were not split; thus, samples for measuring physical properties were not retrieved in this hole. All of

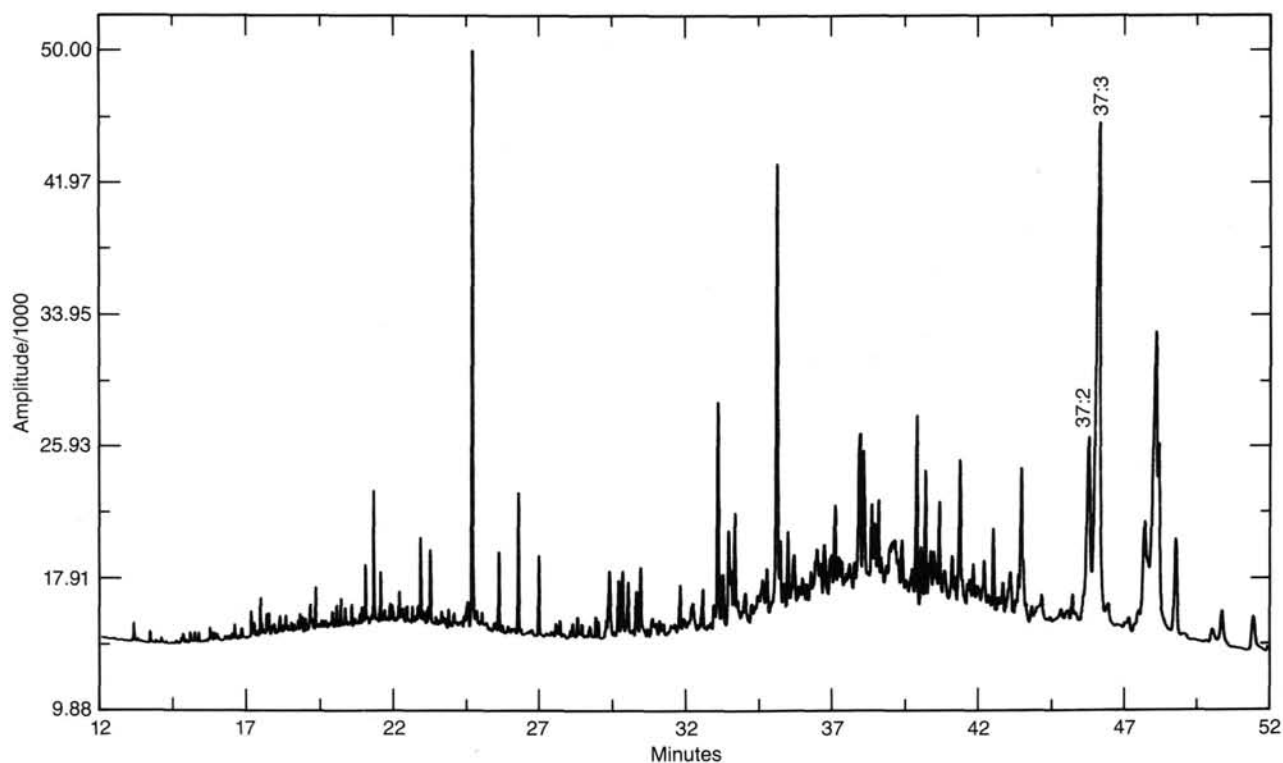


Figure 29. A gas chromatogram of a sediment from Sample 112-684A-7H-3, 30-31 cm, illustrating the abundance of alkenones. 37:2 =  $C_{37}$  alkadienone; 37:3 =  $C_{37}$  alkatrienone.

the cores from Holes 684B and 684C were processed through the GRAPE, with excellent correlations evident between the two holes. In general, the suite of physical-property data shows good correlation with the described lithology at Site 684.

### Index Properties

The index properties measured at Site 684 include water content (presented as a percentage of dry sample weight), porosity, bulk density, and grain density (Table 10). The methods specified in "Explanatory Notes" (this volume) were used to measure the index properties at Site 684. The salinity of the pore water increased with depth at this site, and the measured salinity (see "Inorganic Geochemistry" section, this chapter) was used to calculate index properties. Figure 45 illustrates the downhole trends in water content and porosity with depth and lithology for this site.

Core sections from Hole 684A were run through the GRAPE as time allowed. Usually, two or three sections of each core were processed. Cores from Holes 684B and 684C were processed in their entirety. Figure 46 shows the GRAPE data for the three holes of Site 684. Good correlation between the profiles for Holes 684B and 684C is apparent. The correlation is less obvious between Hole 684A and the other two holes, probably owing to the gaps in the data. This provides a strong case for processing all cores retrieved, particularly when it is important to establish a correlation between holes.

Figure 47 shows the bulk-density data obtained from samples of split cores superimposed on the GRAPE profiles. In general, the correlation of the GRAPE data with the bulk-density values obtained from the index-property samples was excellent. The XCB cores were run through the GRAPE; however, there were no bulk-density samples with which to check the validity of these data. Therefore, the bulk densities obtained from

the GRAPE profiles for the XCB cores must be used with caution. Data from previous sites of Leg 112 show that the GRAPE bulk densities are consistently lower than the sampled bulk densities in XCB cores. This is a result of the drilling slurry and sample disturbance in these cores. Future analyses will involve the detailed study of core descriptions and the selection of GRAPE data that were gathered in zones of apparently undisturbed sediment.

The water contents in lithologic Subunits IA and IB are fairly scattered and range from highs near 220% to lows of 132% to 140% (Fig. 45). A significant decrease in water contents occurs across the boundary between Subunit IB and Unit II, to values of 82% to 93%. The water contents calculated for Hole 684A appear to be slightly higher than those for Hole 684B. Smear slides indicate that the sediments in Hole 684B are generally coarser than those of Hole 684A (see "Lithostratigraphy" section, this chapter). The slightly lower water contents in Hole 684B may reflect some draining while obtaining samples of coarser-grained material or some function of decreased organic content. The general trend is of slightly increasing water content with depth through Units II and III. The data are sparse in Units IV and V, but the trend appears to be of decreasing water content in Unit IV and a sudden increase across the boundary between lithologic Units IV and V.

Porosities are fairly constant in lithologic Subunits IA and IB, ranging from 79% to 85%. A noticeable decrease in porosities (to values of 69%–70%) occurs across the boundary between subunit IB and Unit II. Porosities increase gradually through Units II and III, to values of 76% to 80% at approximately 35 mbsf. In Unit IV, the porosities appear to decrease from a value of 81% at 41 mbsf to a value of 72% at 50 mbsf, and then suddenly to increase across the boundary between Units IV and V, to 84% at 55 mbsf. In Unit V, the porosities appear to decrease with increasing depth.

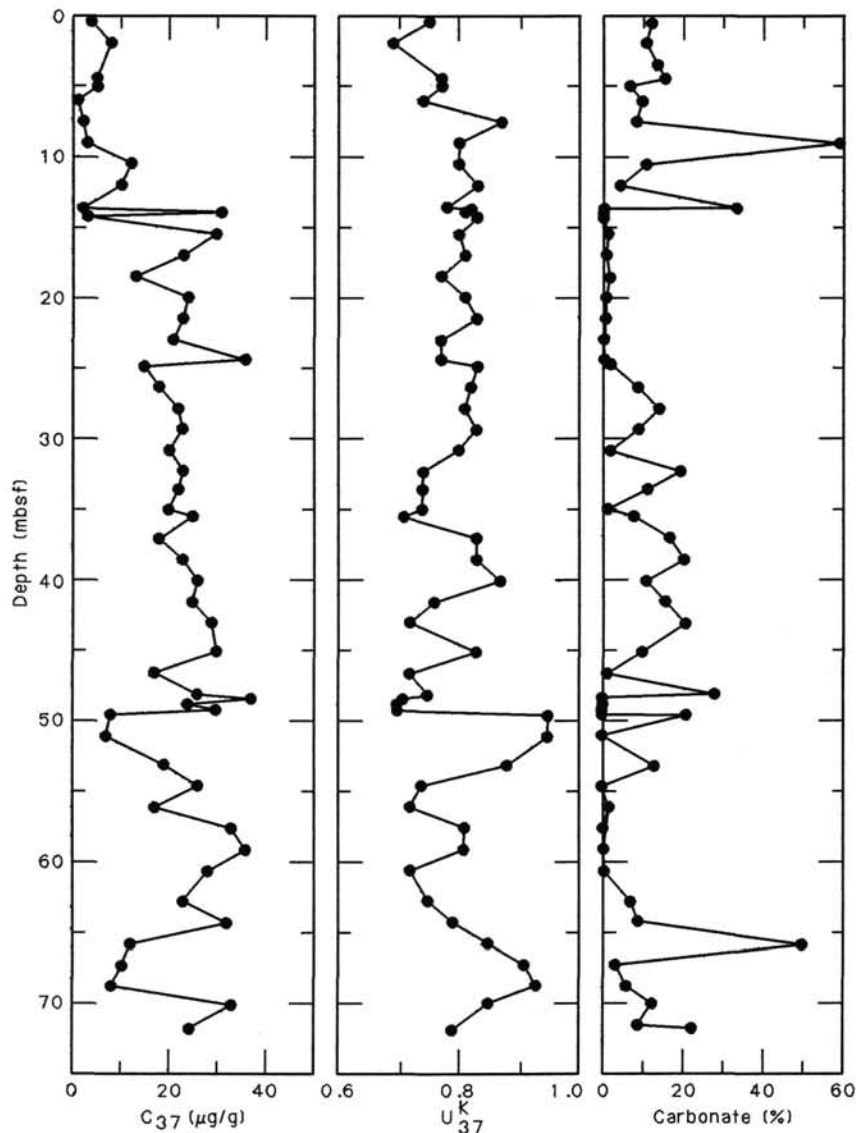


Figure 30.  $C_{37}$  alkadienone content ( $\mu\text{g/g}$ ) and the  $U_{37}^K$  ratio for extracts and the percentage of carbonate for the dry sediment of samples from Hole 684A, plotted vs. depth (mbsf). (Higher  $U_{37}^K$  ratios have been interpreted in terms of warmer water [Brassell et al., 1986a, 1986b]).

The bulk densities in Subunit IA increase from approximately  $1.35 \text{ g/cm}^3$  near the seafloor to values of  $1.42$  to  $1.45 \text{ g/cm}^3$  at just above the Subunit IA/IB boundary in both Holes 684A and 684B (Fig. 47). The two bulk-density samples from Subunit IB show a decrease in bulk density. This feature also shows up clearly in the profile of GRAPE data (Fig. 46). A sudden increase in bulk densities is seen at approximately the center of Subunit IB (at about 12 mbsf), to a value of  $1.7 \text{ g/cm}^3$ . This increase is particularly noticeable in the GRAPE plots for Holes 684B and 684C, where there is a continuous record of bulk density with depth. A shell-rich phosphatic sand layer, which is reflected on the GRAPE profile, occurs at the base of Subunit IB. The bulk densities decrease to  $1.5 \text{ g/cm}^3$  across the Subunit IB/Unit II boundary and continue to decrease gradually through Units II and III to  $1.4 \text{ g/cm}^3$  at the base of Unit IV, at approximately 54 mbsf. There are few data from Unit V, but bulk density appears to decrease across the boundary between Units IV and V, and remain fairly constant at  $1.35 \text{ g/cm}^3$  through Unit V.

### Compressional-Wave Velocity

The *P*-Wave Logger (PWL), which is run in conjunction with the GRAPE, was used to measure velocities through the sediments before the cores were split. Velocity data from the PWL were reduced manually by selecting reasonable values of velocity from shipboard printouts. The PWL velocity data for each hole are shown in Figure 48. The PWL does not provide reliable velocity data for XCB cores (see "Physical Properties" section, Site 682 chapter), and we attempted to retrieve Hamilton Frame samples from intact biscuits in the XCB cores of Site 684. However, we could not obtain samples good enough to give a clear signal.

In general, the velocities obtained are low because of the high water content of the sediments. The velocities range between 1500 and 1600 m/s, with a few values near 1650 m/s that can be correlated to maxima in the bulk densities of the GRAPE profiles. The velocity profiles generally correlate well to the

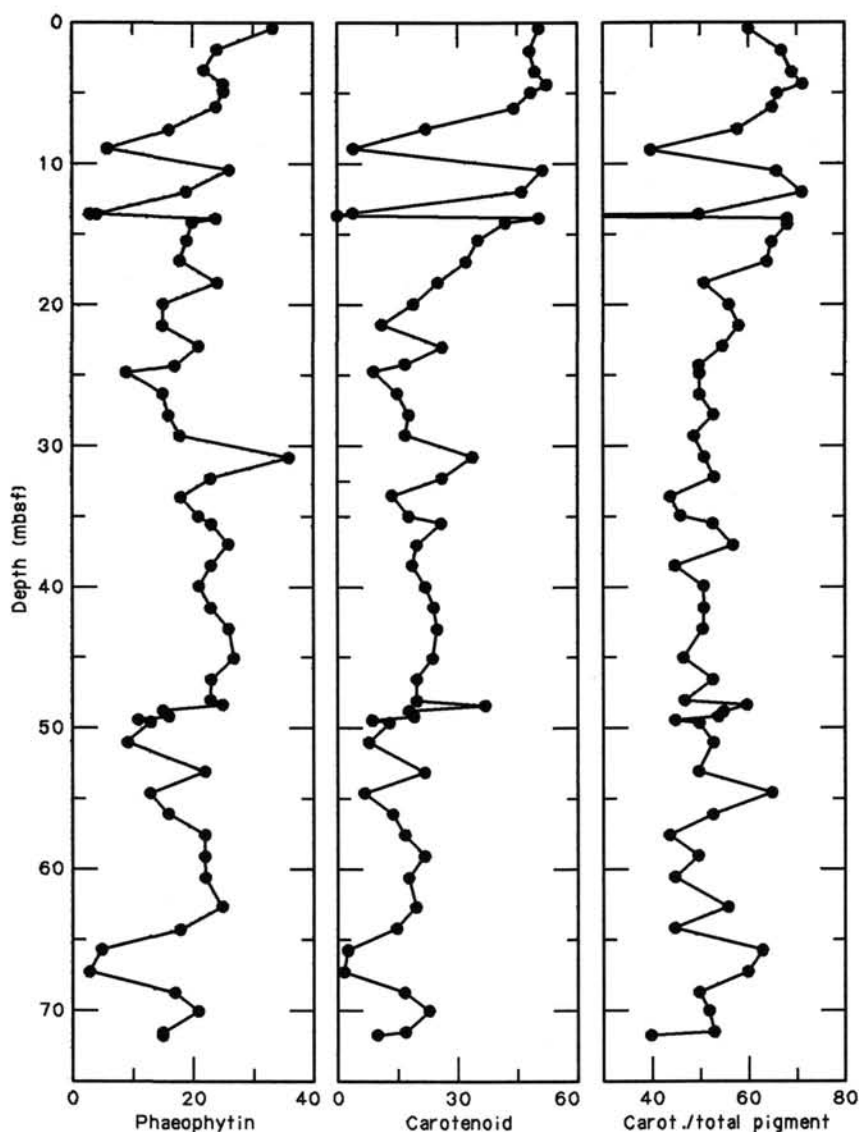


Figure 31. Concentrations (in arbitrary units) of gross "phaeophytin" and "carotenoids," and the ratio of "carotenoids" to total pigment plotted downhole for Hole 684A.

bulk-density profiles. For example, the sudden decrease and then increase in the velocities of Hole 684C at around 20 mbsf is reflected in the same behavior of the bulk-density profile for that hole.

### Vane Shear Strength

The undrained vane-shear-strength measurements for Site 684 were performed with the Wykham Farrance vane apparatus in split cores of Holes 684A and 684B. Values obtained for peak undrained shear strength are presented in Table 11 and are shown vs. depth below seafloor in Figure 49.

The vane shear strengths at Site 684 are low near the mud line, compared with other Leg 112 sites. The values increase fairly uniformly from 27 to 31 kPa near the mud line to 99 kPa at 25 mbsf. The boundaries between lithologic Subunits IA and IB and between Subunit IB and Unit II are not marked by significant changes in shear strength. Such a change was expected at the Subunit IB/Unit II boundary, where a major decrease in water contents occurs. Below 25 mbsf, the data are too scattered to draw any conclusions regarding trends with depth, but shear

strengths appear to be increasing slightly with increasing depth below seafloor.

Total overburden stresses were calculated for Hole 684A, using bulk-density measurements and assuming hydrostatic pore-pressure conditions. The total stress profile and the assumed hydrostatic profile are shown vs. depth below seafloor in Figure 50. Changes in slope of the total stress curve occur at approximately 40 and 54 mbsf, which corresponds to the boundaries between lithologic Units III and IV and Units IV and V, respectively. The ratio of peak undrained vane shear strength to effective overburden pressure ( $C_u/P'$ ) is plotted vs. depth below seafloor for Hole 684A (Fig. 51). Theoretically, the ratio of  $C_u/P'$  should be very high near the mud line and decrease quickly to a constant value with depth.  $C_u/P'$  deviates noticeably from the theoretical profile at several locations. The first corresponds to the low bulk densities of the upper one-half of Subunit IB, at 10.7 mbsf. The three points at 31, 36, and 40.5 mbsf reflect the high shear strengths combined with low bulk densities measured in this sequence. The same conditions cause the deviation in the  $C_u/P'$  profile at 58 mbsf.

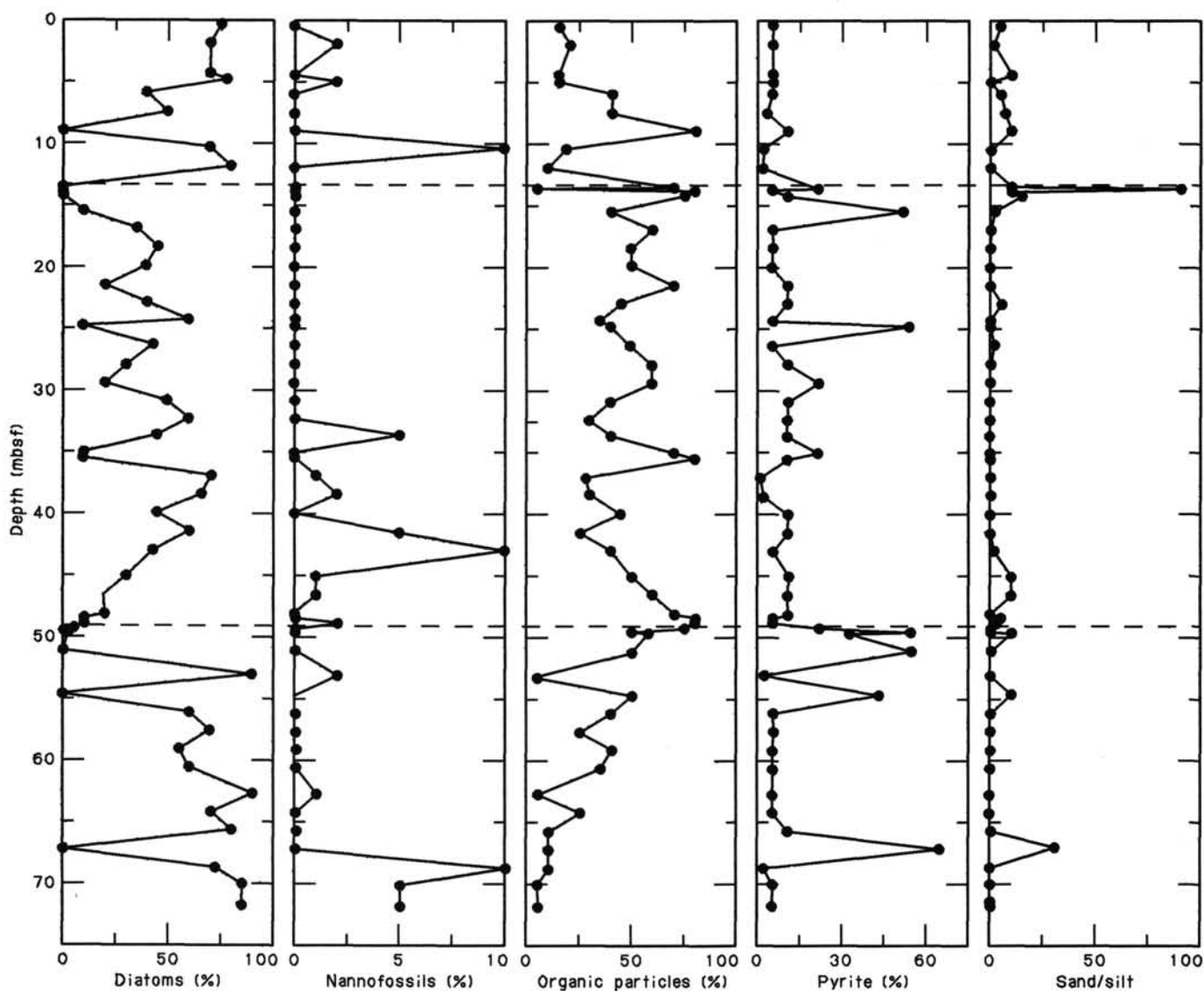


Figure 32. Distribution of particles, estimated microscopically by a smear-slide technique (% of particles), plotted vs. depth at Hole 684A.

### Thermal Conductivity

Thermal conductivity was measured by means of the needle-probe method, mainly on Hole 684B samples. At Hole 684B, a very hard layer was encountered while retrieving Core 112-684B-5H; measurements were possible only to Core 112-684B-4H. Additional measurements were attempted at Hole 684C, but good samples were recovered only to Core 112-684C-5H. In consequence, the thermal conductivity could not be obtained below 40 mbsf. The results are summarized in Table 12 and Figure 52.

The variation of thermal conductivity in lithologic Units I and II correlates well with the variation in GRAPE bulk density (Fig. 46). In Unit III, the thermal conductivity is fairly constant and most of the values are between 0.8 and 0.9 W/m·K. Figure 53 shows that thermal conductivity does not vary significantly with changes in water content. This suggests that the difference in grain thermal conductivity between lithologic Units I and II (and III) compensates for the difference in water content.

### Summary and Discussion

Lithologic Subunits IA and IB are characterized by high water contents (140% to 220%) and high porosities (greater than

80%). Bulk densities increase steadily from 1.35 near the mud line to 1.45 g/cm<sup>3</sup> at the bottom of Subunit IA. The low bulk densities are associated with the upper part of Subunit IB and are probably from drilling disturbance of this sandy interval. Firmer sand gives an abrupt maximum in the profile at the base of Subunit IB, and the layer of shell-laden phosphatic sand at the Subunit IB/Unit II boundary shows up clearly in the GRAPE profiles. There is no obvious correlation with CaCO<sub>3</sub> diagenesis as outlined in the "Inorganic Geochemistry" section (this chapter).

A sudden decrease in water contents and porosities occurs across the boundary between lithologic Subunit IB and Unit II. However, instead of continuing to decrease with increasing depth below seafloor, these values increase through Units II and III. Bulk densities decrease slightly over the same depth. This trend is contrary to the behavior expected of a normally consolidating sediment column. The slightly higher bulk densities in lithologic Units II and IV, noticeable on the GRAPE profiles, are probably the result of the less-diatomaceous, black silty mud having phosphatic nodules that is found in these units.

The values obtained for water content and porosity in Hole 684A appear to be consistently lower than those obtained for Hole 684B in lithologic Unit II and the upper part of Unit III. The GRAPE and vane-shear-strength profiles also appear to be

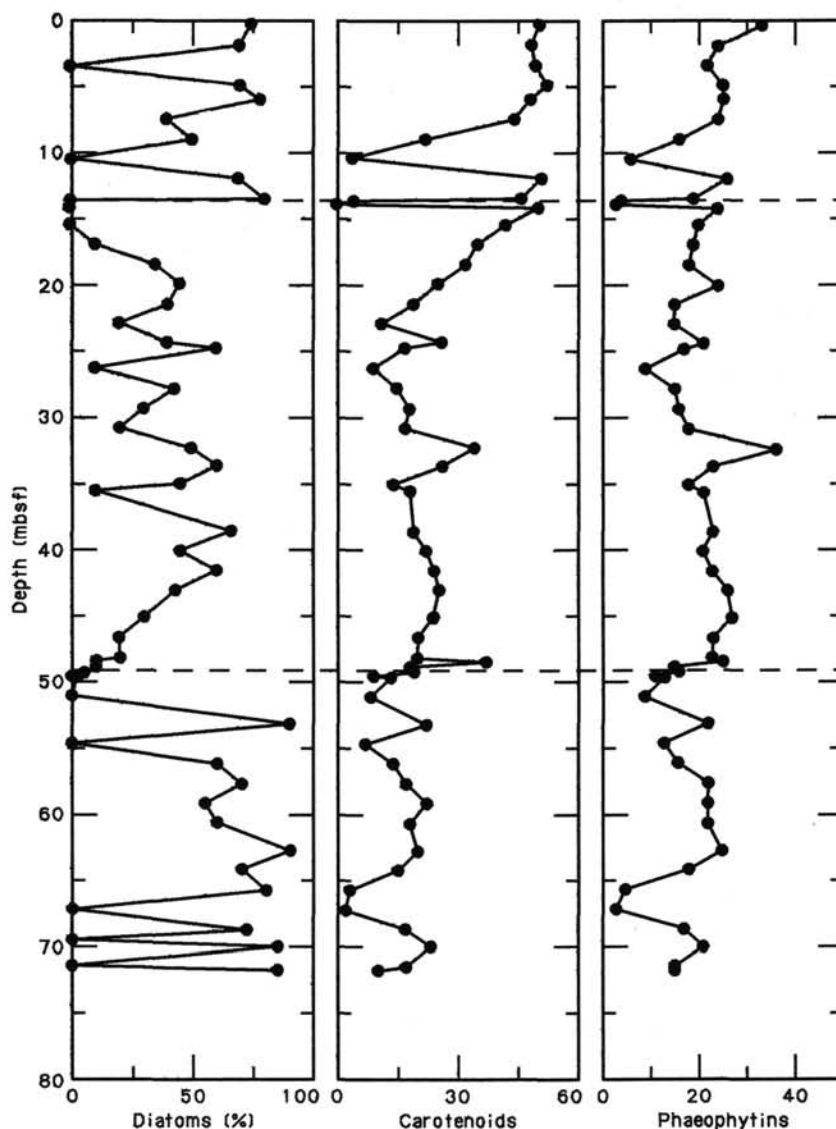


Figure 33. Correlation between independent spectrophotometric and microscopic estimates of phytoplankton contributions to Peru margin sediments for the top 75 m of Hole 684A. Gross "phaeophytin" and "carotenoid" concentrations were measured by extraction of the sediment with aqueous acetone, followed by absorptiometry in the visible spectrum. The data are expressed in relative, but arbitrary units, and are comparable downcore. Diatoms represent percentage abundance of data, as detailed in Fig. 32.

slightly different between the two holes. Lithologic differences between the holes (as indicated by smear slides and visual descriptions) are discussed in the "Lithostratigraphy" section (this chapter). Shore-based grain size and Atterberg limit analyses are expected to verify these suspected differences.

## GEOPHYSICS

### Structure and Seismic Records

Site 684 was located in a small Holocene sediment pond near the seaward flank of the Trujillo Basin. The Trujillo Basin is complexly faulted and, according to Thornburg (1985), reflects a history of superimposed compressional and tensional tectonism. Reverse faults with short vertical displacement are common, and Site 684 was positioned at 424 m of water depth within a structural depression bounded by block-faulted Neogene strata. The pond is approximately 2 km across and, apparently, of limited extent along strike.

The continental shelf off north-central Peru is a broad, shallow, current-swept platform, and the small basin at Site 684 probably intercepted sediments that were transported beyond the shelf break. Site selection was initially based on the SCS Line YALOC #2030 (1-3-72), obtained during the Nazca Plate Project (Kulm et al., 1981; Thornburg and Kulm, 1981). An interpreted section of this line is shown in Figure 54. Seismic information was subsequently improved through MCS Line #2025 (Thornburg, 1985), and a concurrent 3.5-kHz profile also was made. The combined information shows a maximum of about 0.15 s of Holocene sediment in the otherwise barren region. The sediment pond rests on an irregular unconformity surface; shallow reflectors onlap or terminate abruptly against fault blocks, causing sediment thickness to vary rapidly across short distances. A rapid lateral pinch-out of these recent sediments was obvious in the 3.5-kHz record during our approach to the site. About 2 km north-northeast along the strike of the basin, no Holocene sediment cover occurred at all (see "Operations" section, this

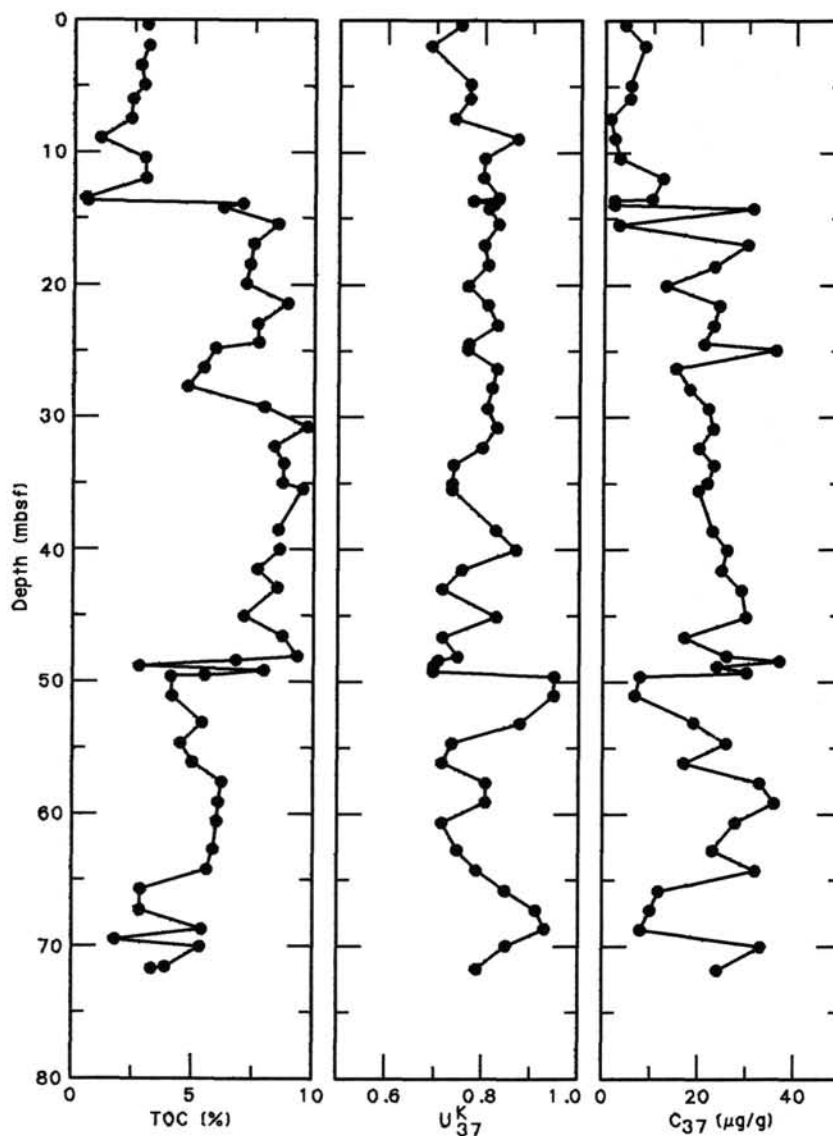


Figure 34. Parallel depth plots downhole at Hole 684A for TOC, determined with the Rock-Eval pyrolysis device, and two lipid parameters. Total amount of the 37:2 alkadienone in  $\mu\text{g/g}$  dry sediment (37K) correlates with TOC, indicating a reasonably consistent composition for the organic matter in the sediment. The ratio  $U_{37}^K$ ,  $(37:2/(37:2 + 37:3))$  behaves independently and shows no readily interpretable distribution.

Table 8. Geochemical data for Site 684.

Core/section interval (cm)	Depth (mbsf)	pH	Salinity (g/kg)	Cl <sup>-</sup> (mmol/L)	Alkalinity (mmol/L)	SO <sub>4</sub> <sup>2-</sup> (mmol/L)	PO <sub>4</sub> <sup>3-</sup> ( $\mu\text{mol/L}$ )	NH <sub>4</sub> <sup>+</sup> (mmol/L)	SiO <sub>2</sub> ( $\mu\text{mol/L}$ )	Ca <sup>2+</sup> (mmol/L)	Mg <sup>2+</sup> (mmol/L)	Mg <sup>2+</sup> /Ca <sup>2+</sup>
112-684B-1H-3, 145-150	4.5	7.6	34.5	557.09	12.82	17.66	5.74	2.03	1095	8.67	51.13	5.90
3H-3, 145-150	21.5	7.7	38.2	638.18	22.58	1.72	—	5.53	1136	8.25	52.76	6.40
112-684C-1H-3, 145-150	4.5	—	34.5	558.05	12.33	17.57	16.55	2.09	1109	8.63	51.01	5.91
2H-3, 145-150	12.3	7.8	35.0	575.22	18.66	7.06	11.63	4.03	1167	6.58	48.17	7.32
3H-3, 145-150	21.8	7.8	37.9	646.76	22.26	2.01	—	5.36	1077	7.79	51.93	6.67
4H-6, 145-150	35.8	7.8	41.8	694.46	23.85	0.78	—	6.64	1055	10.93	57.38	5.25
5H-1, 145-150	37.8	7.8	42.5	724.88	23.56	0.10	—	6.53	1082	11.62	59.99	5.16
6X-1, 145-150	40.5	7.4	44.0	755.56	23.51	0.0	—	7.20	1136	12.91	60.54	4.69
7X-2, 145-150	51.5	7.6	46.4	774.74	20.90	0.44	—	9.02	1454	15.77	62.42	3.96
8X-2, 92-97	60.4	7.5	50.5	861.03	15.66	0.0	8.14	10.23	1181	19.42	66.47	3.42
10X-1, 35-40	<sup>a</sup> 77.4	<sup>a</sup> 7.6	<sup>a</sup> 51.7	<sup>a</sup> 897.47	<sup>a</sup> 15.93	<sup>a</sup> 2.72	<sup>a</sup> 9.12	<sup>a</sup> 11.07	1010	<sup>a</sup> 22.64	<sup>a</sup> 68.15	<sup>a</sup> 3.01
11X-1, 145-150	88.0	7.5	55.8	940.62	17.34	0.30	9.34	12.48	1140	26.78	71.32	2.66
13X-1, 140-145	106.9	7.3	59.7	1028.83	12.95	0.0	4.64	14.20	1041	29.78	73.94	2.48

<sup>a</sup> Core was highly disturbed; data (for example, SO<sub>4</sub><sup>2-</sup>) indicate small amounts of admixed drillhole water; — = solutions developed a brown color instead of a blue color when prepared for colorimetry.

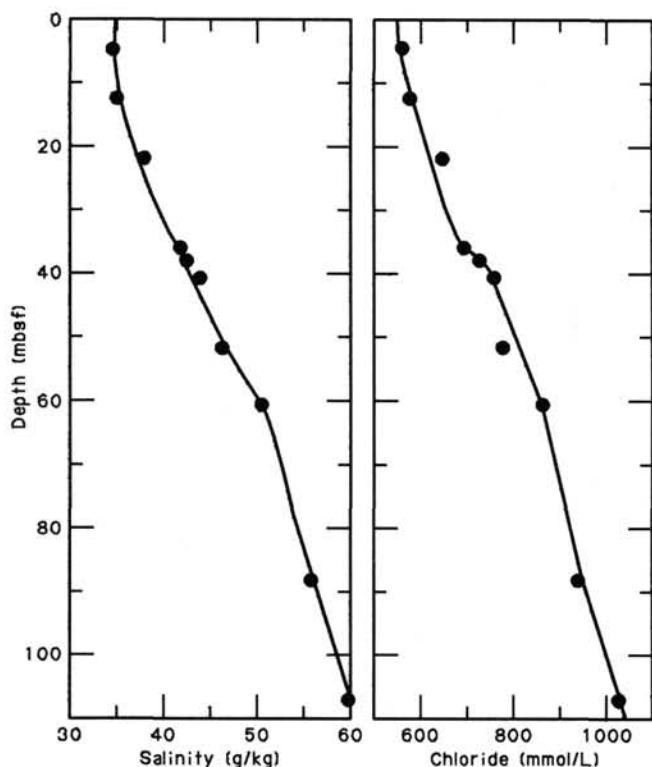


Figure 35. Interstitial salinity and chloride for Site 684.

chapter), whereas subsequent relocation in the opposite direction revealed increasingly thicker strata that eventually were penetrated by drilling at Site 684.

Because of the difficulties anticipated in locating this site, we did not deploy any single-channel seismic gear from the *JOIDES Resolution* so as to maintain better maneuverability. An additional 3.5-kHz record was obtained while drilling Hole 684A, and several sub-bottom reflectors could be correlated to lithologic changes within the recovered section. Two 1-m-thick, sandy shell beds between 10 and 14 mbsf and a massive dolomite bed at 39 mbsf probably correspond to the high-amplitude reflections observed on this record. The SCS line shows a seaward-dipping, disconformable contact about 70 m below the Holocene sediment fill. At this depth, the Pliocene/Miocene hiatus was overlain by more than 10 m of glauconitic and phosphatic sand. Thus, the Holocene sediment ponded in this local basin corresponds to the Pliocene-Quaternary section of the drill hole at Site 684.

### Heat Flow

#### Temperature Measurements

Temperatures were measured twice with the APC tool at Site 684 while retrieving Cores 112-684A-4H and 112-684A-6H. Measurements with the T-probe were not conducted because of very hard sediments. Good quality temperature records were obtained, and the record from Core 112-684A-6H is shown in Figure 55 as an example. The extrapolated final temperatures are 10.4°C ( $\pm 0.4^\circ\text{C}$ ) at 33.8 mbsf (Core 112-684A-4H) and 11.1°C ( $\pm 0.2^\circ\text{C}$ ) at 52.8 mbsf (Core 112-684A-6H).

#### Heat Flow Estimation

The two equilibrium temperatures give a geothermal gradient of  $37 \times 10^{-3} \text{ K/m}$  for the depth range from 33.8 to 52.8 mbsf. This value may have a large error for the short depth interval as these equilibrium temperatures have large errors. Thermal-con-

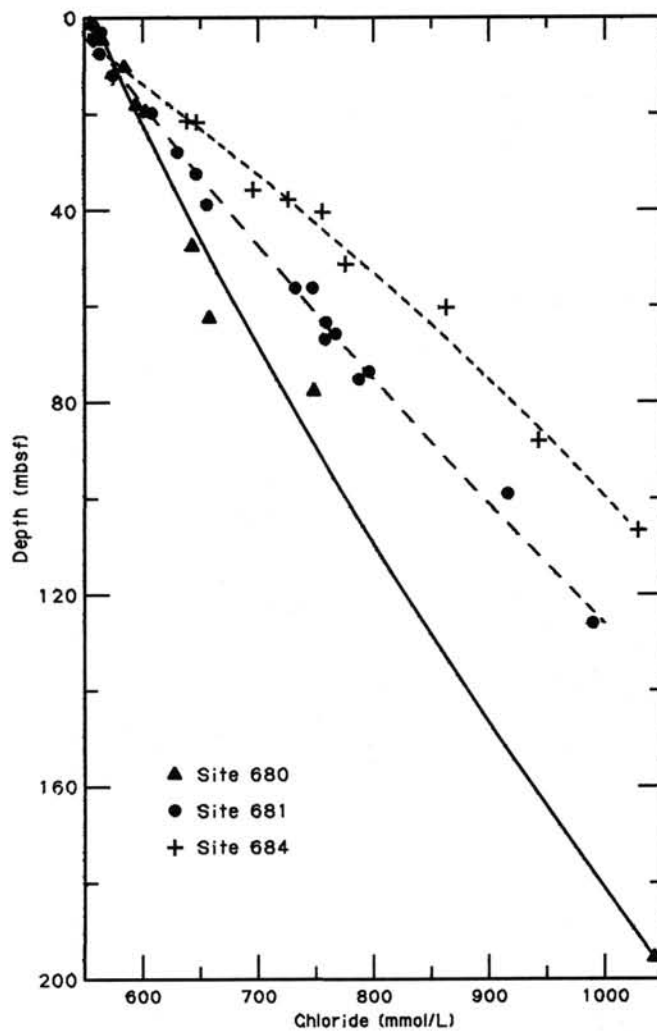


Figure 36. Interstitial chloride for Sites 680, 681, and 684.

ductivity measurements at Site 684 were performed on Cores 112-684B-1H to 112-684A-4H and 112-684C-5H. In consequence, only two thermal-conductivity data points exist for the depth range where the temperature gradient was obtained. The thermal conductivity of ocean sediments is mainly determined by the water content (Ratcliffe, 1960). As the water content of Cores 112-684A-5H and 112-684A-6H seems near that of Core 112-684B-4H (see "Physical Properties" section, this chapter), the thermal-conductivity data of Core 112-684B-4H may be used to calculate heat flow. The average thermal conductivity of Core 112-684B-4H is 0.84 W/m·K, after correcting for temperature and pressure effects. Thus, the heat flow at Site 684 is estimated at about 31 mW/m<sup>2</sup>. The error might exceed 20 mW/m<sup>2</sup>. This heat-flow value is lower than the 45 to 60 mW/m<sup>2</sup> obtained at the southern shelf sites, Sites 686 and 687 (see "Geophysics" sections, Sites 686 and 687 chapters). Considering the large error in the heat flow at Site 684, however, the difference may not be significant.

### SUMMARY AND CONCLUSIONS

Drilling at Site 684 addressed the questions of latitudinal variability of upwelling parameters, facies differentiation from reworking of sediments by the poleward undercurrent, and the influence of hypersaline pore fluids on early diagenesis. The variability of upwelling parameters along the Peruvian coast is expressed by the species composition of biologic assemblages, by

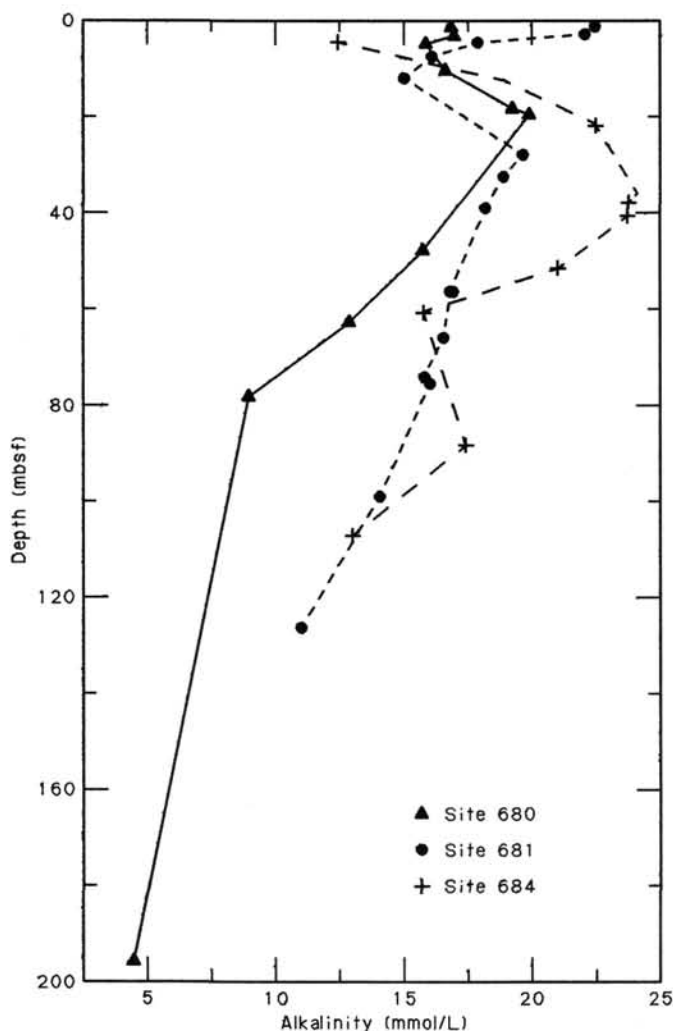


Figure 37. Interstitial alkalinity for Sites 680, 681, and 684.

biomarkers, and by stable-isotope signals of calcareous plankton and benthos that respond to changes in water properties. Sediments at Site 684 may have recorded the extent of equatorial water incursions during upwelling (El Niño-type conditions) in greater detail than did the sediments at more southern sites along the transect. Sediments of the upper continental slope and outer shelf in the south consist of organic-carbon-rich muds that accumulate where the shelf is narrow and steep. In the north, where the shelf is wide and shallow, one can see an accumulation of calcareous organic-carbon-rich muds that are coarser in texture and contain phosphorites and glauconites. This accumulation results from reworking and exporting of fine-grained constituents by a poleward-flowing undercurrent. This undercurrent is an important part of the upwelling circulation system. Site 684 was selected to sample time intervals over which the calcareous and residual facies had been accumulating in the northern part of the operational area of Leg 112. Subsurface hypersaline pore fluids, discovered at Sites 680 and 681, strongly influence diagenetic reaction pathways, particularly those of dolomitization and methanogenesis.

Drilling at Site 684, the northern point of a transect along the Peruvian coastal upwelling regime, contributed to these diverse objectives in several ways. The site was located in a small sediment pond on the seaward flank of the Trujillo Basin in an area otherwise devoid of sediments. The pond has a limited areal extent along strike and rests on an irregular, unconformable

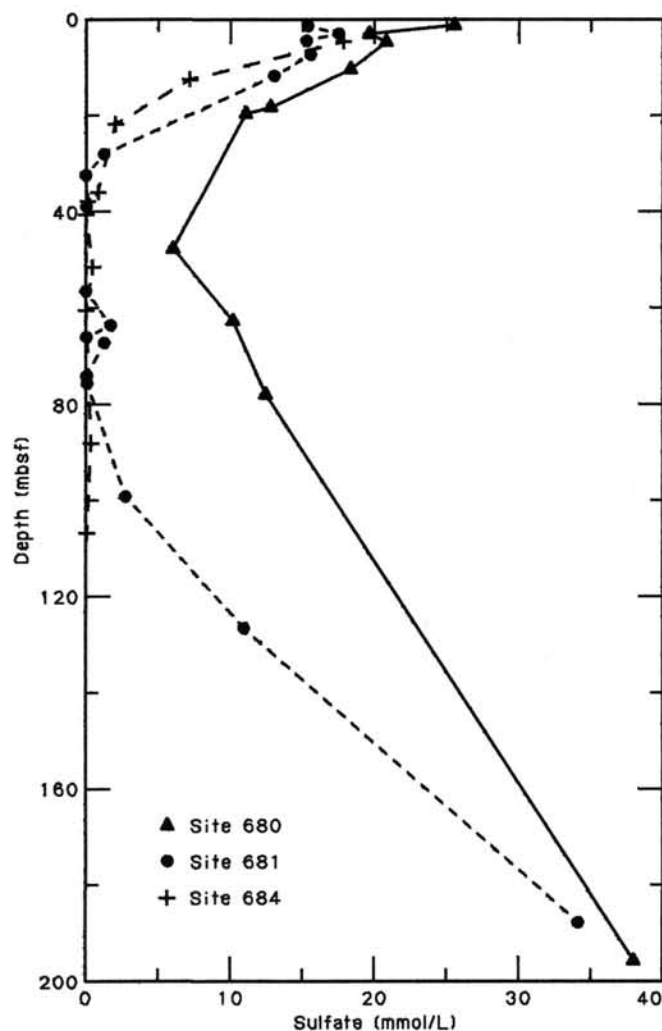


Figure 38. Interstitial sulfate for Sites 680, 681, and 684.

surface that separates the Miocene strata of the Trujillo Basin from Pliocene-Quaternary sediments. The continental shelf is a broad, shallow, and current-swept platform. A sediment pond lies beneath the seaward trail of frequent upwelling plumes that cross this shelf. The sediments at Site 684 provided a record of upwelling in three distinct chronological stratigraphic sections of late Quaternary, Pliocene, and Miocene age. Two hiatuses separate these sections from each other. The first occurs at 13.5 mbsf, where it divides < 0.9-Ma-old, well-laminated, olive and gray diatomaceous muds interbedded with coarse, calcareous, phosphatic and terrigenous beds (< 0.9 Ma) from underlying Pliocene (3.5-4 Ma), bioturbated, dark to olive gray mud with microfossil- and macrofossil-bearing units. The second hiatus at 56.2 mbsf in Hole 684A (59.5 mbsf at Hole 684C) separates these deposits from > 7.8-Ma-old, olive gray, nannofossil-bearing diatomaceous mud of Miocene age with laminated and mottled beds to the bottom of the holes. The six lithologic units and subunits that comprise these three intervals alternate between hemipelagic upwelling facies and a facies that is influenced by current deposition. Perhaps the current-dominated facies represents periods of intense activity of the undercurrent.

The late Quaternary upwelling environment (Subunit IA) is characterized by well-preserved diatom and coccolith assemblages. In the current-dominated section (Subunit IB), normally graded beds of shell debris, foraminifers, bone fragments, and glauconitic and phosphatic grains are common. The Pliocene

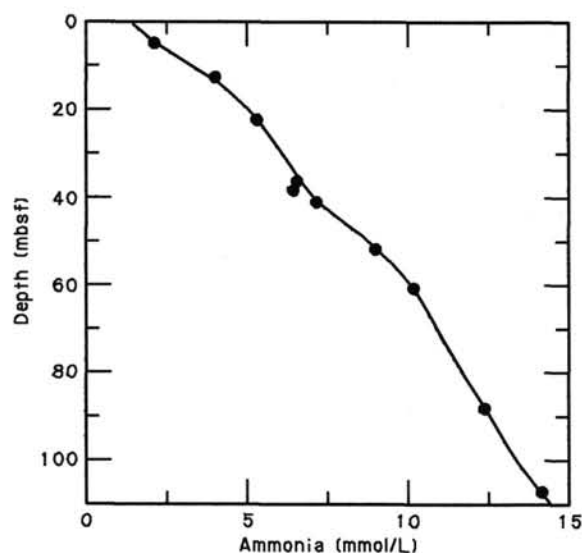


Figure 39. Interstitial ammonia for Site 684.

depositional environment (lithologic Units II, III, and IV) was located in shallow water and generally less influenced by coastal upwelling. Bioturbation, erosional contacts, and coarse-grained beds are prevalent in Units II and IV. Diagnostic diatom and coccolith upwelling assemblages are rare, although organic-matter contents are high (7–9 wt% organic carbon in Unit III). The Miocene “upwelling” environment is characterized by frequent blooms of diatoms and coccoliths that show little evidence of reworking. These indicate a high supply of nutrients to surface waters during brief, alternating cold and warm phases. Perhaps the warm phases represent periods during which upwelling was generated from equatorial rather than Antarctic subsurface waters.

The nature of sedimentary organic matter deposited during Quaternary Subunit IA, Pliocene Unit III, and Miocene Unit V indicate sources from coastal upwelling ecosystems. TOC contents are high during these intervals, as are hydrogen indices and the contents of biomarkers, which are dominated by unsaturated ketones. These biomarkers could potentially record the upwelling temperature distribution and are believed to be produced by coccolithophorids. These algae may be either preferentially associated with or better preserved during the “warm” water incursions noted in the floral assemblages. At this time, these conclusions are tenuous and must be substantiated in much greater detail by shore-based analyses. Interestingly, the nature of the sedimentary organic matter in the reworked intervals indicates high oxygen indices and significantly higher temperatures of maximum pyrolytic release ( $T_{max}$  Rock-Eval parameter), particularly at the unconformities. The total quantity of organic carbon is also much less in these intervals than elsewhere. Such characteristics can be expected from reworking of sediments in an oxygenated environment before burial.

The current-deposited, shallower water units also contain abundant dense phosphate peloids and glauconites. The phosphate-glauconite beds are produced by short-lived winnowing of diatomaceous muds in which grains of these authigenic phases had formed. Beds in lithologic Units II and IV are condensed sequences associated with major hiatuses that correlate with eustatic low stands of sea level. The diatomaceous upwelling units contain authigenic carbonates and friable phosphates. Calcite and dolomite are present as disseminated crystals in unlithified muds and as fully lithified nodules and beds. Intervals having pronounced concentrations of calcite and dolomite coincide with zones of significant changes in the  $Ca^{2+}/Mg^{2+}$  ratio of hypersaline pore waters.

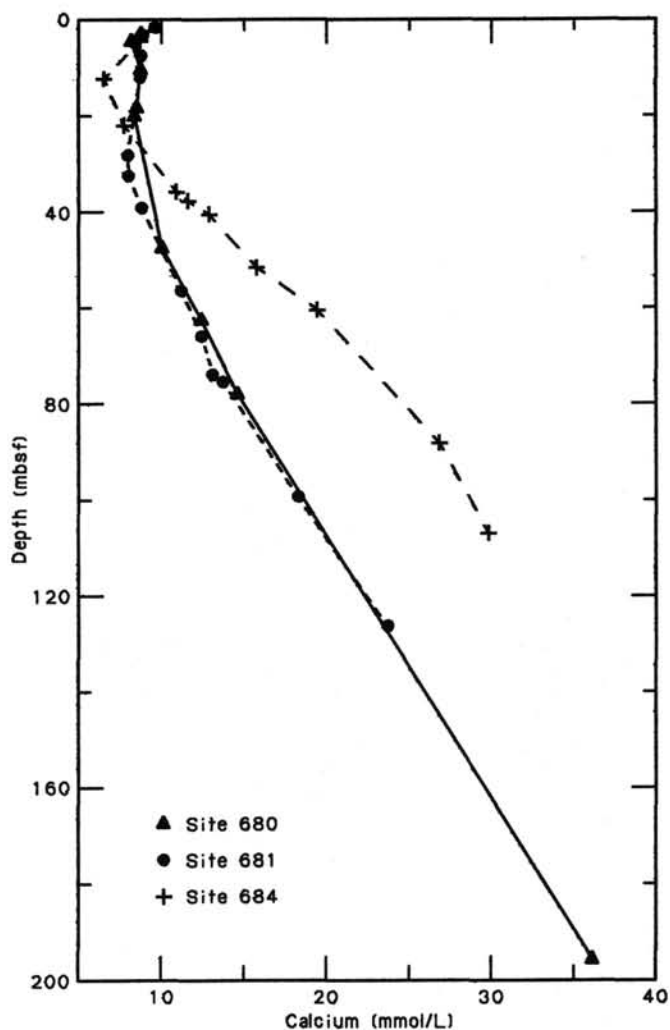


Figure 40. Interstitial calcium for Sites 680, 681, and 684.

These fluids were previously discovered in the subsurface of the Peru outer shelf at Sites 680 and 681 and were encountered again at Site 684, 200 km farther north. Chloride and dissolved major ion contents at the bottom of Hole 684C increased to concentrations twice those of seawater. The areal extent of the subsurface brine over the Peru shelf appears enormous. Its origin remains unknown. Microbial sulfate reduction and methanogenesis, the important driving mechanisms of carbonate and organic-matter diagenesis, are closely controlled by the brine influx. This is documented by the methane, alkalinity, and dissolved sulfate distribution in pore fluids of the sediments from Site 684.

#### REFERENCES

- Barron, J., 1985. Late Eocene to Holocene diatom biostratigraphy of the equatorial Pacific Ocean, Deep Sea Drilling Project Leg 85. In Mayer, L., Thayer, F., Thomas, E., et al., *Init. Repts. DSDP*, 85: Washington (U.S. Govt. Printing Office), 413–456.
- Baturin, G. N., 1971. Stages of phosphorite formation on the ocean floor. *Nature Phys. Sci.*, 232:61–62.
- Berggren, W. A., Aubry, M. P., and Hamilton, N., 1983. Neogene magnetobiostratigraphy of DSDP Site 516 (Rio Grande Rise, South Atlantic). In Barker, P. F., Carlson, R. L., Johnson, D. A., et al., *Init. Repts. DSDP*, 72: Washington (U.S. Govt. Printing Office), 675–706.
- Blow, W. H., 1969. Late middle Eocene to Recent planktonic foraminiferal biostratigraphy. In Brönnimann, R., and Renz, H. H. (Eds.), *Proc. 1st Int. Conf. Planktonic Microfossils*, Geneva, 1967, 1:199–421.

- Brassell, S. C., Eglinton, G., Marlowe, I. T., Sarnthein, M., and Pflaummann, U., 1986a. Molecular stratigraphy: a new tool for climatic assessment. *Nature*, 320:129-133.
- Brassell, S. C., Brereton, R. G., Eglinton, G., Grimalt, J., Liebezeit, G., Marlowe, I. T., Pflaummann, U., and Sarnthein, M., 1986b. Palaeoclimatic signals recognised by chemometric treatment of molecular stratigraphic data. In Leythaeuser, D., and Rullkötter, J. (Eds.), *Advances in Organic Geochemistry 1985*. Org. Geochem., 10:649-660.
- Burnett, W. C., 1977. Geochemistry and origin of phosphorite deposits from off Peru and Chile. *Geol. Soc. Am. Bull.*, 88:813-823.
- Ekdale, A. A., Bromley, R. G., and Pemberton, S. G., 1984. Ichnology. *Soc. Econ. Paleontol. Mineral. Short Course Notes*, 1-317.
- Haq, B. U., Hardenbol, J., and Vail, P. R., 1987. Chronology of fluctuating sea levels since the Triassic (250 million years to present). *Science*, 235:1150-1167.
- Hsü, K. J., et al., 1977. History of the Mediterranean salinity crisis. *Nature*, 267:399-403.
- Kennett, J. P., 1973. Middle and late Cenozoic planktonic foraminiferal biostratigraphy in the southwest Pacific-DSDP Leg 21. In Burns, R. E., Andrews, J. E., et al., *Init. Repts. DSDP*, 21: Washington (U.S. Govt. Printing Office), 575-640.
- Kulm, L. D., Dymond, J., Dash, E. J., and Hussong, D. M. (Eds.), 1981. *Nazca Plate: Crustal Formation and Andean Convergence*. Geol. Soc. Am. Mem. 154.
- Kulm, L. D., Suess, E., and Thornburg, T. M., 1984. Dolomites in organic-rich muds of the Peru forearc basins: analogue to the Monterey Formation. In Garrison, R. E., Kastner, M., and Zenger, D. H. (Eds.), *Dolomites of the Monterey Formation and Other Organic-Rich Units*. Pacific Section Soc. Econ. Paleontol. Mineral., 41:29-47.
- Kvenvolden, K., and McDonald, T. J., 1986. *Organic Geochemistry on the JOIDES Resolution—an Assay*. Ocean Drilling Program Technical Note No. 6.
- Locker, S., and Martini, E., 1986. Silicoflagellates and some sponge spicules from the southwest Pacific, Deep Sea Drilling Project, Leg 90. In Kennett, J. P., von der Borch, C. C., et al., *Init. Repts. DSDP*, 90: Washington (U.S. Govt. Printing Office), 887-924.
- Martini, E., 1969. Nannoplankton aus dem Miozan von Gabon (Westafrika). *Neues Jahrb. Geol. Paläontol. Abhand.*, 132:285-300.
- Parsons, T. R., Maita, Y., and Lalli, C. M., 1984. *In A Manual of Chemical and Biological Methods for Seawater Analysis*: Oxford (Pergamon Press), 4.
- Poutanen, E.-L., and Morris, R. J., 1983. The occurrence of high molecular weight humic compounds in the organic rich sediments of the Peru continental Shelf. *Oceanol. Acta*, 6(1):21-28.
- Ratcliffe, E. H., 1960. The thermal conductivities of ocean sediments. *J. Geophys. Res.*, 65:1535-1541.
- Ridout, P. S., Morris, R. J., and Tibbetts, P.J.C., 1986. Possible origins of a novel carotenoid in sediments from two organic-rich sites. *Chem. Ecol.*, 2:73-78.
- Srinivasan, M. S., and Kennett, J. P., 1981. Neogene planktonic foraminiferal biostratigraphy and evolution: Equatorial to Subantarctic South Pacific. *Mar. Micropaleontol.*, 6:499-533.
- Suess, E., Kulm, L. D., and Killingley, J. S., 1987. Coastal upwelling and a history of organic-rich mudstone deposition off Peru. In Brooks, J., and Fleet, A. J. (Eds.), *Marine Petroleum Source Rocks*. Geol. Soc. Am. Spec. Publ., 24:181-197.
- Thornburg, T. M., 1985. Seismic stratigraphy of Peru forearc basins. In Hussong, D. M., et al. (Eds.), *Atlas of the Ocean Margin Drilling Program, Peru Continental Margin, Region VI*: Woods Hole (Marine Science International), 8.
- Thornburg, T. M., and Kulm, L. D., 1981. Sedimentary basins of the Peru continental margin: structure, stratigraphy and Cenozoic tectonics from 6°S to 16°S latitude. In Kulm, L. D., et al. (Eds.), *Nazca Plate: Crustal Formation and Andean Convergence*. Geol. Soc. Am. Mem., 154:393-422.
- Tissot, B. P., and Welte, D. H., 1984. *Petroleum Formation and Occurrence* (2nd ed.): Berlin-Heidelberg (Springer-Verlag).
- Walker, R. G., 1984. Shelf and shallow marine sands. In Walker, R. G. (Ed.), *Facies Models*. Geosci. Can. Reprint Ser., 1:141-170.

## Ms 112A-115

Table 9. Salinity and chlorinity profiles at three Peru Margin sites affected by brines (Sites 680, 681, and 684).

Site 680 11°03.90'S, 78°04.67'W Water depth: 252 m				Site 681 10°58.60'S, 77°57.46'W Water depth: 150 m				Site 684 8°49.59'S, 79°54.35'W Water depth: 426 m			
Core/section interval (cm)	Depth (mbsf)	Salinity (g/kg)	Cl <sup>-</sup> (mmol/L)	Core/section interval (cm)	Depth (mbsf)	Salinity (g/kg)	Cl <sup>-</sup> (mmol/L)	Core/section interval (cm)	Depth (mbsf)	Salinity (g/kg)	Cl <sup>-</sup> (mmol/L)
112-680C-1H-1, 130-150	1.3	34.2	556.15	112-681C-1H-1, 145-150	1.5	34.2	557.11	112-684B-1H-3, 145-150	4.5	34.5	557.09
112-680B-1H-2, 145-150	3.0	34.5	559.95	112-681B-1H-2, 145-150	3.0	36.0	563.73	112-684C-1H-3, 145-150	4.5	34.5	558.05
112-680C-1H-3, 145-150	4.5	34.5	564.69	112-681C-1H-3, 140-150	4.5	34.5	558.05	2H-3, 145-150	12.3	35.0	575.22
2H-3, 140-150	10.2	34.5	583.68	2H-1, 140-150	7.4	34.8	562.79	112-684B-3H-3, 145-150	21.5	38.2	638.18
3H-2, 145-150	18.3	35.2	595.07	2H-4, 145-150	11.9	34.9	574.16	112-684C-3H-3, 145-150	21.8	37.9	646.76
112-680B-3H-3, 145-150	19.5	35.2	602.66	112-681B-3H-3, 145-150	19.8	35.8	608.27	4H-6, 145-150	35.8	41.8	694.46
6H-3, 145-150	47.5	38.0	643.47	112-681C-4H-2, 145-150	27.9	36.5	630.06	5H-1, 145-150	37.8	42.5	724.88
<i>In situ</i> #1	62.5	39.8	657.70	4H-5, 145-150	32.4	37.0	646.17	6X-1, 145-150	40.5	44.0	755.56
112-680B-9H-4, 140-150	77.9	43.8	747.86	5H-3, 145-150	38.9	38.0	655.64	7X-2, 145-150	51.5	46.4	774.74
<i>In situ</i> #2	195.5	64.0	1043.02	7H-2, 140-150	56.3	43.8	731.44	8X-2, 145-150	60.4	50.5	861.03
				112-681B-7H-2, 140-150	56.3	42.8	746.60	11X-1, 145-150	88.0	55.8	940.62
				112-681C-8H-2, 140-150	65.8	45.2	766.49	13X-1, 140-145	106.9	59.7	1028.83
				112-681B-9H-1, 140-150	73.8	46.0	794.92				
				112-681C-9H-2, 140-150	75.3	51.5	786.39				
				112-681B-12X-3, 140-150	98.9	52.3	914.30				
				15X-1, 135-145	126.0	57.8	989.15				

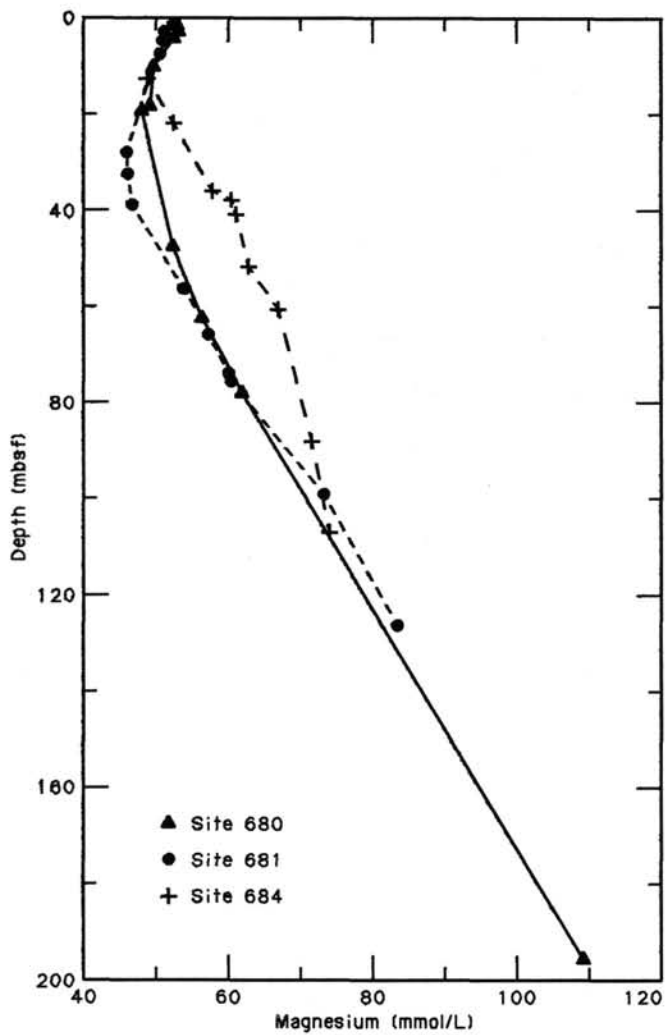


Figure 41. Interstitial magnesium for Sites 680, 681, and 684.

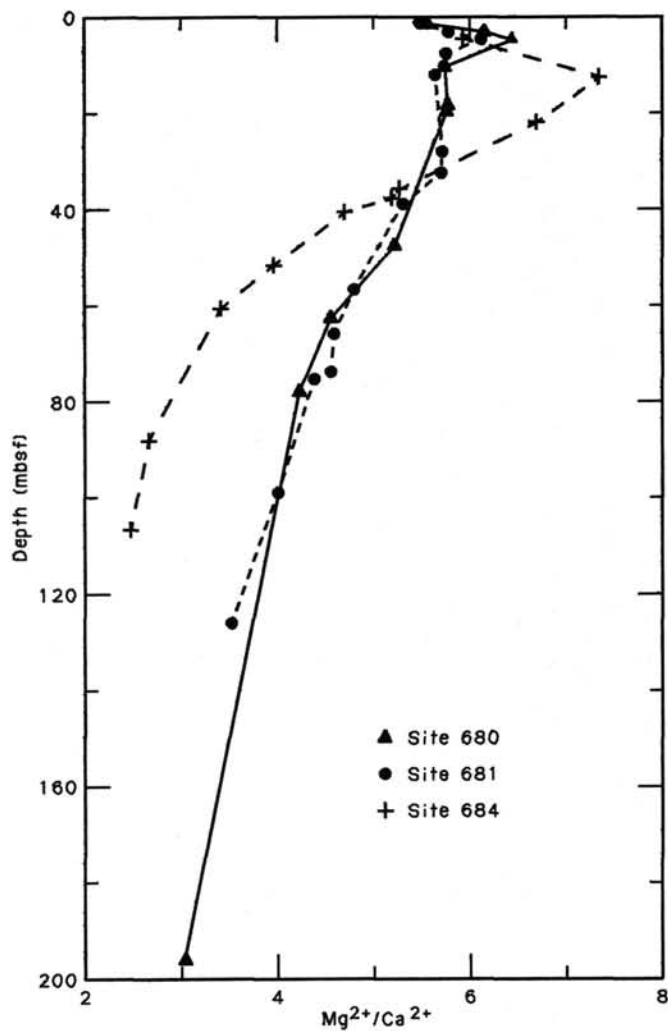


Figure 42. Mg<sup>2+</sup>/Ca<sup>2+</sup> for Sites 680, 681, and 684.

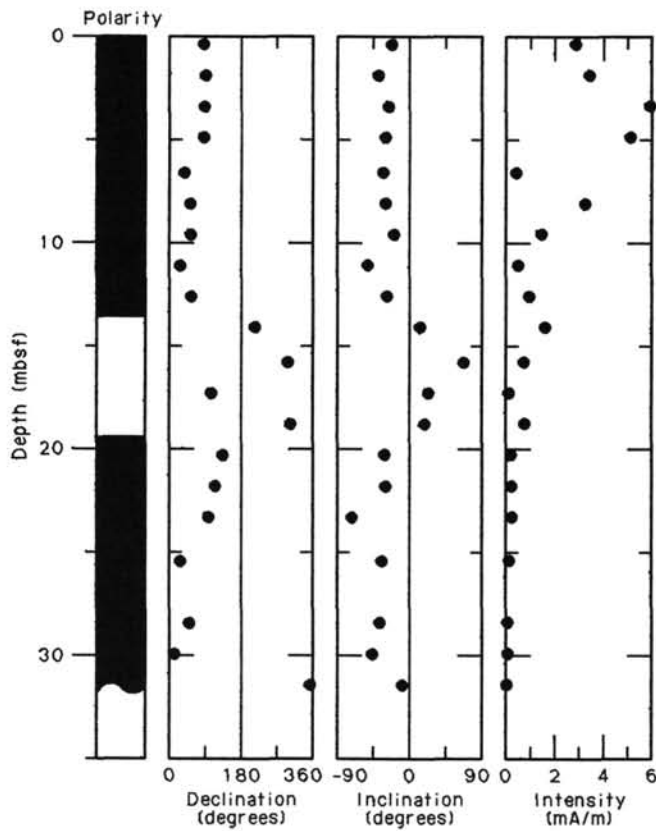


Figure 43. Plot of magnetic declination, inclination, and intensity of magnetization for samples from Hole 684A. Sampling frequency was one sample per section. Intensity values shown are values obtained after an alternating-field treatment of 150 Oe. Exceptions to this are the very low intensity values (<0.1 mA/m) that occur after lower-level alternating-field treatments.

Table 10. Summary of index properties at Site 684.

Core/section interval (cm)	Depth (mbsf)	Water contents (dry wt%)	Porosity (%)	Bulk density (g/cm <sup>3</sup> )	Grain density (g/cm <sup>3</sup> )
112-684A-1H-1, 91	0.91	155.51	81.06	1.36	2.58
1H-3, 80	3.80	154.59	84.04	1.42	2.47
2H-2, 97	7.77	140.23	82.37	1.45	2.61
2H-4, 91	10.71	160.10	83.82	1.40	2.83
2H-7, 16	14.46	93.13	71.45	1.52	2.37
3H-2, 78	17.08	109.17	75.74	1.49	2.40
3H-5, 79	21.59	111.07	77.39	1.51	2.38
4H-2, 69	26.49	112.42	77.04	1.49	2.44
4H-5, 91	31.21	126.46	77.09	1.41	2.12
5H-2, 64	35.94	113.08	75.23	1.45	2.27
5H-5, 72	40.52	128.93	80.28	1.46	2.41
6H-2, 86	45.66	123.60	76.23	1.41	2.38
6H-5, 87	50.17	82.09	71.37	1.62	2.51
7H-2, 75	55.05	154.22	83.82	1.42	2.36
7H-4, 53	57.83	167.65	81.19	1.33	2.22
9X-2, 30	71.40	131.98	76.36	1.38	2.22
112-684B-1H-1, 83	0.83	218.55	85.07	1.27	2.43
1H-3, 66	3.66	164.76	84.89	1.40	2.84
1H-5, 79	6.79	132.47	79.25	1.42	2.52
2H-1, 127	8.77	213.23	85.12	1.28	2.29
2H-4, 76	12.76	92.89	70.60	1.50	2.43
2H-6, 81	15.81	82.24	68.85	1.56	2.59
3H-1, 76	17.76	85.52	69.36	1.54	2.46
3H-3, 77	20.77	88.54	70.33	1.53	2.48
3H-6, 75	25.25	81.74	68.17	1.55	2.54
4H-1, 110	27.60	128.16	77.53	1.41	2.47
4H-3, 69	30.19	101.94	73.85	1.50	2.39
4H-5, 84	33.34	141.46	79.31	1.39	2.35

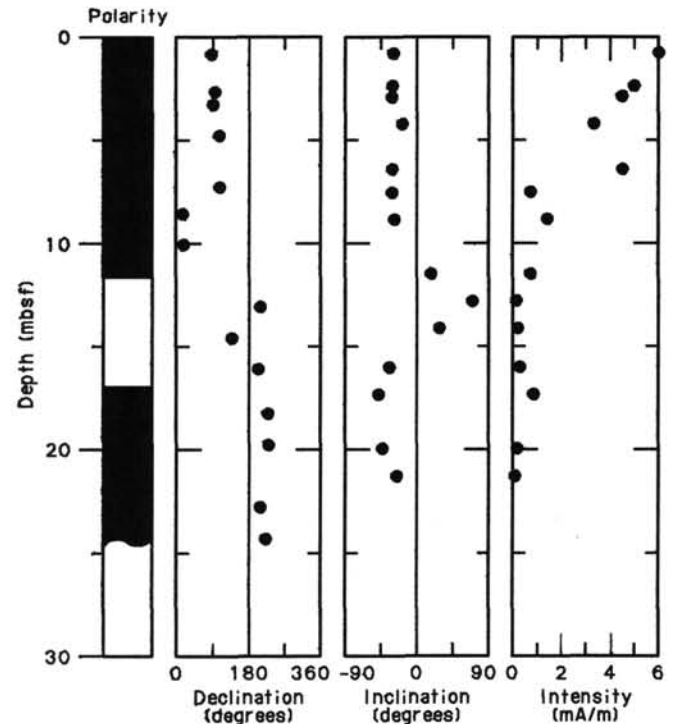


Figure 44. Plot of magnetic declination, inclination, and intensity of magnetization for samples from Hole 684B.

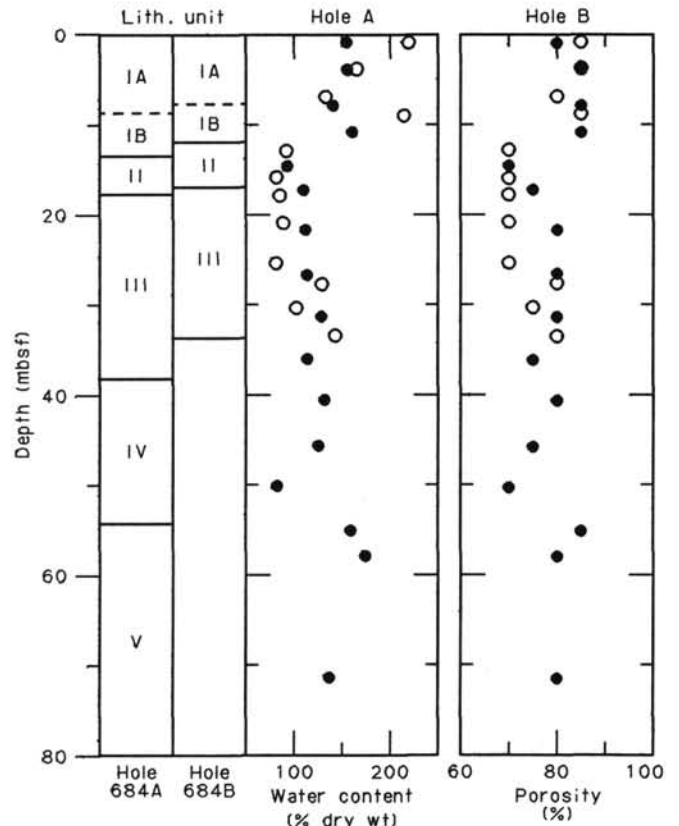


Figure 45. Water content and porosity plotted vs. depth below seafloor for Holes 684A and 684B.

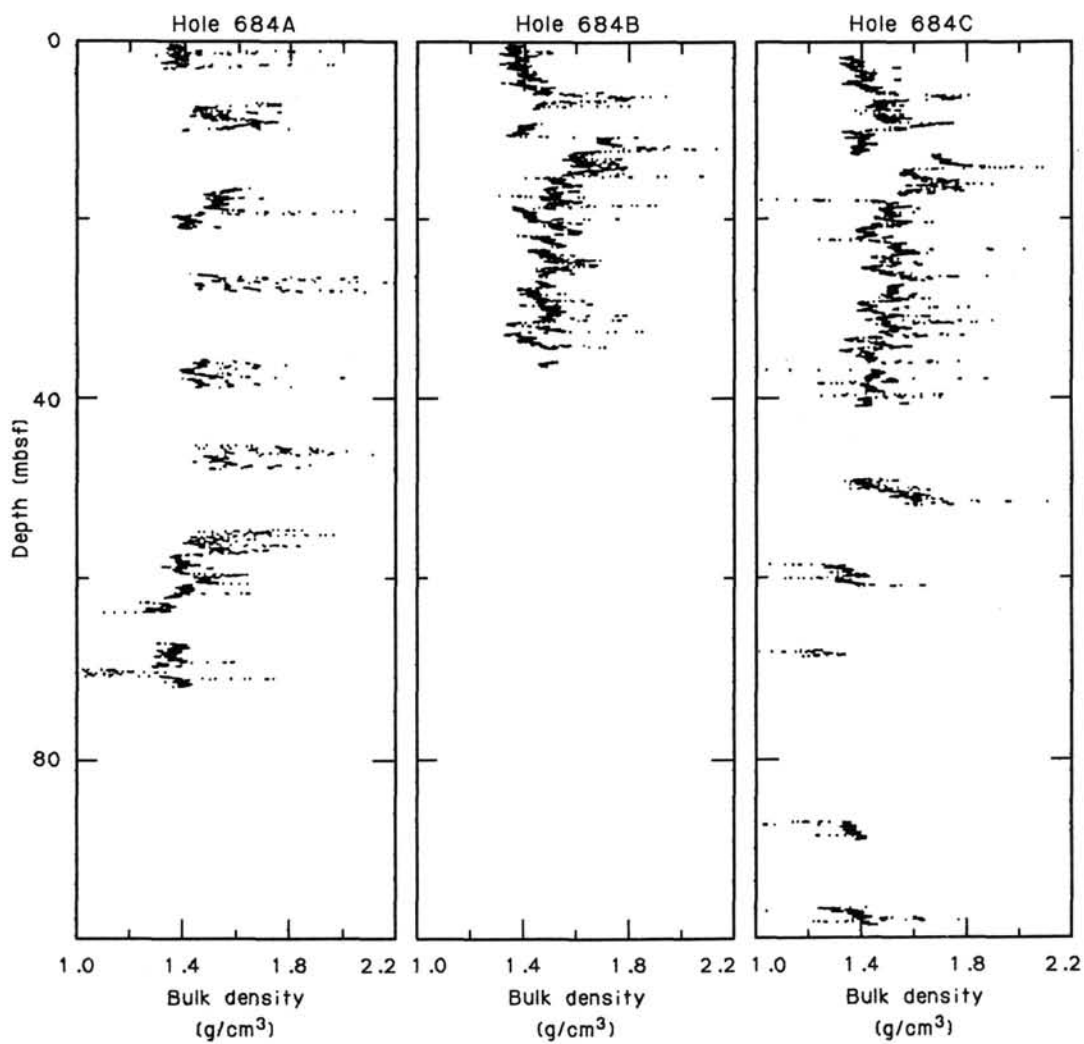


Figure 46. GRAPE bulk density plotted vs. depth below seafloor for Holes 684A, 684B, and 684C.

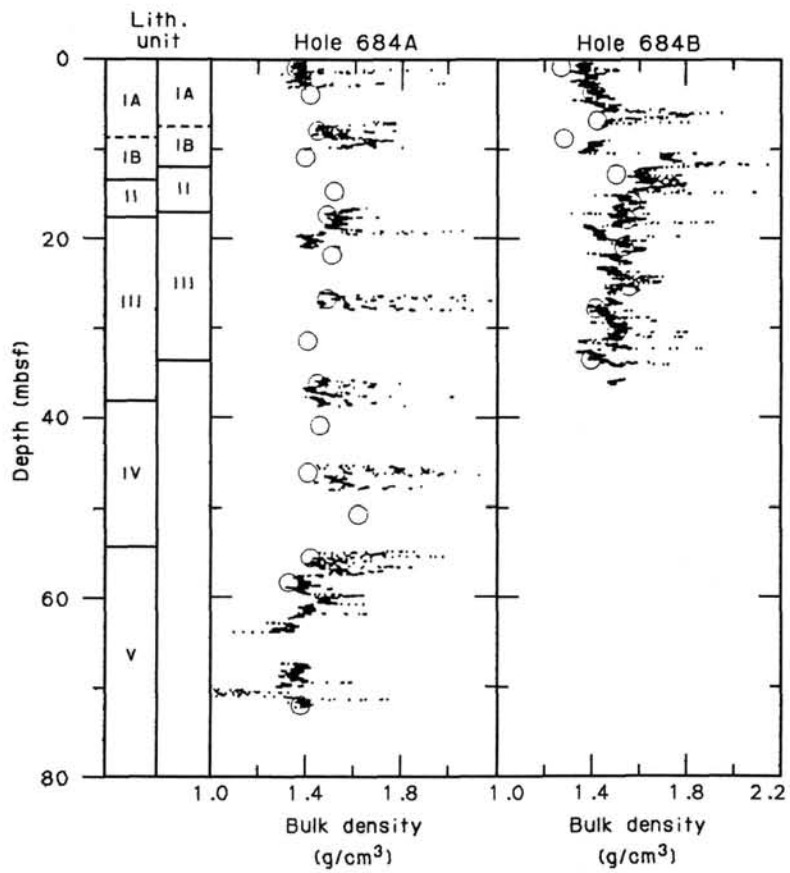


Figure 47. Sample bulk density superimposed on GRAPE bulk density vs. depth below seafloor for Holes 684A and 684B.

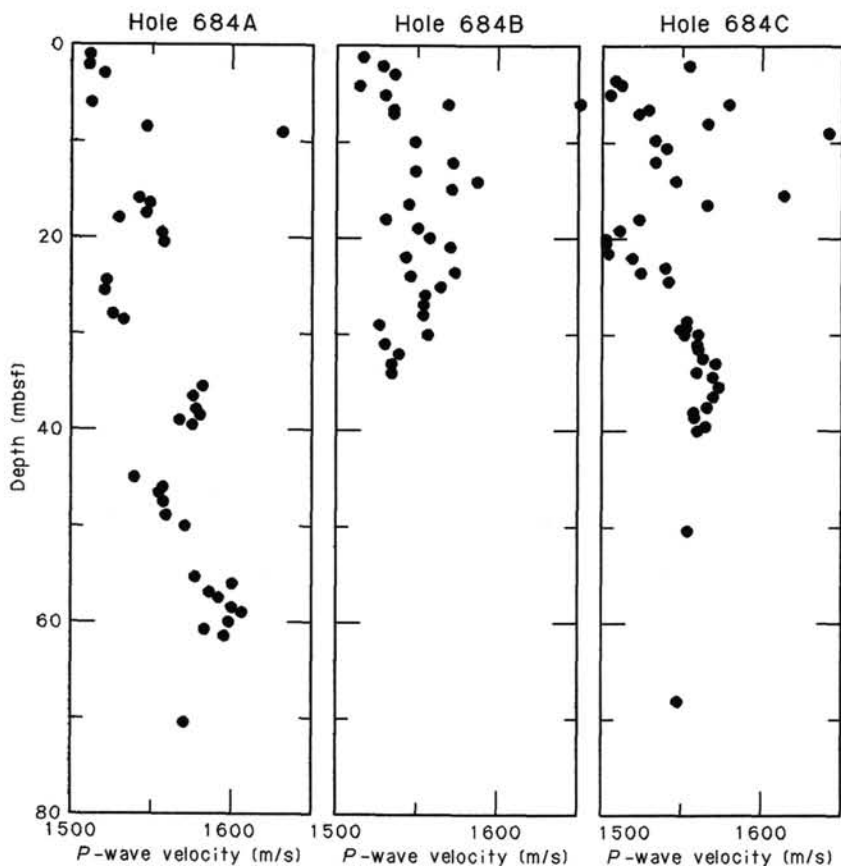


Figure 48. P-wave velocity vs. depth below seafloor for Holes 684A, 684B, and 684C.

Table 11. Summary of vane shear strength for Site 684.

Core/section interval(cm)	Depth (mbsf)	Peak (kPa)
112-684A-1H-1, 91	0.91	68.80
1H-3, 80	3.80	79.30
2H-2, 97	7.77	96.79
2H-4, 91	10.71	121.28
2H-7, 16	14.46	158.60
3H-2, 78	17.08	176.09
3H-5, 79	21.59	225.07
4H-2, 69	26.49	192.41
4H-2, 69	26.49	192.41
4H-5, 91	31.21	326.52
5H-2, 64	35.94	303.20
5H-5, 72	40.52	425.64
6H-2, 86	45.66	201.74
6H-5, 87	50.17	438.47
7H-2, 75	55.05	275.21
7H-4, 53	57.83	409.32
9X-2, 33	71.43	367.33
112-684B-1H-1, 84	0.84	31.37
1H-3, 66	3.66	36.91
1H-5, 78	6.78	39.22
2H-1, 1	7.51	46.14
2H-4, 75	12.75	62.74
2H-6, 8	15.08	59.52
3H-1, 75	17.75	81.66
3H-3, 75	20.75	77.05
3H-6, 75	25.25	98.50
4H-1, 110	27.60	85.81
4H-3, 68	30.18	95.04
4H-5, 85	33.35	85.35
4H-5, 85	33.35	138.11

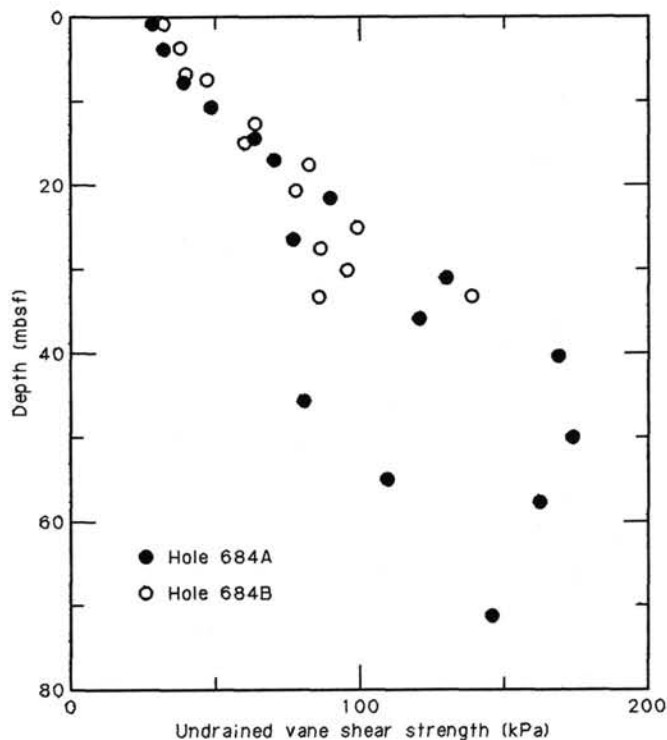


Figure 49. Peak undrained vane shear strength vs. depth below seafloor for Holes 684A and 684B.

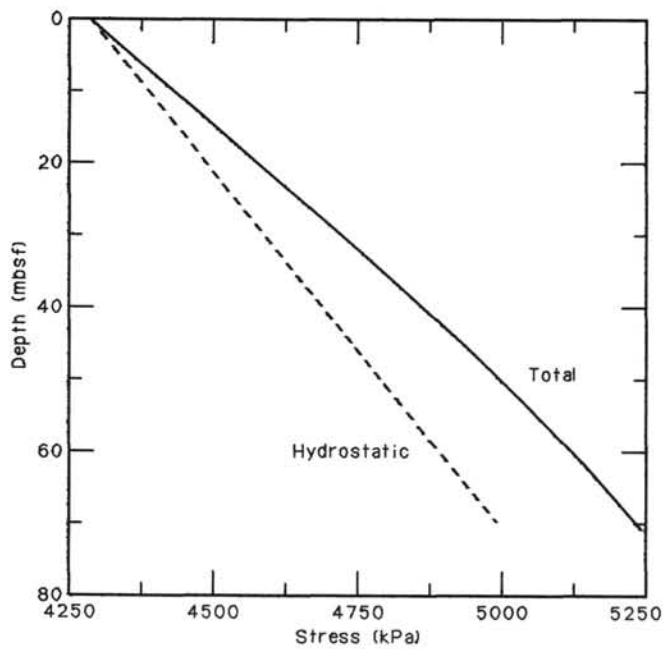


Figure 50. Assumed hydrostatic stress and calculated total stress vs. depth below seafloor for Hole 684A.

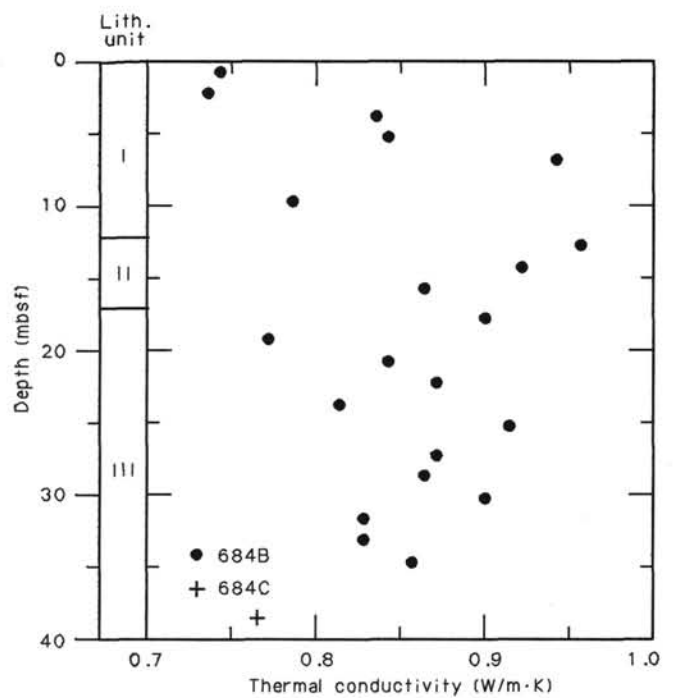


Figure 52. Thermal conductivity vs. depth below seafloor for Holes 684B and 684C.

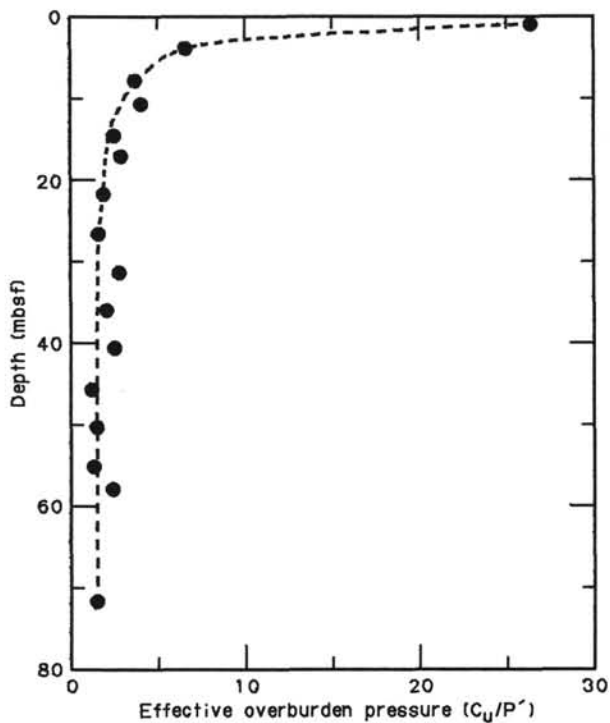


Figure 51. Ratio of peak undrained vane shear strength to effective overburden pressure vs. depth below seafloor for Hole 684A.

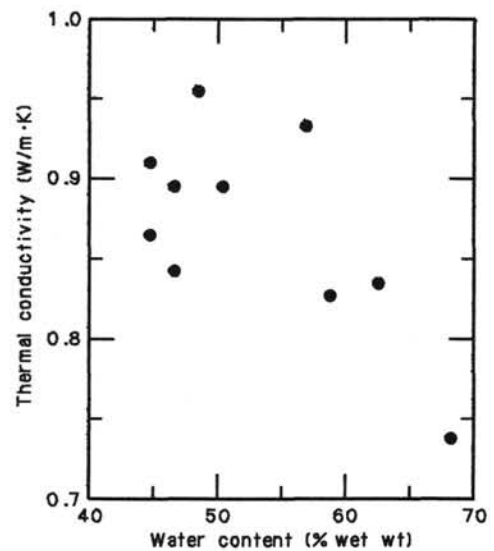


Figure 53. Thermal conductivity vs. water content for Hole 684B.

**Table 12. Thermal-conductivity data for Site 684.**

Core/section interval (cm)	Depth (mbsf)	Thermal conductivity (W/m·K)
112-684B-1H-1, 70	0.70	0.743
1H-2, 70	2.20	0.736
1H-3, 70	3.70	0.835
1H-4, 70	5.20	0.839
1H-5, 70	6.70	0.934
2H-2, 70	9.70	0.783
2H-4, 70	12.70	0.955
2H-5, 70	14.20	0.920
2H-6, 70	15.70	0.865
3H-1, 70	17.70	0.900
3H-2, 70	19.20	0.770
3H-3, 70	20.70	0.843
3H-4, 70	22.20	0.868
3H-5, 70	23.70	0.814
3H-6, 70	25.20	0.914
4H-1, 70	27.20	0.867
4H-2, 70	28.70	0.864
4H-3, 70	30.20	0.898
4H-4, 70	31.70	0.827
4H-5, 70	33.20	0.832
4H-6, 70	34.70	0.857
112-684C-5H-2, 67	38.47	0.809

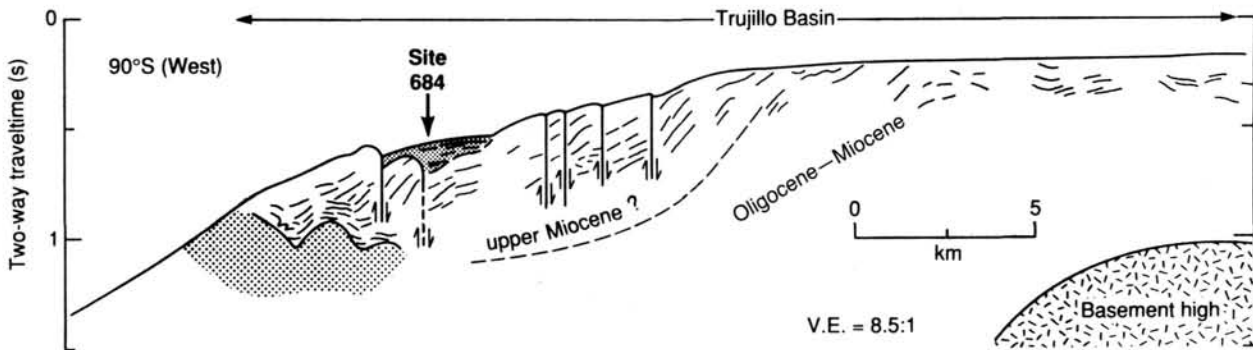


Figure 54. Trujillo Basin seismic stratigraphy and location of Site 684.

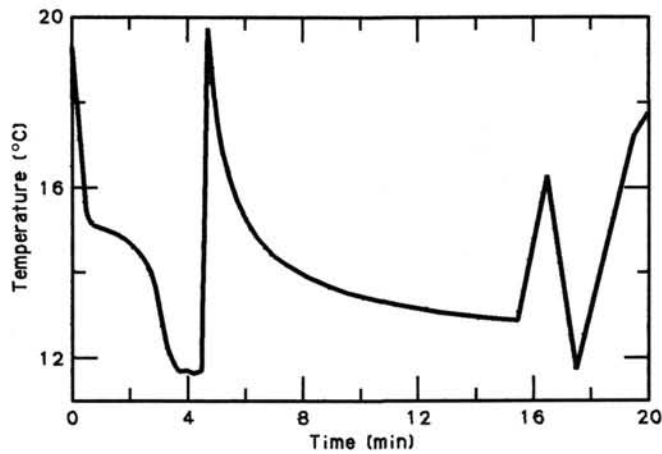
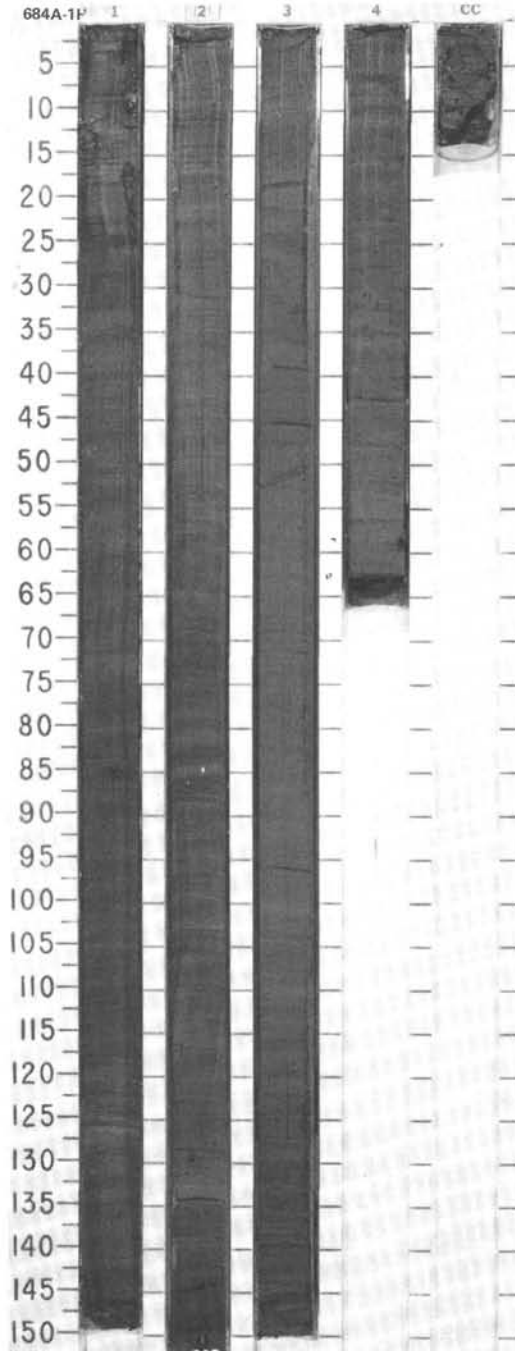


Figure 55. Temperature vs. time record obtained with the APC tool while retrieving Core 112-684A-6H.

SITE 684 HOLE A CORE 1H CORED INTERVAL 426.0-431.3 mbsl; 0.0-5.3 mbsf

TIME-ROCK UNIT	BIOSTRAT. ZONE/ FOSSIL CHARACTER				PALEOMAGNETICS	PHYS. PROPERTIES	CHEMISTRY	SECTION	METERS	GRAPHIC LITHOLOGY	DRILLING DISTURB.	SED. STRUCTURES	SAMPLES	LITHOLOGIC DESCRIPTION																																																																																																									
	FORAMINIFERS	NANNOFOSSILS	RADIOLARIANS	DIATOMS																																																																																																																			
QUATERNARY	* Quaternary	* NN20	* Quaternary	* <i>Pseudoeunotia doliolus</i> Zone				0.0-0.2	0.0-0.2					DIATOMACEOUS MUD, SILTY MUD, and MUD																																																																																																									
								0.2-1.0	0.2-1.0					Major lithology: dark olive (5Y 3/3) laminated diatomaceous mud and silty mud in Sections 1 and 2. Dark olive (5Y 3/3) laminated diatomaceous silty mud and mud in Section 3. Olive gray diatom mud (5Y 4/2) with olive yellow (5Y 6/6) laminae rich in siliceous microfossils in Section 4 through CC.																																																																																																									
								1.0-2.0	1.0-2.0					Minor lithologies: 1. nannofossil- and foraminifer-bearing diatomaceous ooze, Sections 1-2. 2. nannofossil ooze, occasional shell fragments, Section 3. 3. diatom- and foraminifer-bearing silt, Section 4-CC.																																																																																																									
								2.0-3.0	2.0-3.0					SMEAR SLIDE SUMMARY (%):																																																																																																									
								3.0-4.0	3.0-4.0					<table border="1"> <tr> <td></td> <td>1, 12</td> <td>1, 112</td> <td>1, 123</td> <td>2, 112</td> <td>2, 113</td> <td>3, 138</td> </tr> <tr> <td></td> <td>D</td> <td>D</td> <td>M</td> <td>D</td> <td>D</td> <td>M</td> </tr> </table>		1, 12	1, 112	1, 123	2, 112	2, 113	3, 138		D	D	M	D	D	M																																																																																											
	1, 12	1, 112	1, 123	2, 112	2, 113	3, 138																																																																																																																	
	D	D	M	D	D	M																																																																																																																	
								4.0-5.3	4.0-5.3					TEXTURE:																																																																																																									
														<table border="1"> <tr> <td>Sand</td> <td>—</td> <td>—</td> <td>5</td> <td>—</td> <td>—</td> <td>—</td> </tr> <tr> <td>Silt</td> <td>50</td> <td>50</td> <td>80</td> <td>50</td> <td>25</td> <td>20</td> </tr> <tr> <td>Clay</td> <td>50</td> <td>50</td> <td>15</td> <td>50</td> <td>75</td> <td>80</td> </tr> </table>	Sand	—	—	5	—	—	—	Silt	50	50	80	50	25	20	Clay	50	50	15	50	75	80																																																																																				
Sand	—	—	5	—	—	—																																																																																																																	
Silt	50	50	80	50	25	20																																																																																																																	
Clay	50	50	15	50	75	80																																																																																																																	
														COMPOSITION:																																																																																																									
														<table border="1"> <tr> <td>Quartz</td> <td>3</td> <td>1</td> <td>—</td> <td>10</td> <td>Tr</td> <td>Tr</td> </tr> <tr> <td>Rock fragments</td> <td>—</td> <td>—</td> <td>—</td> <td>—</td> <td>Tr</td> <td>Tr</td> </tr> <tr> <td>Mica</td> <td>—</td> <td>—</td> <td>—</td> <td>—</td> <td>—</td> <td>—</td> </tr> <tr> <td>Clay</td> <td>50</td> <td>50</td> <td>10</td> <td>50</td> <td>75</td> <td>20</td> </tr> <tr> <td>Volcanic glass</td> <td>—</td> <td>Tr</td> <td>Tr</td> <td>—</td> <td>Tr</td> <td>2</td> </tr> <tr> <td>Calcite/dolomite</td> <td>5</td> <td>—</td> <td>5</td> <td>5</td> <td>2</td> <td>—</td> </tr> <tr> <td>Accessory minerals</td> <td>—</td> <td>—</td> <td>—</td> <td>—</td> <td>—</td> <td>Tr</td> </tr> <tr> <td>Pyrite</td> <td>—</td> <td>Tr</td> <td>Tr</td> <td>—</td> <td>—</td> <td>—</td> </tr> <tr> <td>Micrite</td> <td>—</td> <td>2</td> <td>—</td> <td>—</td> <td>1</td> <td>1</td> </tr> <tr> <td>Foraminifers</td> <td>—</td> <td>—</td> <td>10</td> <td>15</td> <td>—</td> <td>—</td> </tr> <tr> <td>Nannofossils</td> <td>—</td> <td>—</td> <td>10</td> <td>5</td> <td>—</td> <td>60</td> </tr> <tr> <td>Diatoms</td> <td>40</td> <td>40</td> <td>65</td> <td>15</td> <td>18</td> <td>14</td> </tr> <tr> <td>Sponge spicules</td> <td>1</td> <td>7</td> <td>—</td> <td>—</td> <td>3</td> <td>3</td> </tr> <tr> <td>Silicoflagellates</td> <td>—</td> <td>—</td> <td>—</td> <td>—</td> <td>1</td> <td>—</td> </tr> <tr> <td>Fish remains</td> <td>1</td> <td>—</td> <td>—</td> <td>—</td> <td>—</td> <td>—</td> </tr> </table>	Quartz	3	1	—	10	Tr	Tr	Rock fragments	—	—	—	—	Tr	Tr	Mica	—	—	—	—	—	—	Clay	50	50	10	50	75	20	Volcanic glass	—	Tr	Tr	—	Tr	2	Calcite/dolomite	5	—	5	5	2	—	Accessory minerals	—	—	—	—	—	Tr	Pyrite	—	Tr	Tr	—	—	—	Micrite	—	2	—	—	1	1	Foraminifers	—	—	10	15	—	—	Nannofossils	—	—	10	5	—	60	Diatoms	40	40	65	15	18	14	Sponge spicules	1	7	—	—	3	3	Silicoflagellates	—	—	—	—	1	—	Fish remains	1	—	—	—	—	—
Quartz	3	1	—	10	Tr	Tr																																																																																																																	
Rock fragments	—	—	—	—	Tr	Tr																																																																																																																	
Mica	—	—	—	—	—	—																																																																																																																	
Clay	50	50	10	50	75	20																																																																																																																	
Volcanic glass	—	Tr	Tr	—	Tr	2																																																																																																																	
Calcite/dolomite	5	—	5	5	2	—																																																																																																																	
Accessory minerals	—	—	—	—	—	Tr																																																																																																																	
Pyrite	—	Tr	Tr	—	—	—																																																																																																																	
Micrite	—	2	—	—	1	1																																																																																																																	
Foraminifers	—	—	10	15	—	—																																																																																																																	
Nannofossils	—	—	10	5	—	60																																																																																																																	
Diatoms	40	40	65	15	18	14																																																																																																																	
Sponge spicules	1	7	—	—	3	3																																																																																																																	
Silicoflagellates	—	—	—	—	1	—																																																																																																																	
Fish remains	1	—	—	—	—	—																																																																																																																	
														TEXTURE:																																																																																																									
														<table border="1"> <tr> <td>Sand</td> <td>10</td> <td>10</td> </tr> <tr> <td>Silt</td> <td>70</td> <td>60</td> </tr> <tr> <td>Clay</td> <td>20</td> <td>30</td> </tr> </table>	Sand	10	10	Silt	70	60	Clay	20	30																																																																																																
Sand	10	10																																																																																																																					
Silt	70	60																																																																																																																					
Clay	20	30																																																																																																																					
														COMPOSITION:																																																																																																									
														<table border="1"> <tr> <td>Quartz</td> <td>3</td> <td>25</td> </tr> <tr> <td>Feldspar</td> <td>—</td> <td>5</td> </tr> <tr> <td>Rock fragments</td> <td>—</td> <td>5</td> </tr> <tr> <td>Clay</td> <td>12</td> <td>29</td> </tr> <tr> <td>Calcite/dolomite</td> <td>—</td> <td>5</td> </tr> <tr> <td>Accessory minerals</td> <td>—</td> <td>—</td> </tr> <tr> <td>Pyrite</td> <td>—</td> <td>5</td> </tr> <tr> <td>Glaucinite</td> <td>—</td> <td>Tr</td> </tr> <tr> <td>Foraminifers</td> <td>15</td> <td>10</td> </tr> <tr> <td>Nannofossils</td> <td>10</td> <td>1</td> </tr> <tr> <td>Diatoms</td> <td>60</td> <td>15</td> </tr> </table>	Quartz	3	25	Feldspar	—	5	Rock fragments	—	5	Clay	12	29	Calcite/dolomite	—	5	Accessory minerals	—	—	Pyrite	—	5	Glaucinite	—	Tr	Foraminifers	15	10	Nannofossils	10	1	Diatoms	60	15																																																																								
Quartz	3	25																																																																																																																					
Feldspar	—	5																																																																																																																					
Rock fragments	—	5																																																																																																																					
Clay	12	29																																																																																																																					
Calcite/dolomite	—	5																																																																																																																					
Accessory minerals	—	—																																																																																																																					
Pyrite	—	5																																																																																																																					
Glaucinite	—	Tr																																																																																																																					
Foraminifers	15	10																																																																																																																					
Nannofossils	10	1																																																																																																																					
Diatoms	60	15																																																																																																																					



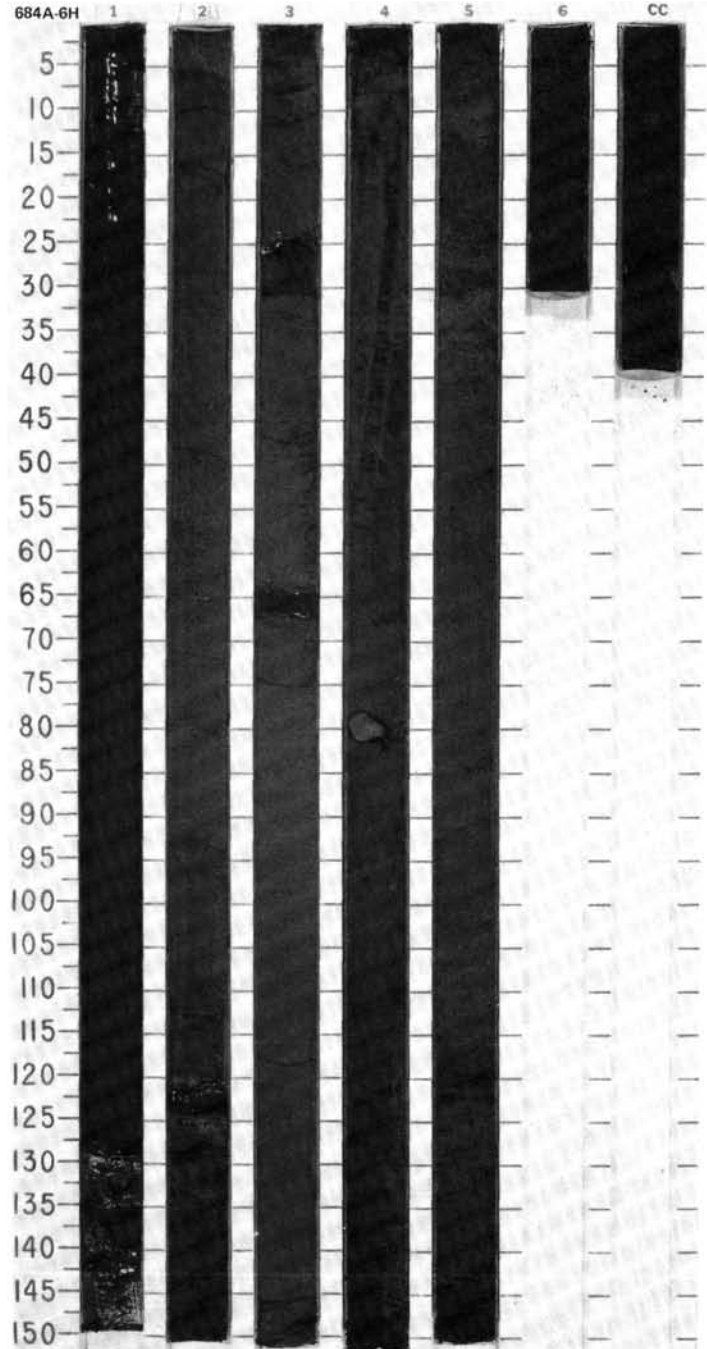






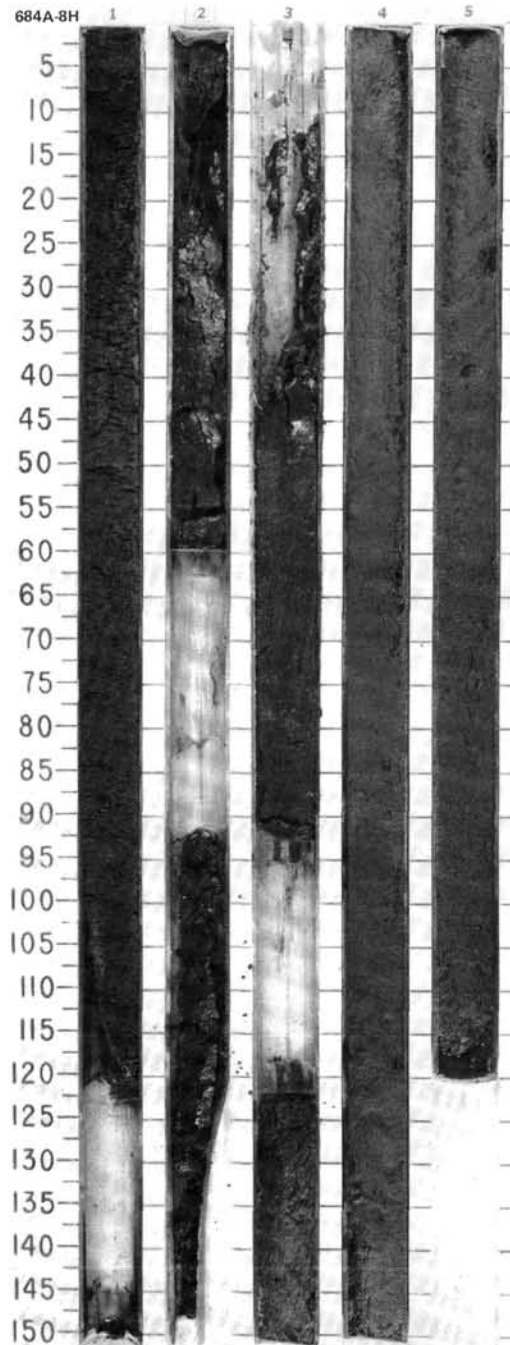


TIME-ROCK UNIT	BIOSTRAT. ZONE/ FOSSIL CHARACTER				PALEOMAGNETICS	PHYS. PROPERTIES CHEMISTRY	SECTION METERS	GRAPHIC LITHOLOGY	DRILLING DISTURB.	SED. STRUCTURES SAMPLES	LITHOLOGIC DESCRIPTION																																																																																																																								
	FORAMINIFERS	NANNOFOSSILS	RADIOLARIANS	DIATOMS																																																																																																																															
UPPER PLIOGENE	* B				● 1.41 ● 0.77.03	1	VOID				<p>MUD, DIATOMACEOUS MUD, and SILT</p> <p>Major lithology: Sections 1 and 2: dark olive gray (5Y 3/2) mud, homogeneous with dispersed foraminifers. Sections 3 and 4: dark olive gray (5Y 3/1) diatomaceous mud, homogeneous. Section 5: black (5Y 2.5/1) mud. Section 6 and CC: black (N 1/, N 2) silt, structureless, a few scattered foraminifers.</p> <p>Minor lithologies:                      1. foraminifer- and nannofossil-bearing silt, Barite(?) phosphatic sandy silt, Sections 3 and 4.                      2. phosphatic muddy silt, Section 5.                      3. glauconitic, phosphatic muddy silt, Section 6-CC.</p> <p>SMEAR SLIDE SUMMARY (%):</p> <table border="1"> <tr> <td></td> <td>3, 98</td> <td>4, 81</td> <td>4, 82</td> <td>5, 29</td> </tr> <tr> <td>D</td> <td></td> <td></td> <td>M</td> <td>D</td> </tr> </table> <p>TEXTURE:</p> <table border="1"> <tr> <td>Sand</td> <td>—</td> <td>10</td> <td>25</td> <td>5</td> </tr> <tr> <td>Silt</td> <td>30</td> <td>50</td> <td>55</td> <td>55</td> </tr> <tr> <td>Clay</td> <td>70</td> <td>40</td> <td>20</td> <td>40</td> </tr> </table> <p>COMPOSITION:</p> <table border="1"> <tr> <td>Quartz</td> <td>5</td> <td>—</td> <td>—</td> <td>—</td> </tr> <tr> <td>Feldspar</td> <td>—</td> <td>—</td> <td>15</td> <td>8</td> </tr> <tr> <td>Rock fragments</td> <td>—</td> <td>—</td> <td>—</td> <td>—</td> </tr> <tr> <td>Mica</td> <td>—</td> <td>—</td> <td>Tr</td> <td>1</td> </tr> <tr> <td>Clay</td> <td>35</td> <td>40</td> <td>15</td> <td>38</td> </tr> <tr> <td>Volcanic glass</td> <td>5</td> <td>—</td> <td>—</td> <td>15</td> </tr> <tr> <td>Calcite/dolomite</td> <td>10</td> <td>10</td> <td>5</td> <td>—</td> </tr> <tr> <td>Accessory minerals</td> <td></td> <td></td> <td></td> <td></td> </tr> <tr> <td>Collophane</td> <td>20</td> <td>10</td> <td>—</td> <td>—</td> </tr> <tr> <td>Pyrite</td> <td>Tr</td> <td>—</td> <td>1</td> <td>3</td> </tr> <tr> <td>Quartz/ microcrystalline</td> <td>5</td> <td>—</td> <td>—</td> <td>—</td> </tr> <tr> <td>Glauconite</td> <td>—</td> <td>5</td> <td>1</td> <td>5</td> </tr> <tr> <td>Sulfate min.</td> <td>—</td> <td>5</td> <td>—</td> <td>—</td> </tr> <tr> <td>Barite/apatite</td> <td>—</td> <td>10</td> <td>35</td> <td>—</td> </tr> <tr> <td>Phosphorites</td> <td>—</td> <td>—</td> <td>20</td> <td>—</td> </tr> <tr> <td>Foraminifers</td> <td>15</td> <td>10</td> <td>5</td> <td>—</td> </tr> <tr> <td>Nannofossils</td> <td>Tr</td> <td>Tr</td> <td>—</td> <td>—</td> </tr> <tr> <td>Diatoms</td> <td>5</td> <td>10</td> <td>3</td> <td>5</td> </tr> <tr> <td>Sponge spicules</td> <td>Tr</td> <td>Tr</td> <td>—</td> <td>—</td> </tr> </table>		3, 98	4, 81	4, 82	5, 29	D			M	D	Sand	—	10	25	5	Silt	30	50	55	55	Clay	70	40	20	40	Quartz	5	—	—	—	Feldspar	—	—	15	8	Rock fragments	—	—	—	—	Mica	—	—	Tr	1	Clay	35	40	15	38	Volcanic glass	5	—	—	15	Calcite/dolomite	10	10	5	—	Accessory minerals					Collophane	20	10	—	—	Pyrite	Tr	—	1	3	Quartz/ microcrystalline	5	—	—	—	Glauconite	—	5	1	5	Sulfate min.	—	5	—	—	Barite/apatite	—	10	35	—	Phosphorites	—	—	20	—	Foraminifers	15	10	5	—	Nannofossils	Tr	Tr	—	—	Diatoms	5	10	3	5	Sponge spicules	Tr	Tr	—	—
		3, 98	4, 81	4, 82		5, 29																																																																																																																													
	D			M		D																																																																																																																													
	Sand	—	10	25		5																																																																																																																													
	Silt	30	50	55		55																																																																																																																													
	Clay	70	40	20		40																																																																																																																													
Quartz	5	—	—	—																																																																																																																															
Feldspar	—	—	15	8																																																																																																																															
Rock fragments	—	—	—	—																																																																																																																															
Mica	—	—	Tr	1																																																																																																																															
Clay	35	40	15	38																																																																																																																															
Volcanic glass	5	—	—	15																																																																																																																															
Calcite/dolomite	10	10	5	—																																																																																																																															
Accessory minerals																																																																																																																																			
Collophane	20	10	—	—																																																																																																																															
Pyrite	Tr	—	1	3																																																																																																																															
Quartz/ microcrystalline	5	—	—	—																																																																																																																															
Glauconite	—	5	1	5																																																																																																																															
Sulfate min.	—	5	—	—																																																																																																																															
Barite/apatite	—	10	35	—																																																																																																																															
Phosphorites	—	—	20	—																																																																																																																															
Foraminifers	15	10	5	—																																																																																																																															
Nannofossils	Tr	Tr	—	—																																																																																																																															
Diatoms	5	10	3	5																																																																																																																															
Sponge spicules	Tr	Tr	—	—																																																																																																																															
* B	* NN16					2																																																																																																																													
* B	* NN16					3																																																																																																																													
* B						4																																																																																																																													
* B						5																																																																																																																													
						6																																																																																																																													
						CC																																																																																																																													



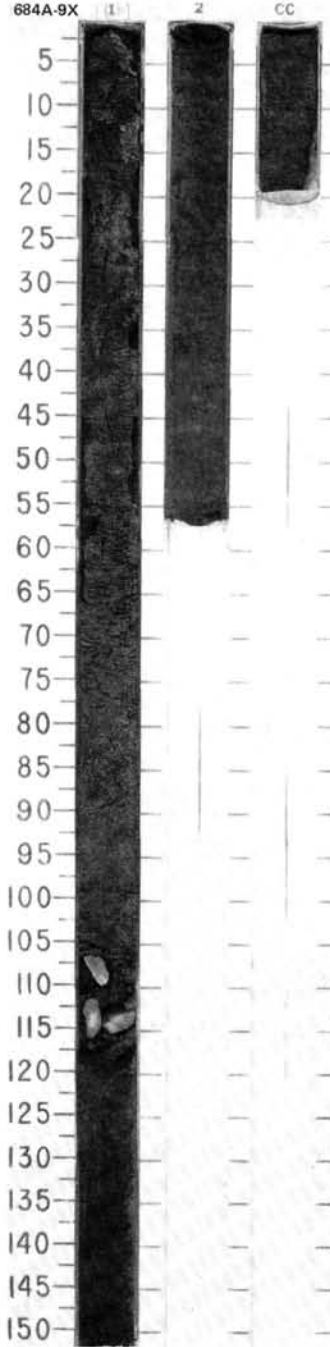


TIME-ROCK UNIT	BIOSTRAT. ZONE/ FOSSIL CHARACTER			PALEOMAGNETICS	PHYS. PROPERTIES	CHEMISTRY	SECTION	METERS	GRAPHIC LITHOLOGY	DRILLING DISTURB.	SED. STRUCTURES	SAMPLES	LITHOLOGIC DESCRIPTION																																																																																																																																																																																																																																																																																	
	FORAMINIFERS	NANNOFOSSILS	RADIOLARIANS																																																																																																																																																																																																																																																																																											
MIDDLE / UPPER MIOCENE	* B	NN9 *					1	0.5 1.0				*	<p><b>MUD and DIATOMACEOUS MUD</b></p> <p>Major lithology: Sections 1-2, and Section 3, 0-91 cm: olive gray (5Y 4/2) to dark olive gray (5Y 3/2) diatomaceous mud; patch of gray ash at Section 3, 77 cm. Section 3, 121-150 cm: very dark grayish brown (2.5Y 3/2) mud, laminated with yellowish ooze. Section 4, 0-91 cm: very dark grayish brown (2.5Y 3/2) mud, laminated; 91-150 cm: black (5Y 2.5/1) mud. Section 5: dark olive gray (5Y 3/2) diatomaceous mud.</p> <p>Minor lithology: 1. diatomaceous ooze. Section 1 through Section 3, 0-91 cm. 2. nannofossil-bearing diatomaceous mud, Section 3, 121-150 cm. 3. calcareous nodule at Section 5, 75 cm. 4. micritic calcite (vein) in Section 5.</p> <p><b>SMEAR SLIDE SUMMARY (%):</b></p> <table border="1"> <thead> <tr> <th></th> <th>1, 30 D</th> <th>1, 102 M</th> <th>3, 131 D</th> <th>4, 64 M</th> <th>4, 76 D</th> <th>4, 110 M</th> </tr> </thead> <tbody> <tr> <td><b>TEXTURE:</b></td> <td></td> <td></td> <td></td> <td></td> <td></td> <td></td> </tr> <tr> <td>Sand</td> <td>5</td> <td>10</td> <td>15</td> <td>5</td> <td>5</td> <td>10</td> </tr> <tr> <td>Silt</td> <td>40</td> <td>60</td> <td>35</td> <td>70</td> <td>25</td> <td>45</td> </tr> <tr> <td>Clay</td> <td>55</td> <td>30</td> <td>50</td> <td>25</td> <td>70</td> <td>45</td> </tr> <tr> <td><b>COMPOSITION:</b></td> <td></td> <td></td> <td></td> <td></td> <td></td> <td></td> </tr> <tr> <td>Quartz</td> <td>5</td> <td>20</td> <td>15</td> <td>2</td> <td>5</td> <td>3</td> </tr> <tr> <td>Feldspar</td> <td>3</td> <td>5</td> <td>5</td> <td>1</td> <td>3</td> <td>5</td> </tr> <tr> <td>Rock fragments</td> <td>1</td> <td>—</td> <td>5</td> <td>Tr</td> <td>2</td> <td>2</td> </tr> <tr> <td>Mica</td> <td>—</td> <td>3</td> <td>—</td> <td>—</td> <td>—</td> <td>—</td> </tr> <tr> <td>Clay</td> <td>20</td> <td>47</td> <td>30</td> <td>20</td> <td>30</td> <td>35</td> </tr> <tr> <td>Volcanic glass</td> <td>—</td> <td>10</td> <td>Tr</td> <td>—</td> <td>Tr</td> <td>—</td> </tr> <tr> <td>Calcite/dolomite</td> <td>5</td> <td>5</td> <td>5</td> <td>Tr</td> <td>—</td> <td>1</td> </tr> <tr> <td><b>Accessory minerals</b></td> <td></td> <td></td> <td></td> <td></td> <td></td> <td></td> </tr> <tr> <td>Pyrite</td> <td>5</td> <td>—</td> <td>10</td> <td>2</td> <td>5</td> <td>4</td> </tr> <tr> <td>Opacues</td> <td>—</td> <td>10</td> <td>—</td> <td>—</td> <td>—</td> <td>—</td> </tr> <tr> <td>Foraminifers</td> <td>1</td> <td>—</td> <td>—</td> <td>5</td> <td>5</td> <td>5</td> </tr> <tr> <td>Nannofossils</td> <td>2</td> <td>—</td> <td>5</td> <td>5</td> <td>10</td> <td>5</td> </tr> <tr> <td>Diatoms</td> <td>55</td> <td>—</td> <td>25</td> <td>65</td> <td>40</td> <td>40</td> </tr> <tr> <td>Sponge spicules</td> <td>3</td> <td>—</td> <td>—</td> <td>—</td> <td>—</td> <td>—</td> </tr> <tr> <td>Silicoflagellates</td> <td>—</td> <td>—</td> <td>—</td> <td>Tr</td> <td>—</td> <td>—</td> </tr> <tr> <td>Fish remains</td> <td>—</td> <td>—</td> <td>Tr</td> <td>—</td> <td>—</td> <td>—</td> </tr> <tr> <td></td> <td>4, 116 M</td> <td>5, 74 M</td> <td></td> <td></td> <td></td> <td></td> </tr> <tr> <td><b>TEXTURE:</b></td> <td></td> <td></td> <td></td> <td></td> <td></td> <td></td> </tr> <tr> <td>Sand</td> <td>15</td> <td>—</td> <td></td> <td></td> <td></td> <td></td> </tr> <tr> <td>Silt</td> <td>40</td> <td>—</td> <td></td> <td></td> <td></td> <td></td> </tr> <tr> <td>Clay</td> <td>45</td> <td>100</td> <td></td> <td></td> <td></td> <td></td> </tr> <tr> <td><b>COMPOSITION:</b></td> <td></td> <td></td> <td></td> <td></td> <td></td> <td></td> </tr> <tr> <td>Quartz</td> <td>2</td> <td>—</td> <td></td> <td></td> <td></td> <td></td> </tr> <tr> <td>Feldspar</td> <td>5</td> <td>—</td> <td></td> <td></td> <td></td> <td></td> </tr> <tr> <td>Rock fragments</td> <td>2</td> <td>—</td> <td></td> <td></td> <td></td> <td></td> </tr> <tr> <td>Clay</td> <td>40</td> <td>—</td> <td></td> <td></td> <td></td> <td></td> </tr> <tr> <td>Volcanic glass</td> <td>Tr</td> <td>—</td> <td></td> <td></td> <td></td> <td></td> </tr> <tr> <td>Calcite/dolomite</td> <td>1</td> <td>100</td> <td></td> <td></td> <td></td> <td></td> </tr> <tr> <td><b>Accessory minerals</b></td> <td></td> <td></td> <td></td> <td></td> <td></td> <td></td> </tr> <tr> <td>Pyrite</td> <td>5</td> <td>—</td> <td></td> <td></td> <td></td> <td></td> </tr> <tr> <td>Foraminifers</td> <td>10</td> <td>—</td> <td></td> <td></td> <td></td> <td></td> </tr> <tr> <td>Nannofossils</td> <td>5</td> <td>—</td> <td></td> <td></td> <td></td> <td></td> </tr> <tr> <td>Diatoms</td> <td>30</td> <td>—</td> <td></td> <td></td> <td></td> <td></td> </tr> </tbody> </table>		1, 30 D	1, 102 M	3, 131 D	4, 64 M	4, 76 D	4, 110 M	<b>TEXTURE:</b>							Sand	5	10	15	5	5	10	Silt	40	60	35	70	25	45	Clay	55	30	50	25	70	45	<b>COMPOSITION:</b>							Quartz	5	20	15	2	5	3	Feldspar	3	5	5	1	3	5	Rock fragments	1	—	5	Tr	2	2	Mica	—	3	—	—	—	—	Clay	20	47	30	20	30	35	Volcanic glass	—	10	Tr	—	Tr	—	Calcite/dolomite	5	5	5	Tr	—	1	<b>Accessory minerals</b>							Pyrite	5	—	10	2	5	4	Opacues	—	10	—	—	—	—	Foraminifers	1	—	—	5	5	5	Nannofossils	2	—	5	5	10	5	Diatoms	55	—	25	65	40	40	Sponge spicules	3	—	—	—	—	—	Silicoflagellates	—	—	—	Tr	—	—	Fish remains	—	—	Tr	—	—	—		4, 116 M	5, 74 M					<b>TEXTURE:</b>							Sand	15	—					Silt	40	—					Clay	45	100					<b>COMPOSITION:</b>							Quartz	2	—					Feldspar	5	—					Rock fragments	2	—					Clay	40	—					Volcanic glass	Tr	—					Calcite/dolomite	1	100					<b>Accessory minerals</b>							Pyrite	5	—					Foraminifers	10	—					Nannofossils	5	—					Diatoms	30	—				
	1, 30 D	1, 102 M	3, 131 D	4, 64 M	4, 76 D	4, 110 M																																																																																																																																																																																																																																																																																								
<b>TEXTURE:</b>																																																																																																																																																																																																																																																																																														
Sand	5	10	15	5	5	10																																																																																																																																																																																																																																																																																								
Silt	40	60	35	70	25	45																																																																																																																																																																																																																																																																																								
Clay	55	30	50	25	70	45																																																																																																																																																																																																																																																																																								
<b>COMPOSITION:</b>																																																																																																																																																																																																																																																																																														
Quartz	5	20	15	2	5	3																																																																																																																																																																																																																																																																																								
Feldspar	3	5	5	1	3	5																																																																																																																																																																																																																																																																																								
Rock fragments	1	—	5	Tr	2	2																																																																																																																																																																																																																																																																																								
Mica	—	3	—	—	—	—																																																																																																																																																																																																																																																																																								
Clay	20	47	30	20	30	35																																																																																																																																																																																																																																																																																								
Volcanic glass	—	10	Tr	—	Tr	—																																																																																																																																																																																																																																																																																								
Calcite/dolomite	5	5	5	Tr	—	1																																																																																																																																																																																																																																																																																								
<b>Accessory minerals</b>																																																																																																																																																																																																																																																																																														
Pyrite	5	—	10	2	5	4																																																																																																																																																																																																																																																																																								
Opacues	—	10	—	—	—	—																																																																																																																																																																																																																																																																																								
Foraminifers	1	—	—	5	5	5																																																																																																																																																																																																																																																																																								
Nannofossils	2	—	5	5	10	5																																																																																																																																																																																																																																																																																								
Diatoms	55	—	25	65	40	40																																																																																																																																																																																																																																																																																								
Sponge spicules	3	—	—	—	—	—																																																																																																																																																																																																																																																																																								
Silicoflagellates	—	—	—	Tr	—	—																																																																																																																																																																																																																																																																																								
Fish remains	—	—	Tr	—	—	—																																																																																																																																																																																																																																																																																								
	4, 116 M	5, 74 M																																																																																																																																																																																																																																																																																												
<b>TEXTURE:</b>																																																																																																																																																																																																																																																																																														
Sand	15	—																																																																																																																																																																																																																																																																																												
Silt	40	—																																																																																																																																																																																																																																																																																												
Clay	45	100																																																																																																																																																																																																																																																																																												
<b>COMPOSITION:</b>																																																																																																																																																																																																																																																																																														
Quartz	2	—																																																																																																																																																																																																																																																																																												
Feldspar	5	—																																																																																																																																																																																																																																																																																												
Rock fragments	2	—																																																																																																																																																																																																																																																																																												
Clay	40	—																																																																																																																																																																																																																																																																																												
Volcanic glass	Tr	—																																																																																																																																																																																																																																																																																												
Calcite/dolomite	1	100																																																																																																																																																																																																																																																																																												
<b>Accessory minerals</b>																																																																																																																																																																																																																																																																																														
Pyrite	5	—																																																																																																																																																																																																																																																																																												
Foraminifers	10	—																																																																																																																																																																																																																																																																																												
Nannofossils	5	—																																																																																																																																																																																																																																																																																												
Diatoms	30	—																																																																																																																																																																																																																																																																																												



SITE 684 HOLE A CORE 9X CORED INTERVAL 495.6-505.1 mbsf; 69.6-79.1 mbsf

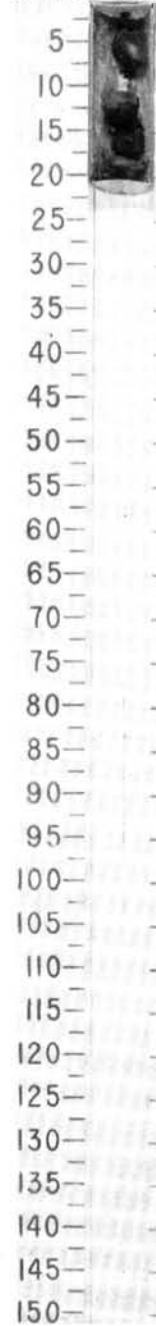
TIME-ROCK UNIT	BIOSTRAT. ZONE/ FOSSIL CHARACTER			PALEOMAGNETICS	PHYS. PROPERTIES	CHEMISTRY	SECTION	METERS	GRAPHIC LITHOLOGY	DRILLING DISTURB.	SED. STRUCTURES	SAMPLES	LITHOLOGIC DESCRIPTION																																																																																																																																																																																																
	FORAMINIFERS	NANNOFOSSILS	RADIOLARIANS																																																																																																																																																																																																										
MIDDLE / UPPER MIOCENE	* N17 to N21	* NN9	* <i>D. antepennulimitus</i>				1	0.5					<p>CALCAREOUS SILTY MUD, LIMESTONE, MUD, and CALCAREOUS MUD</p> <p>Major lithology: Section 1, 0-65 cm: black to dark olive gray (5Y 2.5/2) calcareous silty mud, massive; 65-94 cm: dark grayish brown (2.5Y 4/2) calcareous mud; 94-107 cm: dark olive gray calcareous mud, silty; 107-119 cm: brecciated zone and lithified nodules of limestone; and 117-153 cm: dark olive gray (5Y 3/2) silty calcareous mud, massive. Section 2: dark olive gray (5Y 3/2) and olive gray mud, slightly mottled. CC: dark olive gray (5Y 3/2) calcareous mud with patches of yellowish carbonate-rich ooze.</p> <p>Minor lithology: phosphate nodule at Section 1, 69 cm.</p> <p>SMEAR SLIDE SUMMARY (%):</p> <table border="1"> <tr> <td></td> <td>1, 40</td> <td>1, 69</td> <td>1, 114</td> <td>1, 142</td> <td>2, 41</td> <td>CC, 7</td> <td>CC, 8</td> </tr> <tr> <td></td> <td>D</td> <td>M</td> <td>M</td> <td>D</td> <td>M</td> <td>D</td> <td>D</td> </tr> <tr> <td>Sand</td> <td>5</td> <td>—</td> <td>—</td> <td>5</td> <td>—</td> <td>5</td> <td>10</td> </tr> <tr> <td>Silt</td> <td>35</td> <td>—</td> <td>—</td> <td>35</td> <td>15</td> <td>45</td> <td>10</td> </tr> <tr> <td>Clay</td> <td>60</td> <td>100</td> <td>100</td> <td>60</td> <td>85</td> <td>50</td> <td>80</td> </tr> </table> <p>TEXTURE:</p> <table border="1"> <tr> <td>Sand</td> <td>5</td> <td>—</td> <td>—</td> <td>5</td> <td>—</td> <td>5</td> <td>10</td> </tr> <tr> <td>Silt</td> <td>35</td> <td>—</td> <td>—</td> <td>35</td> <td>15</td> <td>45</td> <td>10</td> </tr> <tr> <td>Clay</td> <td>60</td> <td>100</td> <td>100</td> <td>60</td> <td>85</td> <td>50</td> <td>80</td> </tr> </table> <p>COMPOSITION:</p> <table border="1"> <tr> <td>Quartz</td> <td>3</td> <td>—</td> <td>Tr</td> <td>3</td> <td>—</td> <td>3</td> <td>2</td> </tr> <tr> <td>Feldspar</td> <td>5</td> <td>Tr</td> <td>Tr</td> <td>5</td> <td>—</td> <td>5</td> <td>5</td> </tr> <tr> <td>Rock fragments</td> <td>2</td> <td>—</td> <td>—</td> <td>Tr</td> <td>—</td> <td>Tr</td> <td>1</td> </tr> <tr> <td>Clay</td> <td>30</td> <td>—</td> <td>—</td> <td>35</td> <td>—</td> <td>35</td> <td>10</td> </tr> <tr> <td>Volcanic glass</td> <td>Tr</td> <td>20</td> <td>—</td> <td>—</td> <td>—</td> <td>—</td> <td>—</td> </tr> <tr> <td>Calcite/dolomite</td> <td>Tr</td> <td>—</td> <td>100</td> <td>3</td> <td>85</td> <td>2</td> <td>—</td> </tr> <tr> <td>Accessory minerals</td> <td></td> <td></td> <td></td> <td></td> <td></td> <td></td> <td></td> </tr> <tr> <td>  Pyrite</td> <td>5</td> <td>—</td> <td>—</td> <td>2</td> <td>—</td> <td>5</td> <td>—</td> </tr> <tr> <td>  Apatite</td> <td>—</td> <td>80</td> <td>—</td> <td>—</td> <td>—</td> <td>—</td> <td>80</td> </tr> <tr> <td>  Iron oxide(?)</td> <td>—</td> <td>—</td> <td>—</td> <td>2</td> <td>—</td> <td>—</td> <td>—</td> </tr> <tr> <td>  Glauconite</td> <td>—</td> <td>—</td> <td>—</td> <td>—</td> <td>—</td> <td>—</td> <td>2</td> </tr> <tr> <td>Foraminifers</td> <td>5</td> <td>—</td> <td>—</td> <td>5</td> <td>—</td> <td>5</td> <td>—</td> </tr> <tr> <td>Nannofossils</td> <td>10</td> <td>—</td> <td>—</td> <td>15</td> <td>—</td> <td>15</td> <td>Tr</td> </tr> <tr> <td>Diatoms</td> <td>35</td> <td>—</td> <td>—</td> <td>30</td> <td>15</td> <td>30</td> <td>—</td> </tr> <tr> <td>Silicoflagellates</td> <td>Tr</td> <td>—</td> <td>—</td> <td>—</td> <td>—</td> <td>Tr</td> <td>—</td> </tr> <tr> <td>Fish remains</td> <td>5</td> <td>—</td> <td>—</td> <td>—</td> <td>—</td> <td>—</td> <td>—</td> </tr> </table>		1, 40	1, 69	1, 114	1, 142	2, 41	CC, 7	CC, 8		D	M	M	D	M	D	D	Sand	5	—	—	5	—	5	10	Silt	35	—	—	35	15	45	10	Clay	60	100	100	60	85	50	80	Sand	5	—	—	5	—	5	10	Silt	35	—	—	35	15	45	10	Clay	60	100	100	60	85	50	80	Quartz	3	—	Tr	3	—	3	2	Feldspar	5	Tr	Tr	5	—	5	5	Rock fragments	2	—	—	Tr	—	Tr	1	Clay	30	—	—	35	—	35	10	Volcanic glass	Tr	20	—	—	—	—	—	Calcite/dolomite	Tr	—	100	3	85	2	—	Accessory minerals								Pyrite	5	—	—	2	—	5	—	Apatite	—	80	—	—	—	—	80	Iron oxide(?)	—	—	—	2	—	—	—	Glauconite	—	—	—	—	—	—	2	Foraminifers	5	—	—	5	—	5	—	Nannofossils	10	—	—	15	—	15	Tr	Diatoms	35	—	—	30	15	30	—	Silicoflagellates	Tr	—	—	—	—	Tr	—	Fish remains	5	—	—	—	—	—	—
	1, 40	1, 69	1, 114	1, 142	2, 41	CC, 7	CC, 8																																																																																																																																																																																																						
	D	M	M	D	M	D	D																																																																																																																																																																																																						
Sand	5	—	—	5	—	5	10																																																																																																																																																																																																						
Silt	35	—	—	35	15	45	10																																																																																																																																																																																																						
Clay	60	100	100	60	85	50	80																																																																																																																																																																																																						
Sand	5	—	—	5	—	5	10																																																																																																																																																																																																						
Silt	35	—	—	35	15	45	10																																																																																																																																																																																																						
Clay	60	100	100	60	85	50	80																																																																																																																																																																																																						
Quartz	3	—	Tr	3	—	3	2																																																																																																																																																																																																						
Feldspar	5	Tr	Tr	5	—	5	5																																																																																																																																																																																																						
Rock fragments	2	—	—	Tr	—	Tr	1																																																																																																																																																																																																						
Clay	30	—	—	35	—	35	10																																																																																																																																																																																																						
Volcanic glass	Tr	20	—	—	—	—	—																																																																																																																																																																																																						
Calcite/dolomite	Tr	—	100	3	85	2	—																																																																																																																																																																																																						
Accessory minerals																																																																																																																																																																																																													
Pyrite	5	—	—	2	—	5	—																																																																																																																																																																																																						
Apatite	—	80	—	—	—	—	80																																																																																																																																																																																																						
Iron oxide(?)	—	—	—	2	—	—	—																																																																																																																																																																																																						
Glauconite	—	—	—	—	—	—	2																																																																																																																																																																																																						
Foraminifers	5	—	—	5	—	5	—																																																																																																																																																																																																						
Nannofossils	10	—	—	15	—	15	Tr																																																																																																																																																																																																						
Diatoms	35	—	—	30	15	30	—																																																																																																																																																																																																						
Silicoflagellates	Tr	—	—	—	—	Tr	—																																																																																																																																																																																																						
Fish remains	5	—	—	—	—	—	—																																																																																																																																																																																																						
							2	1.0																																																																																																																																																																																																					



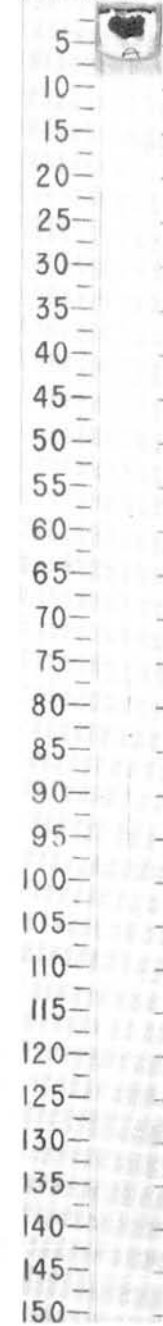
SITE 684 HOLE A CORE 10X CORED INTERVAL 505.1-514.6 mbsl; 79.1-88.6 mbsf

TIME-ROCK UNIT	BIOSTRAT. ZONE/ FOSSIL CHARACTER				PALEOMAGNETICS	PHYS. PROPERTIES	CHEMISTRY	SECTION	METERS	GRAPHIC LITHOLOGY	DRILLING DISTURB.	SED. STRUCTURES	SAMPLES	LITHOLOGIC DESCRIPTION																																																			
	FORAMINIFERS	NANNOFOSSILS	RADIOLARIANS	DIATOMS																																																													
MIDDLE / UPPER MIOCENE	N17 to N21 *	NN9 *												<p>CC</p> <p>CALCAREOUS SILTSTONE and NANNOFOSSIL-BEARING DIATOMACEOUS MUD</p> <p>Major lithology: hard fragments of olive gray (5Y 4/2), slightly calcareous siltstone and nannofossil-bearing diatomaceous mud in CC.</p> <p>SMEAR SLIDE SUMMARY (%):</p> <table border="1"> <tr> <td></td> <td>CC, 7</td> <td>CC, 8</td> </tr> <tr> <td></td> <td>?</td> <td>D</td> </tr> </table> <p>TEXTURE:</p> <table border="1"> <tr> <td>Sand</td> <td>—</td> <td>15</td> </tr> <tr> <td>Silt</td> <td>30</td> <td>50</td> </tr> <tr> <td>Clay</td> <td>70</td> <td>35</td> </tr> </table> <p>COMPOSITION:</p> <table border="1"> <tr> <td>Quartz</td> <td>—</td> <td>3</td> </tr> <tr> <td>Feldspar</td> <td>Tr</td> <td>5</td> </tr> <tr> <td>Rock fragments</td> <td>—</td> <td>Tr</td> </tr> <tr> <td>Clay</td> <td>—</td> <td>20</td> </tr> <tr> <td>Calcite/dolomite</td> <td>100</td> <td>2</td> </tr> <tr> <td>Accessory minerals</td> <td></td> <td></td> </tr> <tr> <td>  Amphibolite</td> <td>Tr</td> <td>—</td> </tr> <tr> <td>  Pyrite</td> <td>—</td> <td>5</td> </tr> <tr> <td>  Foraminifers</td> <td>—</td> <td>10</td> </tr> <tr> <td>  Nannofossils</td> <td>—</td> <td>25</td> </tr> <tr> <td>  Diatoms</td> <td>—</td> <td>30</td> </tr> <tr> <td>  Sponge spicules</td> <td>Tr</td> <td>—</td> </tr> </table>		CC, 7	CC, 8		?	D	Sand	—	15	Silt	30	50	Clay	70	35	Quartz	—	3	Feldspar	Tr	5	Rock fragments	—	Tr	Clay	—	20	Calcite/dolomite	100	2	Accessory minerals			Amphibolite	Tr	—	Pyrite	—	5	Foraminifers	—	10	Nannofossils	—	25	Diatoms	—	30	Sponge spicules	Tr	—
	CC, 7	CC, 8																																																															
	?	D																																																															
Sand	—	15																																																															
Silt	30	50																																																															
Clay	70	35																																																															
Quartz	—	3																																																															
Feldspar	Tr	5																																																															
Rock fragments	—	Tr																																																															
Clay	—	20																																																															
Calcite/dolomite	100	2																																																															
Accessory minerals																																																																	
Amphibolite	Tr	—																																																															
Pyrite	—	5																																																															
Foraminifers	—	10																																																															
Nannofossils	—	25																																																															
Diatoms	—	30																																																															
Sponge spicules	Tr	—																																																															

684A-10X CC



684A-11X CC



SITE 684 HOLE A CORE 11X CORED INTERVAL 514.6-524.1 mbsl; 88.6-98.1 mbsf

TIME-ROCK UNIT	BIOSTRAT. ZONE/ FOSSIL CHARACTER				PALEOMAGNETICS	PHYS. PROPERTIES	CHEMISTRY	SECTION	METERS	GRAPHIC LITHOLOGY	DRILLING DISTURB.	SED. STRUCTURES	SAMPLES	LITHOLOGIC DESCRIPTION																								
	FORAMINIFERS	NANNOFOSSILS	RADIOLARIANS	DIATOMS																																		
MIDDLE / UPPER MIOCENE	Middle Miocene to Upper Miocene *	NN9 *	insignificant *											<p>CC</p> <p>PHOSPHATE NODULE</p> <p>Major lithology: very dark gray (5Y 3/1) hard fragment of phosphate nodule in CC.</p> <p>SMEAR SLIDE SUMMARY (%):</p> <table border="1"> <tr> <td></td> <td>CC</td> </tr> </table> <p>TEXTURE:</p> <table border="1"> <tr> <td>Sand</td> <td>10</td> </tr> <tr> <td>Silt</td> <td>10</td> </tr> <tr> <td>Clay</td> <td>80</td> </tr> </table> <p>COMPOSITION:</p> <table border="1"> <tr> <td>Quartz</td> <td>2</td> </tr> <tr> <td>Feldspar</td> <td>5</td> </tr> <tr> <td>Rock fragments</td> <td>1</td> </tr> <tr> <td>Clay</td> <td>10</td> </tr> <tr> <td>Accessory minerals</td> <td></td> </tr> <tr> <td>  Apatite</td> <td>80</td> </tr> <tr> <td>  Glauconite</td> <td>2</td> </tr> <tr> <td>  Nannofossils</td> <td>Tr</td> </tr> </table>		CC	Sand	10	Silt	10	Clay	80	Quartz	2	Feldspar	5	Rock fragments	1	Clay	10	Accessory minerals		Apatite	80	Glauconite	2	Nannofossils	Tr
	CC																																					
Sand	10																																					
Silt	10																																					
Clay	80																																					
Quartz	2																																					
Feldspar	5																																					
Rock fragments	1																																					
Clay	10																																					
Accessory minerals																																						
Apatite	80																																					
Glauconite	2																																					
Nannofossils	Tr																																					

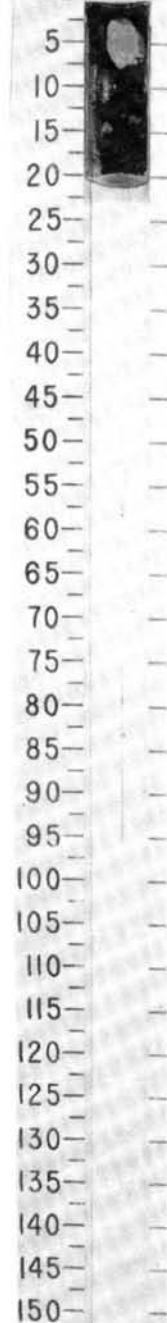
SITE 684 HOLE A CORE 12X CORED INTERVAL 524.1-533.6 mbsf; 98.1-107.6 mbsf

TIME-ROCK UNIT	BIOSTRAT. ZONE/ FOSSIL CHARACTER				PALEOMAGNETICS	PHYS. PROPERTIES	CHEMISTRY	SECTION	METERS	GRAPHIC LITHOLOGY	DRILLING DISTURB.	SED. STRUCTURES	SAMPLES	LITHOLOGIC DESCRIPTION																																																																												
	FORAMINIFERS	NANNOFOSSILS	RADIOLARIANS	DIATOMS																																																																																						
MIDDLE MIOCENE	Middle Miocene *	NN9 *	base <i>D. antepenultimus</i> to top <i>D. alafa</i> *	<i>C. yabei</i> Zone *										<p>CALCAREOUS SILTSTONE and DIATOMACEOUS CALCAREOUS MUD</p> <p>Major lithology: CC, 0-5 cm: calcareous olive gray to olive (5Y 4/2) siltstone, laminated; and 5-20 cm: dark grayish brown (2.5Y 4/2) diatomaceous calcareous mud, mixed with dolomitic glauconitic sand.</p> <p>SMEAR SLIDE SUMMARY (%):</p> <table border="1"> <thead> <tr> <th></th> <th>CC, 2 M</th> <th>CC, 4 D</th> <th>CC, 16 M</th> </tr> </thead> <tbody> <tr> <td>TEXTURE:</td> <td></td> <td></td> <td></td> </tr> <tr> <td>Sand</td> <td>—</td> <td>10</td> <td>40</td> </tr> <tr> <td>Silt</td> <td>1</td> <td>30</td> <td>20</td> </tr> <tr> <td>Clay</td> <td>99</td> <td>60</td> <td>40</td> </tr> </tbody> </table> <p>COMPOSITION:</p> <table border="1"> <thead> <tr> <th></th> <th>Tr</th> <th>Tr</th> <th>3</th> </tr> </thead> <tbody> <tr> <td>Quartz</td> <td>Tr</td> <td>Tr</td> <td>3</td> </tr> <tr> <td>Feldspar</td> <td>Tr</td> <td>Tr</td> <td>5</td> </tr> <tr> <td>Rock fragments</td> <td>—</td> <td>—</td> <td>2</td> </tr> <tr> <td>Clay</td> <td>—</td> <td>33</td> <td>—</td> </tr> <tr> <td>Volcanic glass</td> <td>—</td> <td>Tr</td> <td>—</td> </tr> <tr> <td>Calcite/dolomite</td> <td>100</td> <td>25</td> <td>35</td> </tr> <tr> <td>Accessory minerals</td> <td>—</td> <td>—</td> <td>7</td> </tr> <tr> <td>Pyrite</td> <td>—</td> <td>—</td> <td>40</td> </tr> <tr> <td>Glauconite</td> <td>—</td> <td>—</td> <td>5</td> </tr> <tr> <td>Nannofossils</td> <td>Tr</td> <td>20</td> <td>—</td> </tr> <tr> <td>Diatoms</td> <td>—</td> <td>2</td> <td>—</td> </tr> <tr> <td>Sponge spicules</td> <td>—</td> <td>—</td> <td>3</td> </tr> <tr> <td>Fish remains</td> <td>—</td> <td>—</td> <td>—</td> </tr> </tbody> </table>		CC, 2 M	CC, 4 D	CC, 16 M	TEXTURE:				Sand	—	10	40	Silt	1	30	20	Clay	99	60	40		Tr	Tr	3	Quartz	Tr	Tr	3	Feldspar	Tr	Tr	5	Rock fragments	—	—	2	Clay	—	33	—	Volcanic glass	—	Tr	—	Calcite/dolomite	100	25	35	Accessory minerals	—	—	7	Pyrite	—	—	40	Glauconite	—	—	5	Nannofossils	Tr	20	—	Diatoms	—	2	—	Sponge spicules	—	—	3	Fish remains	—	—	—
	CC, 2 M	CC, 4 D	CC, 16 M																																																																																							
TEXTURE:																																																																																										
Sand	—	10	40																																																																																							
Silt	1	30	20																																																																																							
Clay	99	60	40																																																																																							
	Tr	Tr	3																																																																																							
Quartz	Tr	Tr	3																																																																																							
Feldspar	Tr	Tr	5																																																																																							
Rock fragments	—	—	2																																																																																							
Clay	—	33	—																																																																																							
Volcanic glass	—	Tr	—																																																																																							
Calcite/dolomite	100	25	35																																																																																							
Accessory minerals	—	—	7																																																																																							
Pyrite	—	—	40																																																																																							
Glauconite	—	—	5																																																																																							
Nannofossils	Tr	20	—																																																																																							
Diatoms	—	2	—																																																																																							
Sponge spicules	—	—	3																																																																																							
Fish remains	—	—	—																																																																																							

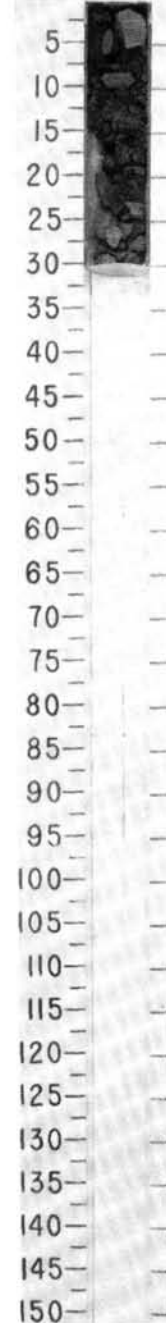
SITE 684 HOLE A CORE 13X CORED INTERVAL 533.6-543.1 mbsf; 107.6-117.1 mbsf

TIME-ROCK UNIT	BIOSTRAT. ZONE/ FOSSIL CHARACTER				PALEOMAGNETICS	PHYS. PROPERTIES	CHEMISTRY	SECTION	METERS	GRAPHIC LITHOLOGY	DRILLING DISTURB.	SED. STRUCTURES	SAMPLES	LITHOLOGIC DESCRIPTION																																																																	
	FORAMINIFERS	NANNOFOSSILS	RADIOLARIANS	DIATOMS																																																																											
MIDDLE MIOCENE / UPPER MIOCENE	Middle Miocene *	NN9 *	<i>D. pettersoni</i> Middle Miocene *	<i>C. yabei</i> Zone *										<p>MUD and LIMESTONE</p> <p>Major lithology: a few fragments of black (5Y 2.5/1) to dark olive gray (5Y 3/2) micritic limestone in a matrix of olive (5Y 4/3) mud, CC.</p> <p>SMEAR SLIDE SUMMARY (%):</p> <table border="1"> <thead> <tr> <th></th> <th>CC, 13 D</th> <th>CC, 13 M</th> <th>CC, 13 D</th> <th>CC, 13 M</th> </tr> </thead> <tbody> <tr> <td>TEXTURE:</td> <td></td> <td></td> <td></td> <td></td> </tr> <tr> <td>Sand</td> <td>5</td> <td>—</td> <td>5</td> <td>30</td> </tr> <tr> <td>Silt</td> <td>20</td> <td>—</td> <td>10</td> <td>20</td> </tr> <tr> <td>Clay</td> <td>75</td> <td>100</td> <td>85</td> <td>50</td> </tr> </tbody> </table> <p>COMPOSITION:</p> <table border="1"> <thead> <tr> <th></th> <th>5</th> <th>—</th> <th>5</th> <th>—</th> </tr> </thead> <tbody> <tr> <td>Quartz</td> <td>5</td> <td>—</td> <td>5</td> <td>—</td> </tr> <tr> <td>Feldspar</td> <td>Tr</td> <td>—</td> <td>Tr</td> <td>—</td> </tr> <tr> <td>Calcite/dolomite</td> <td>95</td> <td>100</td> <td>90</td> <td>70</td> </tr> <tr> <td>Accessory minerals</td> <td>—</td> <td>—</td> <td>—</td> <td>30</td> </tr> <tr> <td>Opaque mineral</td> <td>—</td> <td>Tr</td> <td>—</td> <td>—</td> </tr> <tr> <td>Iron oxide(?)</td> <td>—</td> <td>Tr</td> <td>5</td> <td>—</td> </tr> <tr> <td>Diatoms</td> <td>—</td> <td>Tr</td> <td>—</td> <td>—</td> </tr> </tbody> </table>		CC, 13 D	CC, 13 M	CC, 13 D	CC, 13 M	TEXTURE:					Sand	5	—	5	30	Silt	20	—	10	20	Clay	75	100	85	50		5	—	5	—	Quartz	5	—	5	—	Feldspar	Tr	—	Tr	—	Calcite/dolomite	95	100	90	70	Accessory minerals	—	—	—	30	Opaque mineral	—	Tr	—	—	Iron oxide(?)	—	Tr	5	—	Diatoms	—	Tr	—	—
	CC, 13 D	CC, 13 M	CC, 13 D	CC, 13 M																																																																											
TEXTURE:																																																																															
Sand	5	—	5	30																																																																											
Silt	20	—	10	20																																																																											
Clay	75	100	85	50																																																																											
	5	—	5	—																																																																											
Quartz	5	—	5	—																																																																											
Feldspar	Tr	—	Tr	—																																																																											
Calcite/dolomite	95	100	90	70																																																																											
Accessory minerals	—	—	—	30																																																																											
Opaque mineral	—	Tr	—	—																																																																											
Iron oxide(?)	—	Tr	5	—																																																																											
Diatoms	—	Tr	—	—																																																																											

684A-12X CC



684A-13X CC

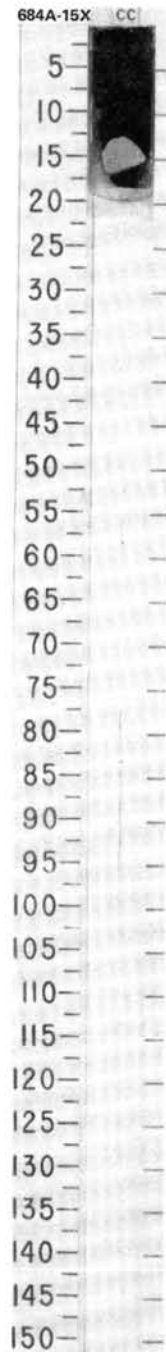
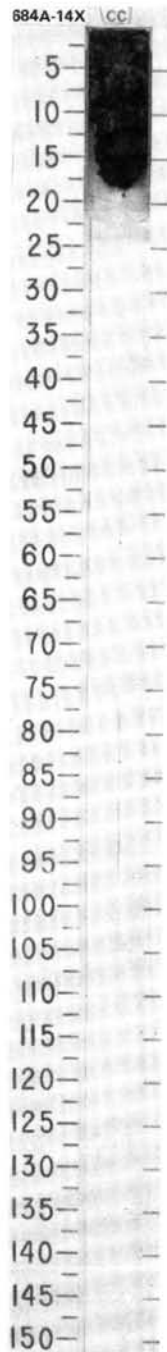


SITE 684 HOLE A CORE 14X CORED INTERVAL 543.1-552.6 mbsl; 117.1-126.6 mbsf

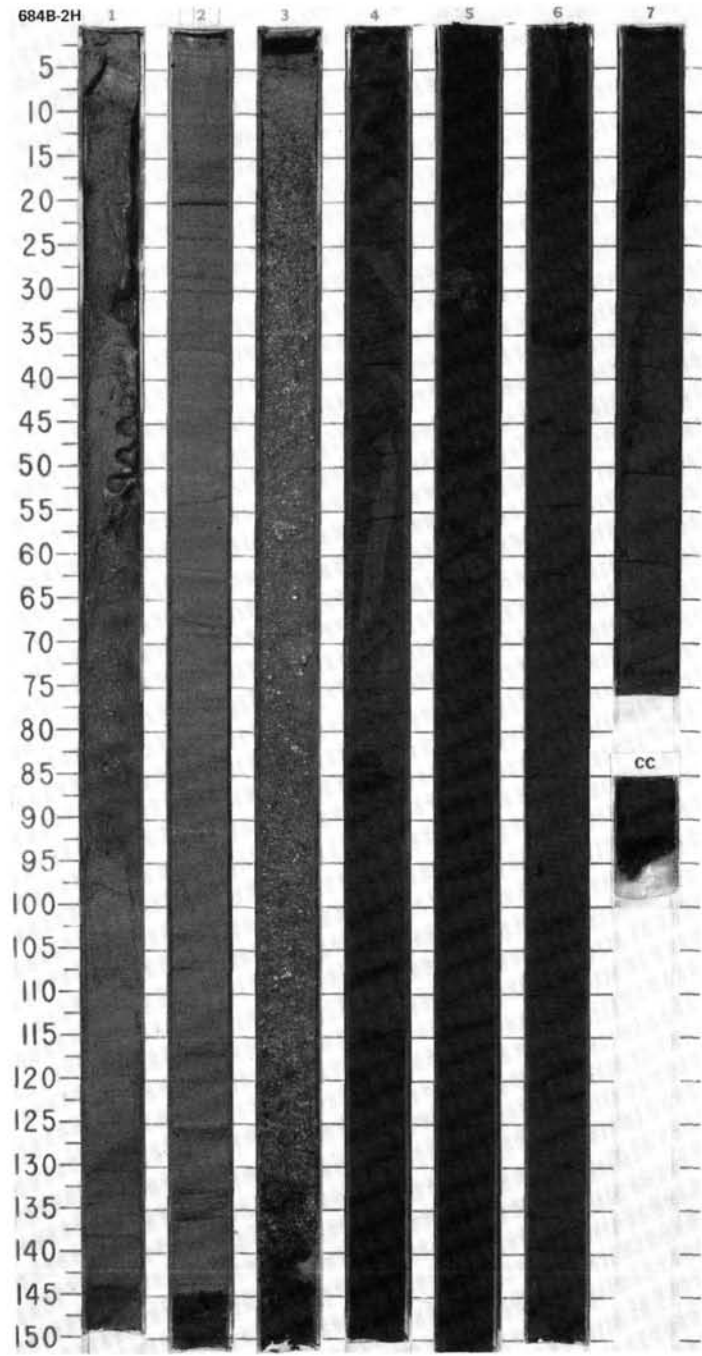
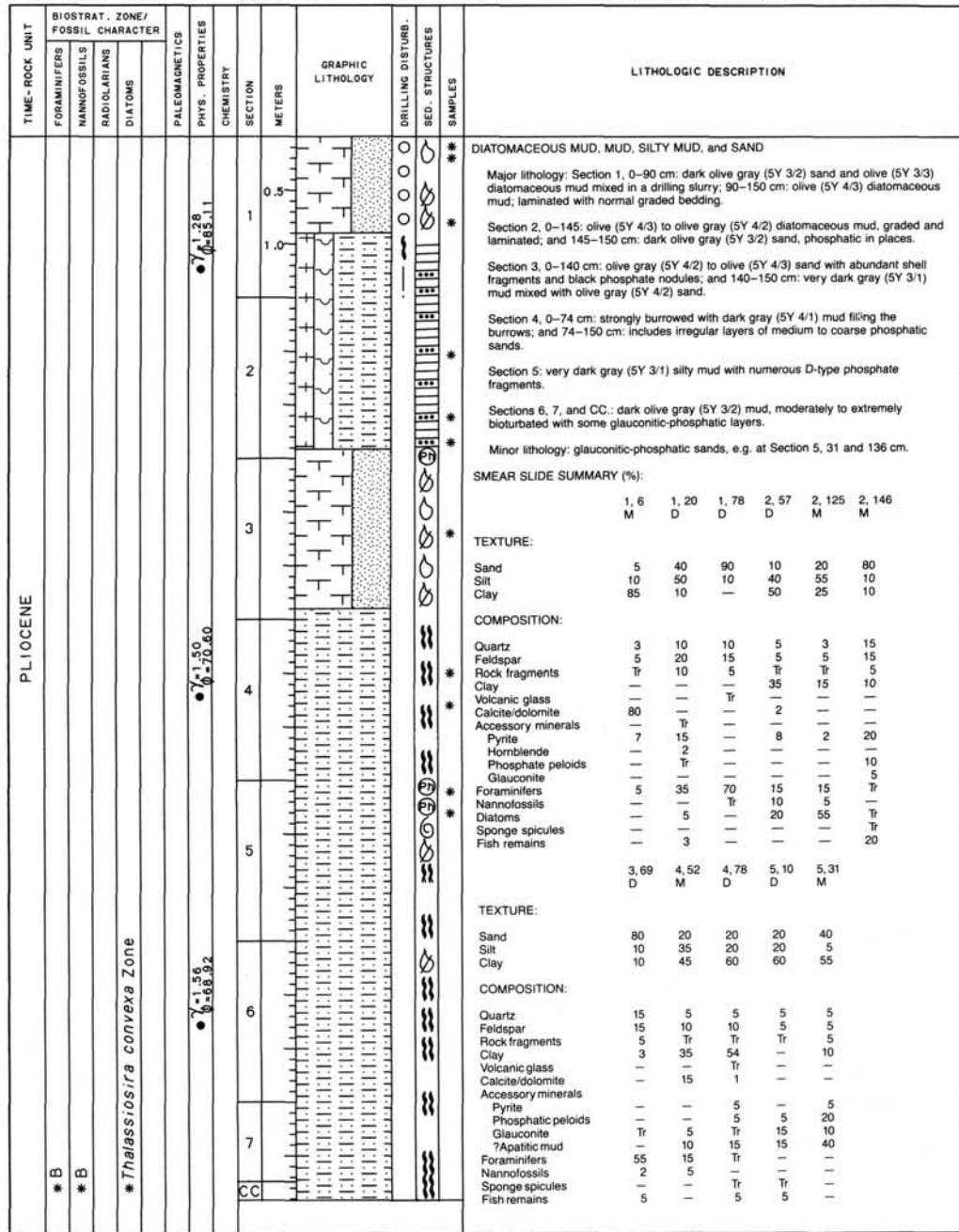
TIME-ROCK UNIT	BIOSTRAT. ZONE/ FOSSIL CHARACTER				PALEOMAGNETICS	PHYS. PROPERTIES	CHEMISTRY	SECTION	METERS	GRAPHIC LITHOLOGY	DRILLING DISTURB.	SED. STRUCTURES	SAMPLES	LITHOLOGIC DESCRIPTION
	FORAMINIFERS	NANNOFOSSILS	RADIOLARIANS	DIATOMS										
MIDDLE MIOCENE / UPPER MIOCENE	B*	NNS*	<i>D. petersoni</i> *	<i>C. yabei</i> Zone*				CC					*	<p>SANDY, CALCAREOUS DIATOMACEOUS MUD</p> <p>Major lithology: dark olive gray (5Y 3/2) sandy, calcareous diatomaceous mud in CC.</p> <p>SMEAR SLIDE SUMMARY (%):</p> <p style="text-align: right;">CC, 8 D</p> <p>TEXTURE:</p> <p>Sand 25 Silt 35 Clay 40</p> <p>COMPOSITION:</p> <p>Quartz 5 Feldspar 10 Rock fragments 5 Clay 27 Calcite/dolomite Tr Accessory minerals Pyrite 3 Foraminifers 10 Nannofossils 10 Diatoms 30</p>

SITE 684 HOLE A CORE 15X CORED INTERVAL 552.6-562.1 mbsl; 126.6-136.1 mbsf

TIME-ROCK UNIT	BIOSTRAT. ZONE/ FOSSIL CHARACTER				PALEOMAGNETICS	PHYS. PROPERTIES	CHEMISTRY	SECTION	METERS	GRAPHIC LITHOLOGY	DRILLING DISTURB.	SED. STRUCTURES	SAMPLES	LITHOLOGIC DESCRIPTION
	FORAMINIFERS	NANNOFOSSILS	RADIOLARIANS	DIATOMS										
MIDDLE / UPPER MIOCENE	Quaternary*		<i>Coscinodiscus yabei</i> *					CC					*	<p>DIATOMACEOUS MUD, SAND, and SHELL FRAGMENTS</p> <p>Major lithology: mixture of olive gray (5Y 4/2) diatomaceous mud and dark gray sand fragments, including shell fragments, in CC. At 15-20 cm: laminated, dolomitic, slightly calcareous.</p> <p>SMEAR SLIDE SUMMARY (%):</p> <p style="text-align: right;">CC, 6 D</p> <p>TEXTURE:</p> <p>Sand 30 Silt 35 Clay 35</p> <p>COMPOSITION:</p> <p>Quartz Tr Feldspar 5 Rock fragments Tr Clay 25 Calcite/dolomite 20 Accessory minerals Pyrite 5 Glauconite Tr Foraminifers 5 Nannofossils 15 Diatoms 20 Fish remains 5</p>

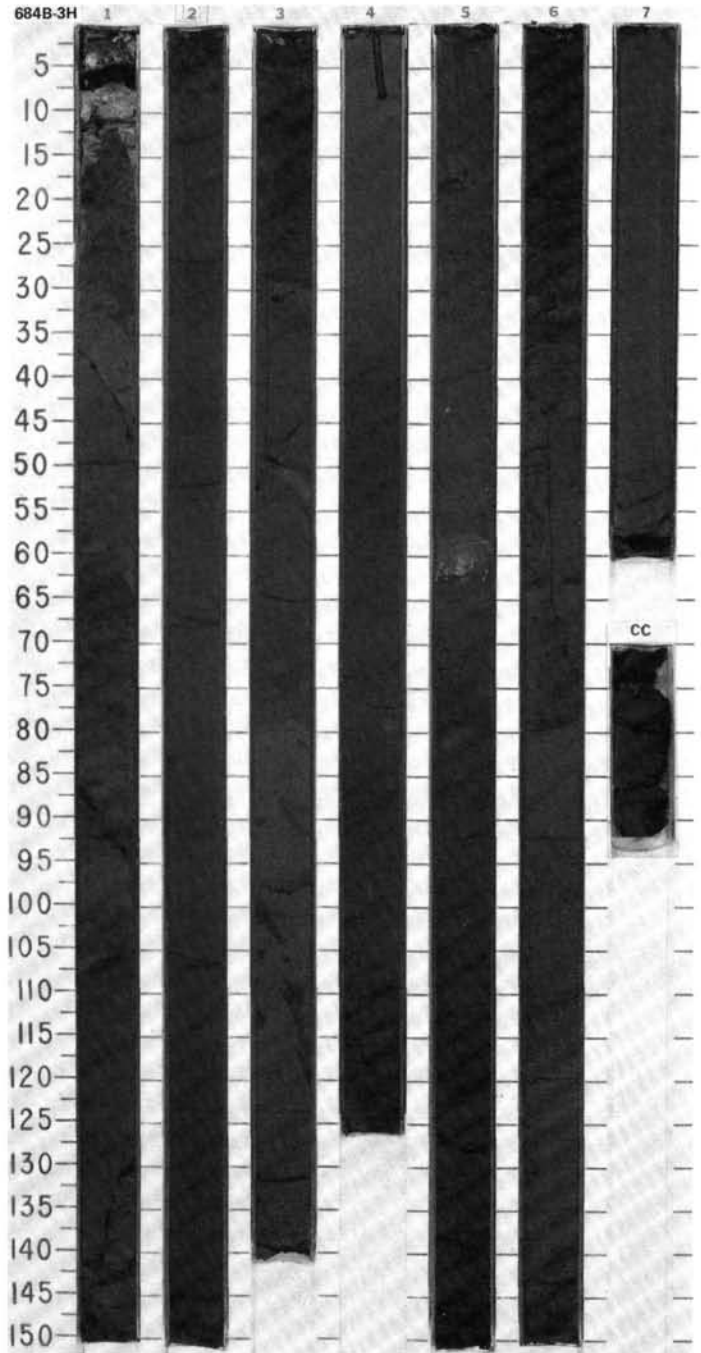




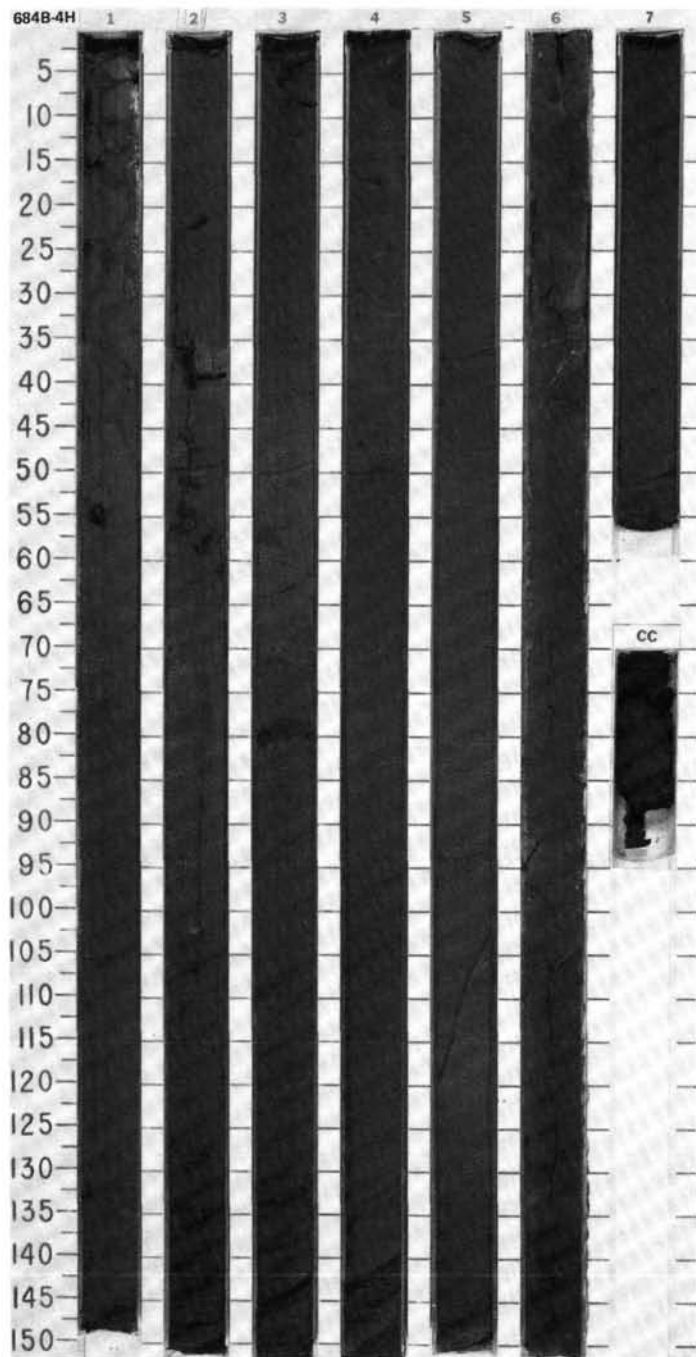


SITE 684 HOLE B CORE 3H CORED INTERVAL 443.5-453.0 mbsl; 17.0-26.5 mbsf

TIME-ROCK UNIT	BIOSTRAT. ZONE/ FOSSIL CHARACTER			PALEOMAGNETICS PHYS. PROPERTIES	CHEMISTRY	SECTION METERS	GRAPHIC LITHOLOGY	DRILLING DISTURB. SED. STRUCTURES	SAMPLES	LITHOLOGIC DESCRIPTION																																																																																																																																					
	FORAMINIFERS	NANNOFOSSILS	RADIOLARIANS								DIATOMS																																																																																																																																				
PLIOCENE	* B					0.5			*	DIATOMACEOUS MUD, SILTY AND SANDY MUD, and MUDDY ASH																																																																																																																																					
	* insignificant					1.0			*	Major lithology: Section 1: black (5Y 2.5/1-5Y 3/1.5) diatomaceous mud, bioturbated and pyritiferous.																																																																																																																																					
	* <i>Thalassiosira convexa</i> Zone					1.5			*	Section 2: olive gray (5Y 3/2) grading to black (5Y 3/1) diatomaceous mud, massive and displaying large burrows.																																																																																																																																					
						2.0			*	Section 3 through 4, 0-35 cm: black (5Y 2.5/1) grading to dark gray (5Y 3/1) diatom-bearing bioturbated mud.																																																																																																																																					
						2.5			*	Section 4, 35-126 cm: very dark gray (5Y 3/1) to black (5Y 2.5/2) silty and sandy mud, moderately bioturbated.																																																																																																																																					
						3.0			*	Section 5, 0-57 cm: black (5Y 2.5/1), grading down into olive gray (5Y 3/2) foraminifer-rich diatomaceous mud; 57-62 cm: olive (5Y 4/4) at top to light olive (5Y 5/3) at base, muddy, diatom-bearing volcanic ash; and 62-150 cm: dark olive gray (5Y 3/2) to black (5Y 2.5/1) silty foraminifer-rich diatomaceous mud, massive to locally burrowed.																																																																																																																																					
						3.5			*	Section 6, 0-42 cm: black (5Y 2.5/1) diatomaceous mud; massive grading down to burrowed with foraminifers visible as white specks; 42-150 cm: dark olive gray (5Y 3/2) foraminifer-bearing diatomaceous mud, some darker burrows visible. Section 7 and CC: black (5Y 2.5/2) foraminifer diatomaceous mud, massive.																																																																																																																																					
					4.0					SMEAR SLIDE SUMMARY (%):																																																																																																																																					
					4.5					<table border="1"> <tr> <td></td> <td>1, 39</td> <td>1, 68</td> <td>2, 8</td> <td>3, 85</td> <td>5, 62</td> <td>7, 12</td> </tr> <tr> <td></td> <td>D</td> <td>D</td> <td>D</td> <td>D</td> <td>M</td> <td>D</td> </tr> </table>		1, 39	1, 68	2, 8	3, 85	5, 62	7, 12		D	D	D	D	M	D																																																																																																																							
	1, 39	1, 68	2, 8	3, 85	5, 62	7, 12																																																																																																																																									
	D	D	D	D	M	D																																																																																																																																									
					5.0					TEXTURE:																																																																																																																																					
					5.5					<table border="1"> <tr> <td>Sand</td> <td>10</td> <td>10</td> <td>30</td> <td>5</td> <td>35</td> <td>25</td> </tr> <tr> <td>Silt</td> <td>40</td> <td>30</td> <td>30</td> <td>20</td> <td>40</td> <td>35</td> </tr> <tr> <td>Clay</td> <td>50</td> <td>60</td> <td>40</td> <td>75</td> <td>25</td> <td>40</td> </tr> </table>	Sand	10	10	30	5	35	25	Silt	40	30	30	20	40	35	Clay	50	60	40	75	25	40																																																																																																																
Sand	10	10	30	5	35	25																																																																																																																																									
Silt	40	30	30	20	40	35																																																																																																																																									
Clay	50	60	40	75	25	40																																																																																																																																									
					6.0					COMPOSITION:																																																																																																																																					
					6.5					<table border="1"> <tr> <td>Quartz</td> <td>10</td> <td>10</td> <td>5</td> <td>5</td> <td>5</td> <td>5</td> </tr> <tr> <td>Feldspar</td> <td>5</td> <td>2</td> <td>2</td> <td>Tr</td> <td>Tr</td> <td>Tr</td> </tr> <tr> <td>Rock fragments</td> <td>5</td> <td>3</td> <td>3</td> <td>5</td> <td>5</td> <td>Tr</td> </tr> <tr> <td>Mica</td> <td>—</td> <td>—</td> <td>—</td> <td>—</td> <td>Tr</td> <td>—</td> </tr> <tr> <td>Clay</td> <td>30</td> <td>50</td> <td>35</td> <td>65</td> <td>10</td> <td>35</td> </tr> <tr> <td>Volcanic glass</td> <td>1</td> <td>Tr</td> <td>—</td> <td>—</td> <td>75</td> <td>Tr</td> </tr> <tr> <td>Calcite/dolomite</td> <td>2</td> <td>Tr</td> <td>Tr</td> <td>—</td> <td>—</td> <td>—</td> </tr> <tr> <td>Accessory minerals</td> <td></td> <td></td> <td></td> <td></td> <td></td> <td></td> </tr> <tr> <td>  Glauconite</td> <td>2</td> <td>5</td> <td>—</td> <td>—</td> <td>Tr</td> <td>—</td> </tr> <tr> <td>  Pyrite</td> <td>10</td> <td>10</td> <td>5</td> <td>5</td> <td>Tr</td> <td>2</td> </tr> <tr> <td>  Micrite</td> <td>5</td> <td>—</td> <td>5</td> <td>5</td> <td>—</td> <td>10</td> </tr> <tr> <td>  Phosphate peloids</td> <td>—</td> <td>—</td> <td>Tr</td> <td>—</td> <td>—</td> <td>—</td> </tr> <tr> <td>  Hornblende</td> <td>—</td> <td>—</td> <td>—</td> <td>—</td> <td>Tr</td> <td>—</td> </tr> <tr> <td>Foraminifers</td> <td>—</td> <td>Tr</td> <td>Tr</td> <td>—</td> <td>—</td> <td>20</td> </tr> <tr> <td>Nannofossils</td> <td>—</td> <td>—</td> <td>Tr</td> <td>—</td> <td>—</td> <td>—</td> </tr> <tr> <td>Diatoms</td> <td>30</td> <td>20</td> <td>45</td> <td>15</td> <td>5</td> <td>25</td> </tr> <tr> <td>Radiolarians</td> <td>—</td> <td>—</td> <td>Tr</td> <td>—</td> <td>Tr</td> <td>—</td> </tr> <tr> <td>Sponge spicules</td> <td>Tr</td> <td>Tr</td> <td>Tr</td> <td>Tr</td> <td>Tr</td> <td>3</td> </tr> <tr> <td>Fish remains</td> <td>—</td> <td>—</td> <td>—</td> <td>—</td> <td>Tr</td> <td>—</td> </tr> </table>	Quartz	10	10	5	5	5	5	Feldspar	5	2	2	Tr	Tr	Tr	Rock fragments	5	3	3	5	5	Tr	Mica	—	—	—	—	Tr	—	Clay	30	50	35	65	10	35	Volcanic glass	1	Tr	—	—	75	Tr	Calcite/dolomite	2	Tr	Tr	—	—	—	Accessory minerals							Glauconite	2	5	—	—	Tr	—	Pyrite	10	10	5	5	Tr	2	Micrite	5	—	5	5	—	10	Phosphate peloids	—	—	Tr	—	—	—	Hornblende	—	—	—	—	Tr	—	Foraminifers	—	Tr	Tr	—	—	20	Nannofossils	—	—	Tr	—	—	—	Diatoms	30	20	45	15	5	25	Radiolarians	—	—	Tr	—	Tr	—	Sponge spicules	Tr	Tr	Tr	Tr	Tr	3	Fish remains	—	—	—	—	Tr	—
Quartz	10	10	5	5	5	5																																																																																																																																									
Feldspar	5	2	2	Tr	Tr	Tr																																																																																																																																									
Rock fragments	5	3	3	5	5	Tr																																																																																																																																									
Mica	—	—	—	—	Tr	—																																																																																																																																									
Clay	30	50	35	65	10	35																																																																																																																																									
Volcanic glass	1	Tr	—	—	75	Tr																																																																																																																																									
Calcite/dolomite	2	Tr	Tr	—	—	—																																																																																																																																									
Accessory minerals																																																																																																																																															
Glauconite	2	5	—	—	Tr	—																																																																																																																																									
Pyrite	10	10	5	5	Tr	2																																																																																																																																									
Micrite	5	—	5	5	—	10																																																																																																																																									
Phosphate peloids	—	—	Tr	—	—	—																																																																																																																																									
Hornblende	—	—	—	—	Tr	—																																																																																																																																									
Foraminifers	—	Tr	Tr	—	—	20																																																																																																																																									
Nannofossils	—	—	Tr	—	—	—																																																																																																																																									
Diatoms	30	20	45	15	5	25																																																																																																																																									
Radiolarians	—	—	Tr	—	Tr	—																																																																																																																																									
Sponge spicules	Tr	Tr	Tr	Tr	Tr	3																																																																																																																																									
Fish remains	—	—	—	—	Tr	—																																																																																																																																									
					7.0					CC																																																																																																																																					



TIME-ROCK UNIT	BIOSTRAT. ZONE/ FOSSIL CHARACTER			PALEOMAGNETICS	PHYS. PROPERTIES	CHEMISTRY	SECTION	METERS	GRAPHIC LITHOLOGY	DRILLING DISTURB.	SED. STRUCTURES	SAMPLES	LITHOLOGIC DESCRIPTION																																																																																																																																																																																																																
	FORAMINIFERS	NANNOFOSSILS	RADIOLARIANS																																																																																																																																																																																																																										
PLIOCENE	* B							0.5					<p>DIATOM-BEARING MUD, DIATOMACEOUS MUD, SANDY MUD, and FORAMINIFER-BEARING DIATOMACEOUS MUD</p> <p>Major lithology: Section 1, 0-70 cm: very dark gray (5Y 3/1) to dark olive gray (5Y 3/2) diatom-bearing mud; and 70-150 cm: olive gray (5Y 4/2) foraminifer-bearing sandy mud.</p> <p>Section 2, 0-125 cm: dark olive gray (5Y 3/2) mud, moderately bioturbated with lenses of glauconitic sand (e.g. 67 cm); and 125-150 cm: very dark gray (5Y 3/1) silty mud with thin layer of glauconitic-phosphatic sand.</p> <p>Sections 3-4 and Section 5, 0-147 cm: very dark gray (5Y 3/1) to dark olive gray (5Y 3/2) foraminifer-bearing diatomaceous mud, massive to diffusely laminated.</p> <p>Section 5, 147 cm, through CC: black (5Y 2.5/2, 5Y 2.5/1) foraminifer-bearing diatomaceous mud, massive, locally showing burrows filled with olive (5Y 4/4) material and calcareous veining (e.g., Section 6, 34 cm) and an apatite vein (Section 6, 36.5 cm).</p> <p>Minor lithology: dark olive gray (5Y 3/2) glauconitic sand, e.g., Section 3, 77-81 and 128-32 cm.</p> <p>SMEAR SLIDE SUMMARY (%):</p> <table border="1"> <thead> <tr> <th></th> <th>1, 66</th> <th>3, 40</th> <th>3, 79</th> <th>4, 32</th> <th>5, 31</th> <th>6, 36</th> <th>6, 87</th> </tr> <tr> <th></th> <th>D</th> <th>D</th> <th>M</th> <th>M</th> <th>D</th> <th>M</th> <th>D</th> </tr> </thead> <tbody> <tr> <td>Sand</td> <td>15</td> <td>25</td> <td>55</td> <td>20</td> <td>5</td> <td>—</td> <td>50</td> </tr> <tr> <td>Silt</td> <td>40</td> <td>30</td> <td>25</td> <td>20</td> <td>65</td> <td>90</td> <td>15</td> </tr> <tr> <td>Clay</td> <td>45</td> <td>45</td> <td>20</td> <td>60</td> <td>30</td> <td>10</td> <td>35</td> </tr> </tbody> </table> <p>TEXTURE:</p> <table border="1"> <thead> <tr> <th></th> <th>1, 66</th> <th>3, 40</th> <th>3, 79</th> <th>4, 32</th> <th>5, 31</th> <th>6, 36</th> <th>6, 87</th> </tr> </thead> <tbody> <tr> <td>Sand</td> <td>15</td> <td>25</td> <td>55</td> <td>20</td> <td>5</td> <td>—</td> <td>50</td> </tr> <tr> <td>Silt</td> <td>40</td> <td>30</td> <td>25</td> <td>20</td> <td>65</td> <td>90</td> <td>15</td> </tr> <tr> <td>Clay</td> <td>45</td> <td>45</td> <td>20</td> <td>60</td> <td>30</td> <td>10</td> <td>35</td> </tr> </tbody> </table> <p>COMPOSITION:</p> <table border="1"> <thead> <tr> <th></th> <th>1, 66</th> <th>3, 40</th> <th>3, 79</th> <th>4, 32</th> <th>5, 31</th> <th>6, 36</th> <th>6, 87</th> </tr> </thead> <tbody> <tr> <td>Quartz</td> <td>5</td> <td>5</td> <td>5</td> <td>5</td> <td>5</td> <td>—</td> <td>10</td> </tr> <tr> <td>Feldspar</td> <td>10</td> <td>15</td> <td>15</td> <td>5</td> <td>5</td> <td>Tr</td> <td>20</td> </tr> <tr> <td>Rock fragments</td> <td>5</td> <td>5</td> <td>5</td> <td>Tr</td> <td>Tr</td> <td>Tr</td> <td>5</td> </tr> <tr> <td>Clay</td> <td>35</td> <td>35</td> <td>10</td> <td>15</td> <td>30</td> <td>10</td> <td>30</td> </tr> <tr> <td>Calcite/dolomite</td> <td>5</td> <td>7</td> <td>5</td> <td>42</td> <td>10</td> <td>Tr</td> <td>2</td> </tr> <tr> <td>Accessory minerals</td> <td></td> <td></td> <td></td> <td></td> <td></td> <td></td> <td></td> </tr> <tr> <td>Pyrite</td> <td>5</td> <td>10</td> <td>—</td> <td>—</td> <td>—</td> <td>—</td> <td>10</td> </tr> <tr> <td>Glauconite</td> <td>—</td> <td>5</td> <td>—</td> <td>—</td> <td>—</td> <td>—</td> <td>5</td> </tr> <tr> <td>Phosphate peloids</td> <td>—</td> <td>5</td> <td>20</td> <td>—</td> <td>—</td> <td>—</td> <td>—</td> </tr> <tr> <td>Apatite</td> <td>—</td> <td>—</td> <td>10</td> <td>—</td> <td>—</td> <td>80</td> <td>—</td> </tr> <tr> <td>Foraminifers</td> <td>10</td> <td>10</td> <td>20</td> <td>10</td> <td>20</td> <td>—</td> <td>15</td> </tr> <tr> <td>Nannofossils</td> <td>5</td> <td>—</td> <td>—</td> <td>3</td> <td>5</td> <td>—</td> <td>3</td> </tr> <tr> <td>Diatoms</td> <td>20</td> <td>—</td> <td>—</td> <td>20</td> <td>20</td> <td>10</td> <td>—</td> </tr> <tr> <td>Radiolarians</td> <td>—</td> <td>Tr</td> <td>—</td> <td>—</td> <td>—</td> <td>—</td> <td>—</td> </tr> <tr> <td>Sponge spicules</td> <td>—</td> <td>3</td> <td>—</td> <td>—</td> <td>5</td> <td>—</td> <td>—</td> </tr> <tr> <td>Fish remains</td> <td>—</td> <td>Tr</td> <td>10</td> <td>—</td> <td>—</td> <td>—</td> <td>—</td> </tr> </tbody> </table>		1, 66	3, 40	3, 79	4, 32	5, 31	6, 36	6, 87		D	D	M	M	D	M	D	Sand	15	25	55	20	5	—	50	Silt	40	30	25	20	65	90	15	Clay	45	45	20	60	30	10	35		1, 66	3, 40	3, 79	4, 32	5, 31	6, 36	6, 87	Sand	15	25	55	20	5	—	50	Silt	40	30	25	20	65	90	15	Clay	45	45	20	60	30	10	35		1, 66	3, 40	3, 79	4, 32	5, 31	6, 36	6, 87	Quartz	5	5	5	5	5	—	10	Feldspar	10	15	15	5	5	Tr	20	Rock fragments	5	5	5	Tr	Tr	Tr	5	Clay	35	35	10	15	30	10	30	Calcite/dolomite	5	7	5	42	10	Tr	2	Accessory minerals								Pyrite	5	10	—	—	—	—	10	Glauconite	—	5	—	—	—	—	5	Phosphate peloids	—	5	20	—	—	—	—	Apatite	—	—	10	—	—	80	—	Foraminifers	10	10	20	10	20	—	15	Nannofossils	5	—	—	3	5	—	3	Diatoms	20	—	—	20	20	10	—	Radiolarians	—	Tr	—	—	—	—	—	Sponge spicules	—	3	—	—	5	—	—	Fish remains	—	Tr	10	—	—	—	—
		1, 66	3, 40	3, 79	4, 32	5, 31	6, 36	6, 87																																																																																																																																																																																																																					
		D	D	M	M	D	M	D																																																																																																																																																																																																																					
	Sand	15	25	55	20	5	—	50																																																																																																																																																																																																																					
	Silt	40	30	25	20	65	90	15																																																																																																																																																																																																																					
	Clay	45	45	20	60	30	10	35																																																																																																																																																																																																																					
		1, 66	3, 40	3, 79	4, 32	5, 31	6, 36	6, 87																																																																																																																																																																																																																					
Sand	15	25	55	20	5	—	50																																																																																																																																																																																																																						
Silt	40	30	25	20	65	90	15																																																																																																																																																																																																																						
Clay	45	45	20	60	30	10	35																																																																																																																																																																																																																						
	1, 66	3, 40	3, 79	4, 32	5, 31	6, 36	6, 87																																																																																																																																																																																																																						
Quartz	5	5	5	5	5	—	10																																																																																																																																																																																																																						
Feldspar	10	15	15	5	5	Tr	20																																																																																																																																																																																																																						
Rock fragments	5	5	5	Tr	Tr	Tr	5																																																																																																																																																																																																																						
Clay	35	35	10	15	30	10	30																																																																																																																																																																																																																						
Calcite/dolomite	5	7	5	42	10	Tr	2																																																																																																																																																																																																																						
Accessory minerals																																																																																																																																																																																																																													
Pyrite	5	10	—	—	—	—	10																																																																																																																																																																																																																						
Glauconite	—	5	—	—	—	—	5																																																																																																																																																																																																																						
Phosphate peloids	—	5	20	—	—	—	—																																																																																																																																																																																																																						
Apatite	—	—	10	—	—	80	—																																																																																																																																																																																																																						
Foraminifers	10	10	20	10	20	—	15																																																																																																																																																																																																																						
Nannofossils	5	—	—	3	5	—	3																																																																																																																																																																																																																						
Diatoms	20	—	—	20	20	10	—																																																																																																																																																																																																																						
Radiolarians	—	Tr	—	—	—	—	—																																																																																																																																																																																																																						
Sponge spicules	—	3	—	—	5	—	—																																																																																																																																																																																																																						
Fish remains	—	Tr	10	—	—	—	—																																																																																																																																																																																																																						
				● 6-17, 72				1.0																																																																																																																																																																																																																					
				● 6-17, 72				2																																																																																																																																																																																																																					
				● 6-17, 72				3																																																																																																																																																																																																																					
				● 6-17, 72				4																																																																																																																																																																																																																					
				● 6-17, 72				5																																																																																																																																																																																																																					
				● 6-17, 72				6																																																																																																																																																																																																																					
				● 6-17, 72				7																																																																																																																																																																																																																					
				● 6-17, 72				CC																																																																																																																																																																																																																					

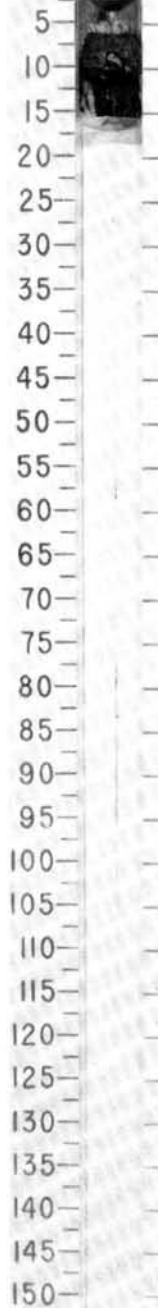


SITE 684 HOLE B CORE 5H CORED INTERVAL 462.5-472.0 mbsl; 36.0-45.5 mbsf

TIME-ROCK UNIT	BIOSTRAT. ZONE/ FOSSIL CHARACTER				PALEOMAGNETICS	PHYS. PROPERTIES	CHEMISTRY	SECTION	METERS	GRAPHIC LITHOLOGY	DRILLING DISTURB. SED. STRUCTURES	SAMPLES	LITHOLOGIC DESCRIPTION
	FORAMINIFERS	NANNOFOSSILS	RADIOLARIANS	DIATOMS									
PLIOCENE	B *	B *											<p>FORAMINIFER-BEARING DIATOMACEOUS MUDSTONE</p> <p>Major lithology: dark olive gray (5Y 3/2) foraminifer-bearing diatomaceous mudstone in CC.</p> <p>SMEAR SLIDE SUMMARY (%): CC, 7</p> <p>TEXTURE:</p> <p>Sand 5 Silt 80 Clay 15</p> <p>COMPOSITION:</p> <p>Quartz 15 Feldspar 5 Clay 15 Calcite/dolomite, some rhombs. 10 Accessory minerals 5 Phosphatic debris 3 Pyrite 3 Foraminifers 15 Nannofossils Tr Diatoms 30 Radiolarians Tr Sponge spicules 2 Fish remains Tr</p>

CORE 112-684B-6X NO RECOVERY

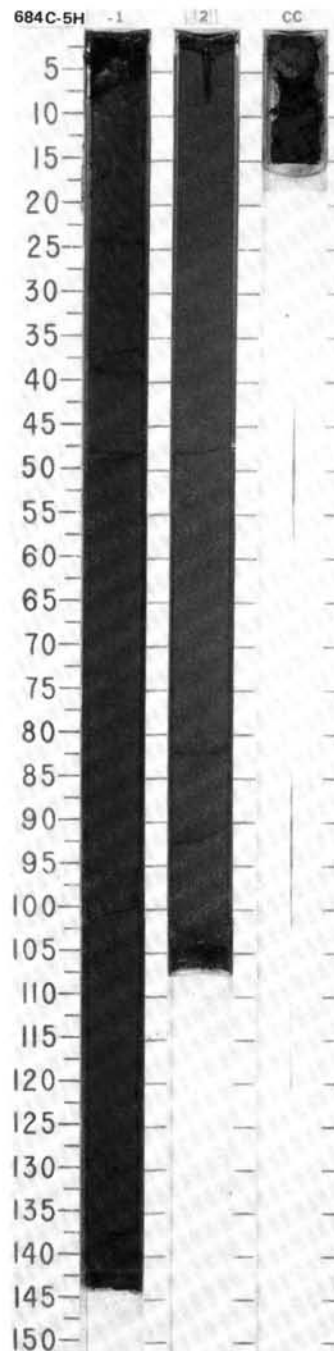
684B-5H CC



CORES 112-684C-1HTO -4H NOT OPENED

SITE 684 HOLE C CORE 5H CORED INTERVAL 462.8-465.5 mbsl: 36.3-39.0 mbsf

TIME-ROCK UNIT	BIOSTRAT. ZONE/ FOSSIL CHARACTER				PALEOMAGNETICS	PHYS. PROPERTIES	CHEMISTRY	SECTION	METERS	GRAPHIC LITHOLOGY	DRILLING DISTURB.	SED. STRUCTURES	SAMPLES	LITHOLOGIC DESCRIPTION																																																																																																																								
	FORAMINIFERS	NANNOFOSSILS	RADIOLARIANS	DIATOMS																																																																																																																																		
PLIOCENE	* B							1	0.5					<p>SILTY MUD and DIATOMACEOUS MUD</p> <p>Major lithology: CC, 1-9 cm: olive gray (5Y 4/4) dolomitized silty mud; and 9-15 cm: dark olive gray (5Y 3/2) diatomaceous mud.</p> <p>Major lithology: Sections 1-2: dark olive gray (5Y 3/2) to olive (5Y 4/3) foraminifer-bearing diatomaceous mud. CC, 1-9 cm: olive gray (5Y 4/4) dolomitized silty mud; and CC, 9-15 cm: dark olive gray (5Y 3/2) diatomaceous mud.</p> <p>Minor lithology: glauconitic-phosphoric sand at Section 1, 130 cm.</p> <p>SMEAR SLIDE SUMMARY (%):</p> <table border="1"> <thead> <tr> <th></th> <th>1, 82 D</th> <th>1, 129 M</th> <th>CC, 7 M</th> <th>CC, 7 D</th> </tr> </thead> <tbody> <tr> <td>Sand</td> <td>5</td> <td>40</td> <td>—</td> <td>5</td> </tr> <tr> <td>Silt</td> <td>35</td> <td>30</td> <td>50</td> <td>80</td> </tr> <tr> <td>Clay</td> <td>60</td> <td>30</td> <td>50</td> <td>15</td> </tr> </tbody> </table> <p>TEXTURE:</p> <table border="1"> <tbody> <tr> <td>Sand</td> <td>5</td> <td>40</td> <td>—</td> <td>5</td> </tr> <tr> <td>Silt</td> <td>35</td> <td>30</td> <td>50</td> <td>80</td> </tr> <tr> <td>Clay</td> <td>60</td> <td>30</td> <td>50</td> <td>15</td> </tr> </tbody> </table> <p>COMPOSITION:</p> <table border="1"> <tbody> <tr> <td>Quartz</td> <td>5</td> <td>—</td> <td>—</td> <td>15</td> </tr> <tr> <td>Feldspar</td> <td>5</td> <td>—</td> <td>—</td> <td>5</td> </tr> <tr> <td>Clay</td> <td>50</td> <td>30</td> <td>—</td> <td>15</td> </tr> <tr> <td>Volcanic glass</td> <td>—</td> <td>Tr</td> <td>—</td> <td>—</td> </tr> <tr> <td>Calcite/dolomite</td> <td>10</td> <td>5</td> <td>—</td> <td>10</td> </tr> <tr> <td>Accessory minerals</td> <td></td> <td></td> <td></td> <td></td> </tr> <tr> <td>  Glauconite</td> <td>Tr</td> <td>30</td> <td>—</td> <td>—</td> </tr> <tr> <td>  Opaques (pyrite and phosphorite)</td> <td>—</td> <td>30</td> <td>5</td> <td>3</td> </tr> <tr> <td>  Micrite</td> <td>—</td> <td>—</td> <td>90</td> <td>—</td> </tr> <tr> <td>  Phosphatic debris</td> <td>—</td> <td>—</td> <td>—</td> <td>5</td> </tr> <tr> <td>Foraminifers</td> <td>10</td> <td>—</td> <td>—</td> <td>15</td> </tr> <tr> <td>Nannofossils</td> <td>10</td> <td>—</td> <td>—</td> <td>Tr</td> </tr> <tr> <td>Diatoms</td> <td>10</td> <td>5</td> <td>5</td> <td>30</td> </tr> <tr> <td>Radiolarians</td> <td>—</td> <td>—</td> <td>—</td> <td>Tr</td> </tr> <tr> <td>Sponge spicules</td> <td>—</td> <td>Tr</td> <td>—</td> <td>2</td> </tr> <tr> <td>Silicoflagellates</td> <td>Tr</td> <td>Tr</td> <td>—</td> <td>—</td> </tr> <tr> <td>Fish remains</td> <td>—</td> <td>—</td> <td>—</td> <td>Tr</td> </tr> </tbody> </table>		1, 82 D	1, 129 M	CC, 7 M	CC, 7 D	Sand	5	40	—	5	Silt	35	30	50	80	Clay	60	30	50	15	Sand	5	40	—	5	Silt	35	30	50	80	Clay	60	30	50	15	Quartz	5	—	—	15	Feldspar	5	—	—	5	Clay	50	30	—	15	Volcanic glass	—	Tr	—	—	Calcite/dolomite	10	5	—	10	Accessory minerals					Glauconite	Tr	30	—	—	Opaques (pyrite and phosphorite)	—	30	5	3	Micrite	—	—	90	—	Phosphatic debris	—	—	—	5	Foraminifers	10	—	—	15	Nannofossils	10	—	—	Tr	Diatoms	10	5	5	30	Radiolarians	—	—	—	Tr	Sponge spicules	—	Tr	—	2	Silicoflagellates	Tr	Tr	—	—	Fish remains	—	—	—	Tr
		1, 82 D	1, 129 M	CC, 7 M	CC, 7 D																																																																																																																																	
Sand	5	40	—	5																																																																																																																																		
Silt	35	30	50	80																																																																																																																																		
Clay	60	30	50	15																																																																																																																																		
Sand	5	40	—	5																																																																																																																																		
Silt	35	30	50	80																																																																																																																																		
Clay	60	30	50	15																																																																																																																																		
Quartz	5	—	—	15																																																																																																																																		
Feldspar	5	—	—	5																																																																																																																																		
Clay	50	30	—	15																																																																																																																																		
Volcanic glass	—	Tr	—	—																																																																																																																																		
Calcite/dolomite	10	5	—	10																																																																																																																																		
Accessory minerals																																																																																																																																						
Glauconite	Tr	30	—	—																																																																																																																																		
Opaques (pyrite and phosphorite)	—	30	5	3																																																																																																																																		
Micrite	—	—	90	—																																																																																																																																		
Phosphatic debris	—	—	—	5																																																																																																																																		
Foraminifers	10	—	—	15																																																																																																																																		
Nannofossils	10	—	—	Tr																																																																																																																																		
Diatoms	10	5	5	30																																																																																																																																		
Radiolarians	—	—	—	Tr																																																																																																																																		
Sponge spicules	—	Tr	—	2																																																																																																																																		
Silicoflagellates	Tr	Tr	—	—																																																																																																																																		
Fish remains	—	—	—	Tr																																																																																																																																		
	* B							2	1.0																																																																																																																													

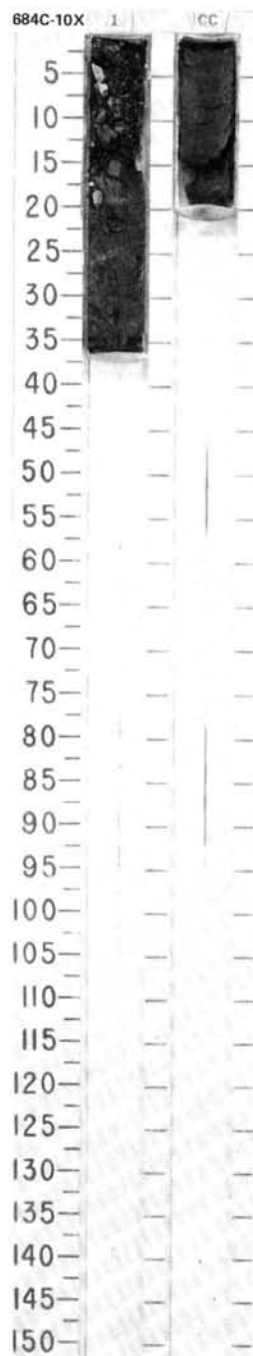




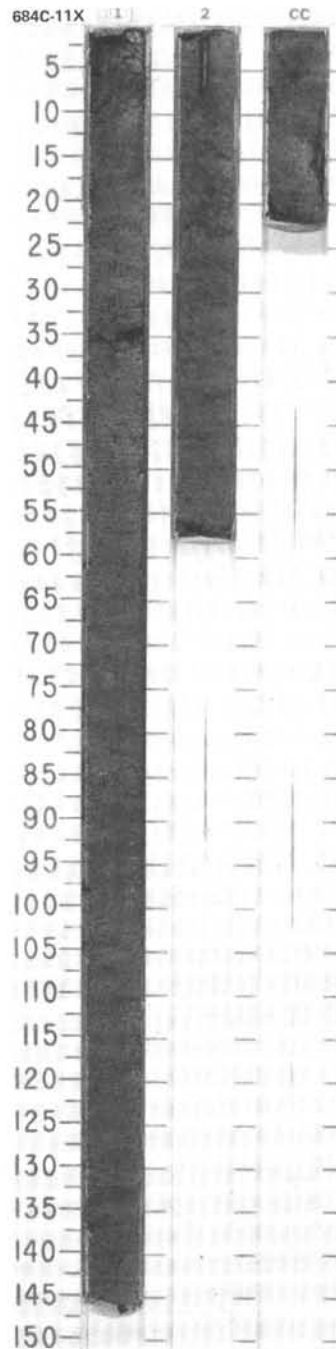


SITE 684 HOLE C CORE 10X CORED INTERVAL 503.5-513.0 mbsl; 77.0-86.5 mbsf

TIME-ROCK UNIT	BIOSTRAT. ZONE/ FOSSIL CHARACTER				PALEOMAGNETICS	PHYS. PROPERTIES	CHEMISTRY	SECTION	METERS	GRAPHIC LITHOLOGY	DRILLING DISTURB. SED. STRUCTURES	SAMPLES	LITHOLOGIC DESCRIPTION																																																																
	FORAMINIFERS	NANNOFOSSILS	RADIOLARIANS	DIATOMS																																																																									
MIDDLE/UPPER MIOCENE	not diagnostic *	NN9 *	<i>D. antepenultimus</i> (Upper Miocene) *	<i>C. yabei</i> *			10.3 OC. 5.1.1	1					<p>DOLOMITE and DIATOMACEOUS MUD</p> <p>Major lithology: Section 1, 0-15 cm: olive gray (5Y 4/2) drilling breccia containing fragments of dolomite either cut by carbonate veins (brecciated) or massive and porous (moldic?); 15-37 cm: olive gray (5Y 4/2) laminated diatomaceous mud; and CC: dark olive gray (5Y 3/2) to olive (5Y 5/4) nannofossil-bearing diatomaceous mud to ooze, cut by vein (dewatering?) structures.</p> <p>Minor lithology: pale olive stringer of "(dolo)micrite" in Section 1, 15-37 cm.</p> <p>SMEAR SLIDE SUMMARY (%):</p> <table border="1"> <thead> <tr> <th></th> <th>1, 26 M</th> <th>CC, 3 M</th> <th>CC, 6 D</th> </tr> </thead> <tbody> <tr> <td>Silt</td> <td>30</td> <td>90</td> <td>55</td> </tr> <tr> <td>Clay</td> <td>70</td> <td>10</td> <td>45</td> </tr> </tbody> </table> <p>TEXTURE:</p> <p>COMPOSITION:</p> <table border="1"> <tbody> <tr> <td>Quartz</td> <td>—</td> <td>5</td> <td>5</td> </tr> <tr> <td>Clay</td> <td>30</td> <td>5</td> <td>35</td> </tr> <tr> <td>Volcanic glass</td> <td>Tr</td> <td>—</td> <td>—</td> </tr> <tr> <td>Calcite/dolomite</td> <td>—</td> <td>2</td> <td>—</td> </tr> <tr> <td>Accessory minerals</td> <td></td> <td></td> <td></td> </tr> <tr> <td>  Micrite</td> <td>50</td> <td>—</td> <td>—</td> </tr> <tr> <td>  Pyrite</td> <td>—</td> <td>2</td> <td>2</td> </tr> <tr> <td>  Phosphatic</td> <td>—</td> <td>3</td> <td>1</td> </tr> <tr> <td>Foraminifers</td> <td>—</td> <td>—</td> <td>2</td> </tr> <tr> <td>Nannofossils</td> <td>—</td> <td>10</td> <td>5</td> </tr> <tr> <td>Diatoms</td> <td>20</td> <td>73</td> <td>50</td> </tr> <tr> <td>Sponge spicules</td> <td>Tr</td> <td>—</td> <td>—</td> </tr> <tr> <td>Silicoflagellates</td> <td>—</td> <td>Tr</td> <td>Tr</td> </tr> </tbody> </table>		1, 26 M	CC, 3 M	CC, 6 D	Silt	30	90	55	Clay	70	10	45	Quartz	—	5	5	Clay	30	5	35	Volcanic glass	Tr	—	—	Calcite/dolomite	—	2	—	Accessory minerals				Micrite	50	—	—	Pyrite	—	2	2	Phosphatic	—	3	1	Foraminifers	—	—	2	Nannofossils	—	10	5	Diatoms	20	73	50	Sponge spicules	Tr	—	—	Silicoflagellates	—	Tr	Tr
	1, 26 M	CC, 3 M	CC, 6 D																																																																										
Silt	30	90	55																																																																										
Clay	70	10	45																																																																										
Quartz	—	5	5																																																																										
Clay	30	5	35																																																																										
Volcanic glass	Tr	—	—																																																																										
Calcite/dolomite	—	2	—																																																																										
Accessory minerals																																																																													
Micrite	50	—	—																																																																										
Pyrite	—	2	2																																																																										
Phosphatic	—	3	1																																																																										
Foraminifers	—	—	2																																																																										
Nannofossils	—	10	5																																																																										
Diatoms	20	73	50																																																																										
Sponge spicules	Tr	—	—																																																																										
Silicoflagellates	—	Tr	Tr																																																																										

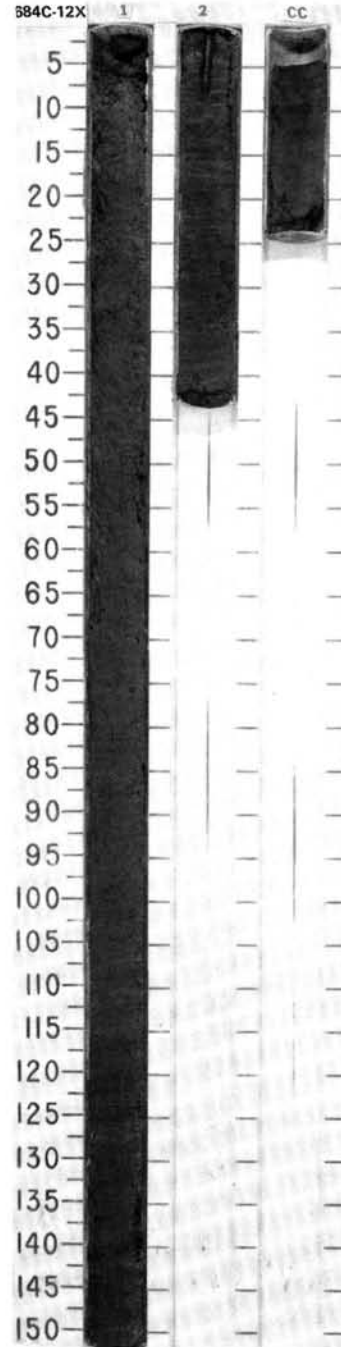


TIME-ROCK UNIT	BIOSTRAT. ZONE/ FOSSIL CHARACTER	PALEOMAGNETICS	PHYS. PROPERTIES	CHEMISTRY	SECTION	METERS	GRAPHIC LITHOLOGY	DRILLING DISTURB.	SED. STRUCTURES	SAMPLES	LITHOLOGIC DESCRIPTION																																																																																																																																																																	
UPPER MIOCENE	*UPPER MIOCENE * NN9 * insignificant * <i>C. yabei</i> Zone			IC: 1.05 OC: 5.57	1 2 CC	0.5 1.0					<p>SANDY DIATOMACEOUS MUD and NANNOFOSSIL-BEARING DIATOM OOZE</p> <p>Major lithology: dark olive gray (5Y 3/2) to olive (5Y 4/4) sandy diatomaceous mud and nannofossil-bearing diatom ooze; laminated on mm and cm scale and disrupted by mud-filled micro-faults, mainly extensional in nature; in Section 1, 2, and CC.</p> <p>Minor lithology: pale yellow nannofossil ooze, Section 1, 129 cm. Also diatomaceous and nannofossil-bearing spiculitic silt, Section 2, 19 cm.</p> <p>SMEAR SLIDE SUMMARY (%):</p> <table border="1"> <thead> <tr> <th></th> <th>1, 70 M</th> <th>1, 85 M</th> <th>1, 127 D</th> <th>1, 132 M</th> <th>2, 19 M</th> <th>2, 26 D</th> </tr> </thead> <tbody> <tr> <td>Texture:</td> <td></td> <td></td> <td></td> <td></td> <td></td> <td></td> </tr> <tr> <td>Silt</td> <td>70</td> <td>60</td> <td>50</td> <td>35</td> <td>75</td> <td>60</td> </tr> <tr> <td>Clay</td> <td>30</td> <td>40</td> <td>50</td> <td>65</td> <td>25</td> <td>40</td> </tr> </tbody> </table> <p>COMPOSITION:</p> <table border="1"> <thead> <tr> <th></th> <th>1, 70</th> <th>1, 85</th> <th>1, 127</th> <th>1, 132</th> <th>2, 19</th> <th>2, 26</th> </tr> </thead> <tbody> <tr> <td>Quartz</td> <td>2</td> <td>2</td> <td>1</td> <td>—</td> <td>2</td> <td>2</td> </tr> <tr> <td>Feldspar</td> <td>3</td> <td>—</td> <td>—</td> <td>—</td> <td>3</td> <td>3</td> </tr> <tr> <td>Rock fragments</td> <td>—</td> <td>—</td> <td>—</td> <td>—</td> <td>—</td> <td>2</td> </tr> <tr> <td>Clay</td> <td>30</td> <td>25</td> <td>50</td> <td>10</td> <td>22</td> <td>25</td> </tr> <tr> <td>Volcanic glass</td> <td>3</td> <td>10</td> <td>—</td> <td>—</td> <td>—</td> <td>2</td> </tr> <tr> <td>Calcite/dolomite</td> <td>Tr</td> <td>—</td> <td>—</td> <td>—</td> <td>3</td> <td>3</td> </tr> <tr> <td>Accessory minerals</td> <td></td> <td></td> <td></td> <td></td> <td></td> <td></td> </tr> <tr> <td>Pyrite</td> <td>2</td> <td>10</td> <td>2</td> <td>Tr</td> <td>2</td> <td>1</td> </tr> <tr> <td>Barite</td> <td>Tr</td> <td>—</td> <td>—</td> <td>—</td> <td>—</td> <td>—</td> </tr> <tr> <td>Phosphate</td> <td>—</td> <td>3</td> <td>—</td> <td>—</td> <td>5</td> <td>5</td> </tr> <tr> <td>Micrite</td> <td>—</td> <td>—</td> <td>1</td> <td>—</td> <td>—</td> <td>—</td> </tr> <tr> <td>Glauconite</td> <td>—</td> <td>—</td> <td>—</td> <td>—</td> <td>Tr</td> <td>Tr</td> </tr> <tr> <td>Foraminifers</td> <td>5</td> <td>—</td> <td>—</td> <td>—</td> <td>3</td> <td>5</td> </tr> <tr> <td>Nannofossils</td> <td>5</td> <td>10</td> <td>3</td> <td>55</td> <td>8</td> <td>15</td> </tr> <tr> <td>Diatoms</td> <td>50</td> <td>20</td> <td>39</td> <td>5</td> <td>50</td> <td>35</td> </tr> <tr> <td>Sponge spicules</td> <td>—</td> <td>20</td> <td>3</td> <td>30</td> <td>—</td> <td>—</td> </tr> <tr> <td>Silicoflagellates</td> <td>—</td> <td>—</td> <td>1</td> <td>—</td> <td>—</td> <td>Tr</td> </tr> <tr> <td>Pellets</td> <td>—</td> <td>—</td> <td>—</td> <td>—</td> <td>2</td> <td>2</td> </tr> </tbody> </table>		1, 70 M	1, 85 M	1, 127 D	1, 132 M	2, 19 M	2, 26 D	Texture:							Silt	70	60	50	35	75	60	Clay	30	40	50	65	25	40		1, 70	1, 85	1, 127	1, 132	2, 19	2, 26	Quartz	2	2	1	—	2	2	Feldspar	3	—	—	—	3	3	Rock fragments	—	—	—	—	—	2	Clay	30	25	50	10	22	25	Volcanic glass	3	10	—	—	—	2	Calcite/dolomite	Tr	—	—	—	3	3	Accessory minerals							Pyrite	2	10	2	Tr	2	1	Barite	Tr	—	—	—	—	—	Phosphate	—	3	—	—	5	5	Micrite	—	—	1	—	—	—	Glauconite	—	—	—	—	Tr	Tr	Foraminifers	5	—	—	—	3	5	Nannofossils	5	10	3	55	8	15	Diatoms	50	20	39	5	50	35	Sponge spicules	—	20	3	30	—	—	Silicoflagellates	—	—	1	—	—	Tr	Pellets	—	—	—	—	2	2
	1, 70 M	1, 85 M	1, 127 D	1, 132 M	2, 19 M	2, 26 D																																																																																																																																																																						
Texture:																																																																																																																																																																												
Silt	70	60	50	35	75	60																																																																																																																																																																						
Clay	30	40	50	65	25	40																																																																																																																																																																						
	1, 70	1, 85	1, 127	1, 132	2, 19	2, 26																																																																																																																																																																						
Quartz	2	2	1	—	2	2																																																																																																																																																																						
Feldspar	3	—	—	—	3	3																																																																																																																																																																						
Rock fragments	—	—	—	—	—	2																																																																																																																																																																						
Clay	30	25	50	10	22	25																																																																																																																																																																						
Volcanic glass	3	10	—	—	—	2																																																																																																																																																																						
Calcite/dolomite	Tr	—	—	—	3	3																																																																																																																																																																						
Accessory minerals																																																																																																																																																																												
Pyrite	2	10	2	Tr	2	1																																																																																																																																																																						
Barite	Tr	—	—	—	—	—																																																																																																																																																																						
Phosphate	—	3	—	—	5	5																																																																																																																																																																						
Micrite	—	—	1	—	—	—																																																																																																																																																																						
Glauconite	—	—	—	—	Tr	Tr																																																																																																																																																																						
Foraminifers	5	—	—	—	3	5																																																																																																																																																																						
Nannofossils	5	10	3	55	8	15																																																																																																																																																																						
Diatoms	50	20	39	5	50	35																																																																																																																																																																						
Sponge spicules	—	20	3	30	—	—																																																																																																																																																																						
Silicoflagellates	—	—	1	—	—	Tr																																																																																																																																																																						
Pellets	—	—	—	—	2	2																																																																																																																																																																						



SITE 684 HOLE C CORE 12X CORED INTERVAL 522.5-532.0 mbsl; 96.0-105.5 mbsf

TIME-ROCK UNIT	BIOSTRAT. ZONE/ FOSSIL CHARACTER				PALEOMAGNETICS	PHYS. PROPERTIES	CHEMISTRY	SECTION	METERS	GRAPHIC LITHOLOGY	DRILLING DISTURB.	SED. STRUCTURES	SAMPLES	LITHOLOGIC DESCRIPTION																									
	FORAMINIFERS	NANNOFOSSILS	RADIOLARIANS	DIATOMS																																			
MIDDLE MIOCENE																																							
	*Upper Miocene							1	0.5					DOLOMITE, DIATOMACEOUS OOZE, and MUD Major lithology: Section 1, 0-4 cm: dark olive gray (5Y 4/1) dolomite. Section 1 through Section 2, 0-49 cm: dark olive gray (5Y 3.5/2) diatomaceous mud. Fine, pale laminations throughout, disrupted by low-angle truncations and high-angle parting. Pale laminations are nannofossil-spicule (at Section 1, 66 cm) and nannofossil-spicule-diatom (at Section 1, 86 cm) oozes. CC: black (5Y 2.5/1) mud, some laminations. SMEAR SLIDE SUMMARY (%): <table border="1"> <thead> <tr> <th></th> <th>1, 65</th> <th>1, 85</th> <th>2, 19</th> <th>2, 33</th> </tr> <tr> <th></th> <th>M</th> <th>M</th> <th>D</th> <th>M</th> </tr> </thead> <tbody> <tr> <td>Sand</td> <td>—</td> <td>—</td> <td>5</td> <td>—</td> </tr> <tr> <td>Silt</td> <td>50</td> <td>60</td> <td>45</td> <td>75</td> </tr> <tr> <td>Clay</td> <td>50</td> <td>40</td> <td>50</td> <td>25</td> </tr> </tbody> </table> TEXTURE: Sand — — 5 — Silt 50 60 45 75 Clay 50 40 50 25 COMPOSITION: Quartz — — 2 — Clay — — 30 10 Volcanic glass Tr — 1 — Accessory minerals Pyrite — 2 2 — Micrite — 5 Tr — Nannofossils 49 38 20 15 Diatoms 25 20 25 75 Radiolarians Tr — — — Sponge spicules 25 30 20 — Silicoflagellates 1 — — — — 5 — —		1, 65	1, 85	2, 19	2, 33		M	M	D	M	Sand	—	—	5	—	Silt	50	60	45	75	Clay	50	40	50	25
	1, 65	1, 85	2, 19	2, 33																																			
	M	M	D	M																																			
Sand	—	—	5	—																																			
Silt	50	60	45	75																																			
Clay	50	40	50	25																																			
							2	1.0																															
							CC																																



TIME-ROCK UNIT	BIOSTRAT. ZONE/ FOSSIL CHARACTER			PALEOMAGNETICS	PHYS. PROPERTIES	CHEMISTRY	SECTION	METERS	GRAPHIC LITHOLOGY	DRILLING DISTURB.	SED. STRUCTURES	SAMPLES	LITHOLOGIC DESCRIPTION																																																																																																														
	FORAMINIFERS	NANNOFOSSILS	RADIOLARIANS											DIATOMS																																																																																																													
MIDDLE/UPPER MIOCENE	Upper Miocene *	NN9 *					1	0.5 1.0					MUD, DIATOM-RICH MUDSTONE, NANNOFOSSIL OOZE, and PHOSPHATIC NODULES  Major lithology: Section 1: dark olive gray (5Y 3/2), finely laminated, diatom-rich mudstone; some phosphatic nodules (e.g., at 124 cm) and thin pale layers comprised of nannofossil oozes (at 8 cm) and diatom-bearing nannofossil ooze (at 35 cm).  CC: black (5Y 2.5/1) mud, drilling slurry.  SMEAR SLIDE SUMMARY (%): <table border="1"> <thead> <tr> <th></th> <th>1, 7 M</th> <th>1, 34 D</th> <th>1, 124 M</th> <th>1, 126 D</th> </tr> </thead> <tbody> <tr> <td>Sand</td> <td>—</td> <td>5</td> <td>—</td> <td>—</td> </tr> <tr> <td>Silt</td> <td>40</td> <td>80</td> <td>20</td> <td>70</td> </tr> <tr> <td>Clay</td> <td>60</td> <td>15</td> <td>80</td> <td>30</td> </tr> </tbody> </table> TEXTURE: <table border="1"> <tbody> <tr> <td>Sand</td> <td>—</td> <td>5</td> <td>—</td> <td>—</td> </tr> <tr> <td>Silt</td> <td>40</td> <td>80</td> <td>20</td> <td>70</td> </tr> <tr> <td>Clay</td> <td>60</td> <td>15</td> <td>80</td> <td>30</td> </tr> </tbody> </table> COMPOSITION: <table border="1"> <tbody> <tr> <td>Quartz</td> <td>1</td> <td>1</td> <td>1</td> <td>3</td> </tr> <tr> <td>Feldspar</td> <td>1</td> <td>1</td> <td>1</td> <td>3</td> </tr> <tr> <td>Clay</td> <td>6</td> <td>15</td> <td>5</td> <td>30</td> </tr> <tr> <td>Volcanic glass</td> <td>—</td> <td>—</td> <td>—</td> <td>2</td> </tr> <tr> <td>Calcite/dolomite</td> <td>Tr</td> <td>3</td> <td>5</td> <td>2</td> </tr> <tr> <td>Accessory minerals</td> <td></td> <td></td> <td></td> <td></td> </tr> <tr> <td>  Phosphate</td> <td>3</td> <td>20</td> <td>80</td> <td>—</td> </tr> <tr> <td>  Pyrite</td> <td>—</td> <td>1</td> <td>—</td> <td>1</td> </tr> <tr> <td>  Glauconite</td> <td>—</td> <td>—</td> <td>—</td> <td>1</td> </tr> <tr> <td>Foraminifers</td> <td>2</td> <td>5</td> <td>—</td> <td>5</td> </tr> <tr> <td>Nannofossils</td> <td>75</td> <td>30</td> <td>8</td> <td>30</td> </tr> <tr> <td>Diatoms</td> <td>10</td> <td>20</td> <td>—</td> <td>15</td> </tr> <tr> <td>Sponge spicules</td> <td>2</td> <td>3</td> <td>—</td> <td>7</td> </tr> <tr> <td>Silicoflagellates</td> <td>—</td> <td>Tr</td> <td>—</td> <td>—</td> </tr> <tr> <td>Pellets</td> <td>—</td> <td>1</td> <td>—</td> <td>1</td> </tr> </tbody> </table>		1, 7 M	1, 34 D	1, 124 M	1, 126 D	Sand	—	5	—	—	Silt	40	80	20	70	Clay	60	15	80	30	Sand	—	5	—	—	Silt	40	80	20	70	Clay	60	15	80	30	Quartz	1	1	1	3	Feldspar	1	1	1	3	Clay	6	15	5	30	Volcanic glass	—	—	—	2	Calcite/dolomite	Tr	3	5	2	Accessory minerals					Phosphate	3	20	80	—	Pyrite	—	1	—	1	Glauconite	—	—	—	1	Foraminifers	2	5	—	5	Nannofossils	75	30	8	30	Diatoms	10	20	—	15	Sponge spicules	2	3	—	7	Silicoflagellates	—	Tr	—	—	Pellets	—	1	—	1
	1, 7 M	1, 34 D	1, 124 M	1, 126 D																																																																																																																							
Sand	—	5	—	—																																																																																																																							
Silt	40	80	20	70																																																																																																																							
Clay	60	15	80	30																																																																																																																							
Sand	—	5	—	—																																																																																																																							
Silt	40	80	20	70																																																																																																																							
Clay	60	15	80	30																																																																																																																							
Quartz	1	1	1	3																																																																																																																							
Feldspar	1	1	1	3																																																																																																																							
Clay	6	15	5	30																																																																																																																							
Volcanic glass	—	—	—	2																																																																																																																							
Calcite/dolomite	Tr	3	5	2																																																																																																																							
Accessory minerals																																																																																																																											
Phosphate	3	20	80	—																																																																																																																							
Pyrite	—	1	—	1																																																																																																																							
Glauconite	—	—	—	1																																																																																																																							
Foraminifers	2	5	—	5																																																																																																																							
Nannofossils	75	30	8	30																																																																																																																							
Diatoms	10	20	—	15																																																																																																																							
Sponge spicules	2	3	—	7																																																																																																																							
Silicoflagellates	—	Tr	—	—																																																																																																																							
Pellets	—	1	—	1																																																																																																																							
							CC																																																																																																																				

